The Role of Gut Bacteria in Tacrolimus Disposition

BY

YUKUANG GUO
B.S. Chengdu University of Traditional Chinese Medicine, Chengdu, China, 2013
M.S. King's College London, London, UK, 2014

THESIS

Submitted as partial fulfillment of the requirements for the degree of Doctor of
Philosophy in Pharmacognosy in the Graduate College of the
University of Illinois at Chicago, 2021 Chicago, Illinois

Defense Committee:

      Hyunyoung Jeong, Chair and Advisor, Pharmaceutical Sciences
      Hyunwoo Lee, Co-advisor, Pharmaceutical Sciences
      Alexander Mankin, Pharmaceutical Sciences
      Jimmy Orjala, Pharmaceutical Sciences
      John Richard Lee, Weill Cornell Medical College

ACKNOWLEDGEMENTS

First and foremost, I would like to thank my advisor Dr. Hyunyoung Jeong for her guidance and support throughout my PhD study. She is a great mentor who taught me how to think critically as a scientist and present research work in a way both professionals and general public can understand. She is passionate about her work, always available for a scientific discussion and willing to give insightful suggestions. Her level of working ethic consistently inspires me to keep learning and growing to be a better scientist.

I would also like to thank my co-advisor Dr. Hyunwoo Lee. He taught me the fundamentals of bacteria related research and helped me in finding the right directions for the project.

I am very honored to have great committee members who offered a broad range of expertise. I want to express my appreciation to Dr. Jimmy Orjala and his previous student Dr. Camila Manoel Crnkovic for assisting with metabolite identification; Dr. John Richard Lee for his efforts on bridging the gap between lab and clinical research; Last but not least, Dr. Alexander Mankin for his expertise in microbiology and contribution on my overall project. All these supports were invaluable to me in completing my PhD study.

I am also thankful to have an enjoyable lab environment to work with our previous (Sungjoon and Miaoran) and current lab members (Kyoung-jae, Ashu, Xiaotong and Giokdjen). They not only helped me with my project but also gave me warmth whenever I was experiencing difficulty.

CONTRIBUTION OF AUTHORS

Chapter 1 is a literature review that summarizes (1) tacrolimus PK and (2) gut bacteria in reductive drug metabolism. The latter has been published as a review paper (include complete citation), in which I, Yukuang Guo, my research advisors Dr. Hyunyoung Jeong and Dr. Hyunwoo Lee, contributed to the writing of the manuscript.

Chapter 2 represents two published manuscripts (include complete citation) and some unpublished work in which I was the main investigator. Dr. Camila M. Crnkovic, a former member of Dr. Jimmy Orjala lab determined the structure of the metabolite using mass and NMR spectroscopic methods. Dr. Kyoung-jae Won, a postdoctoral fellow in our lab, performed the immunosuppression assay. Fecal and blood samples from kidney transplant patients were provided by Dr. John Richard Lee from Weill Cornell Medical College. Ziwei Zhang, a former member of our lab participated in finding tacrolimus metabolizing enzymes in *F. pruasnitzii*. My research advisors Dr. Hyunyoung Jeong and Dr. Hyunwoo Lee, and the researchers mentioned above contributed to the analysis of the data and writing of the manuscripts.

Permission to use the manuscripts in this thesis was granted by the publishers for all published manuscripts used (Permission letters see appendices).

TABLE OF CONTENTS

TABLE OF CONTENTS (Continued)

LIST OF TABLES

LIST OF FIGURES

LIST OF ABBREVIATIONS OR
NOMENCLATURE

ACN   Acetonitrile

ABRs   Aldo/keto reductases

ABX   Antibiotics

AUC   Aera under the curve

BLAST   Basic local alignment search tool

CYP   Cytochrome P450

CON   Control

CBRs   Carbonyl reductases

C_{max} Peak concentration

DDI   Drug-drug interaction

EC   Enzyme commission

ELISA   Enzyme-linked immunosorbent assay

FKBP   FK506 binding protein

GI   Gastrointestinal

HRMS   High-resolution mass spectrometry

IR   Infrared spectroscopy

IC_{50} Concentration required for 50% inhibition

$K_{RBC/PL}$ Blood to plasma ratio

MeOH	Methanol
Met-ID	Metabolite identification
MS	Mass spectrometry
MEIA	Microparticle enzyme immunoassay
NAD	Nicotinamide–adenine- dinucleotide
NADP	Nicotinamide–adenine- dinucleotide phosphate
NMR	Nuclear magnetic resonance
P-gp	P-glycoprotein
PK	Pharmacokinetics
P_{app}	Apparent permeability
RBC	Red blood cells
TLC	Thin layer chromatography
T_{max}	Time to achieve peak concentration
TMB	3,3',5,5'-Tetramethylbenzidine

SUMMARY

Tacrolimus is the mainstay immunosuppressant drug used after solid organ and hematopoietic stem cell transplantation. Tacrolimus exhibits a low and variable oral bioavailability, with an average of 25% of the oral dose reaching the systemic circulation. The major site of drug loss is in the gut, and the gut extraction ratio was reported as 85% and 74% in healthy and liver transplant patients, respectively. However, inhibition of known tacrolimus disposition enzymes (i.e., CYP3A4/5 and P-gp) by co-administration of ketoconazole orally did not fully prevent drug loss. More than 50% of tacrolimus still fail to reach the systemic circulation, suggesting other contributing factors are yet to be well defined. Lack of knowledge regarding other contributing factors to tacrolimus thus constitutes a substantial gap in optimizing tacrolimus dosage regimen and improving graft outcomes in transplant recipients. Recent studies suggest a potential role of gut bacteria in decreasing tacrolimus oral exposure. For example, (1) fecal abundance of *F. prausnitzii* was positively correlated with tacrolimus dosing in kidney transplant patients, and (2) co-treatment of tacrolimus with antibiotics that do not affect tacrolimus disposition enzymes increased tacrolimus trough blood concentration in kidney transplant patients. Together, we hypothesized that bacteria metabolize tacrolimus and decrease oral drug exposure.

In Chapter 1, we summarized knowledge regarding tacrolimus pharmacokinetics and the role of gut bacteria in reductive drug metabolism.

In Chapter 2, we determined bacterial metabolism as an important elimination pathway of tacrolimus in humans. *In vitro* incubation of tacrolimus with *F. prausnitzii* and human stool showed a significant parent drug disappearance and formation of new peaks, which were not produced when tacrolimus was incubated with human hepatic microsomes. And the major

metabolite M1 was identified as hydroxyl tacrolimus, where the ketone group at C-9 position was reduced to the hydroxyl group. To determine the impact of bacterial metabolism on the pharmacological activity of tacrolimus, we compared the immunosuppressive and anti-fungal activity between tacrolimus and M1. The results showed the 15-fold lower activity of M1 as compared to tacrolimus. We further examined the capability of M1 formation by 25 representative human gut bacteria belonging to major taxa. The result showed that 22 of them can metabolize tacrolimus, demonstrating the prevalence of tacrolimus metabolism by human gut bacteria. We also bridged the gap between *in vitro* and *in vivo* studies by detecting M1 in stool and blood samples from kidney transplant patients after oral administration of tacrolimus. To estimate the contribution of bacterial metabolism in tacrolimus oral exposure, we performed the kinetic study of M1 formation using *F. prausnitzii* as a model bacterium, and the result was extrapolated to estimate M1 formation in the human small intestine. The estimation indicated an extensive tacrolimus metabolism by bacteria, where 38% of tacrolimus is converted to M1 at a typical oral dose (i.e., 5 mg). Last but not least, to determine the responsible metabolizing enzymes, we overexpressed 24 oxidoreductases of *F. prausnitzii* and identified 4 of them are capable of producing M1.

In conclusion, our study demonstrated the bacterial metabolism of tacrolimus as an important elimination pathway in humans. In detail, human gut bacteria can convert tacrolimus to M1, a much less active form, through ketone reduction and reduce tacrolimus oral exposure.

CHAPTER 1. OVERVIEW OF TACROLIMUS PK AND GUT BACTERIA IN REDUCTIVE DRUG METABOLISM

Part of this chapter was previously published as Guo, Y., Lee, H., & Jeong, H. (2020). Gut microbiota in reductive drug metabolism. Progress in Molecular Biology and Translational Science, 171, 61-93.

1.1. Tacrolimus PK

1.1.1. Introduction

Tacrolimus is an immunosuppressant used to prevent organ rejection after transplantation. Tacrolimus has a narrow therapeutic window, and supra- and under-therapeutic concentrations of tacrolimus are associated with drug toxicity (nephrotoxicity and neurotoxicity) and graft rejection, respectively (Gardiner et al., 2016). Maintaining tacrolimus concentrations within the therapeutic range is difficult; however, because of its low and variable oral bioavailability (ranging from 5% to 93%; average 25%) (Zou et al., 2019). The activity of CYP3A4/5 and the drug efflux pump P-gp in the liver and intestine had been proposed to explain the tacrolimus bioavailability (Figure 1). However, drug-drug interaction studies of tacrolimus and ketoconazole (an inhibitor of both hepatic and intestinal CYP3A4/5 and P-glycoprotein) showed that even after CYP3A4/5 and P-glycoprotein inhibition, a significant (>50%) fraction of the dose failed to reach systemic circulation, suggesting the presence of additional route(s) of tacrolimus elimination (Floren et al., 1997; Tuteja et al., 2001). Lack of this knowledge thus constitutes a substantial gap in optimizing tacrolimus dosage regimen and improving graft outcomes in transplant recipients.
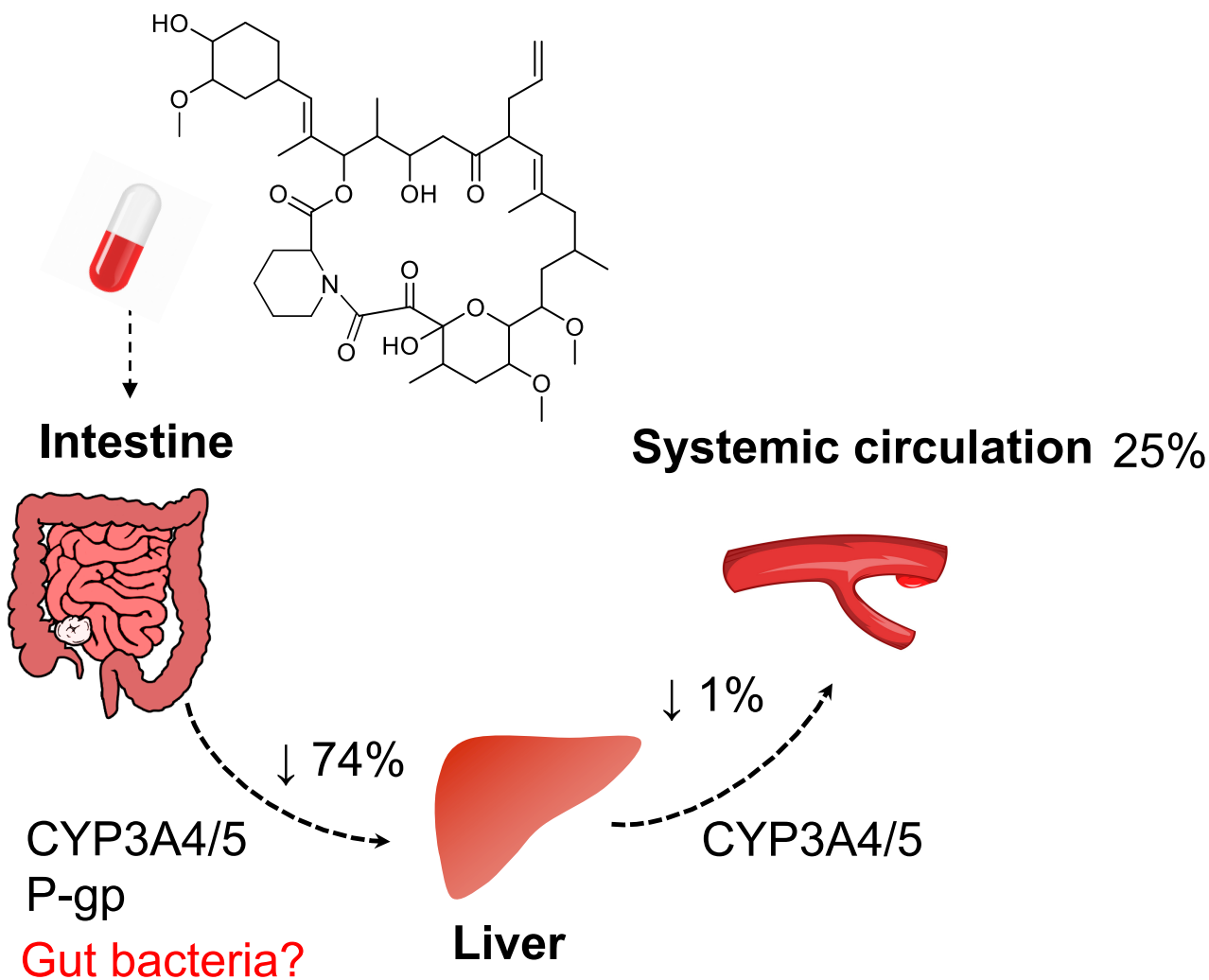
Figure 1. Tacrolimus shows extensive gut metabolism and poor oral bioavailability

1.1.2. Absorption

Tacrolimus is a macrocycle compound that was discoverd in 1987 from the soil bacterium *Streptomyces tsukubaensis* (Starzl, 1987). It exhibits poor water solubility (<1 mg/L) (Patel et al., 2012). For intravenous injection, it is dissolved in a mixture of surfactant HCO-60 and ethanol (Patel et al., 2012). Oral administration is a more common route of administration. To resolve the solubility issue, tacrolimus was formulated into a solid dispersion formulation (Prograf) by mixing with hydrophilic ingredient hydroxyl-

propylmethylcellucose (Yamashita et al., 2003). In addition to this immediate release dosage form, sustained release formulation (Advagraf) is also available to reduce dosing frequency to once a day (Caillard et al., 2016).

As a BCS II compound, tacrolimus exhibits an excellent permeability, which makes it be absorbed rapidly by the small intestine. Most of the patients taking Prograf show peak concentration (T_{max}) between 0.5 to 2 h (Venkataramanan et al., 1991; Gruber et al., 1994). The isolated rat jejunum model is a useful tool to study drug permeability in the human intestine (Peternel et al., 2012). In an *ex vivo* perfusion study using rat jejunum, tacrolimus showed an apparent permeability (P_{app}) of 0.35 ± 0.05 cm/s. Jejunum appears to be the major absorption site, as the permeability was only half of that in the ileum and even lower in the colon (Tamura et al., 2002; Tamura et al., 2003). And the major reason is due to higher expression of the efflux transporter P-glycoprotein (P-gp) in the distal intestine (Mouly and Paine, 2003; MacLean et al., 2008). Treatment of the different rat small intestinal segments with verapamil, a potent P-gp inhibitor, eliminated the difference in permeability (Tamura et al., 2002). *In vitro* Caco-2 study also gave the same conclusion, where the apparent permeability from basolateral to apical is more than 3-fold of that from the opposite direction (Tamura et al., 2002).

In addition to efflux by P-gp, another known factor that decreases oral tacrolimus absorption is intestinal metabolism by CYP3A4/5 (Kolars et al., 1994). Metabolizing enzymes may also work together with P-gp to produce a synergistic effect in decrease the fraction of tacrolimus being absorbed (Christians et al., 2005). Incubation of tacrolimus with human and pig small intestinal microsomes showed a significant loss of parent drug and metabolite formation. Noticeably, the extent of metabolism was declined in the order of duodenum > jejunum > ileum > colon. The potential explanation is likely due to the

higher expression of CYP3A in the proximal region of the intestine (Fritz et al., 2019). *Ex vivo* perfusion study showed 50% and 20% of the absorbed tacrolimus was degraded in rat jejunum and ileum, respectively (Tamura et al., 2003). Treatment with ketoconazole, a potent inhibitor for both CYP3A and P-gp, can increase the absorption from 47.8% to 88.1% in the jejunum (Tamura et al., 2003). Notably, the permeability was not altered by ketoconazole, suggesting inhibition of CYP3A mediated metabolism is the reason for the increased absorption. Treatment with CYP3A4 substrate midazolam also showed a similar extent of enhancement in tacrolimus absorption (Tamura et al., 2003). Together, these studies demonstrate a major role of CYP3A in tacrolimus absorption in proximal small intestine while P-gp-mediated efflux may affect absorption in distal intestine.

1.1.3. Distribution

The majority of tacrolimus is distributed into the red blood cells (RBC). In a human study using ^{3}H-dihydro-tacrolimus, the result showed 85.3% to 98% of the drug is associated with erythrocytes (Nagase et al., 1994; Zahir et al., 2001). As a comparison, tacrolimus is much less distributed into the plasma and lymphocytes, with an average of 14.3% and 0.46%, respectively (Nagase et al., 1994; Zahir et al., 2001). Nagase *et al.* studied the subcellular distribution of tacrolimus in the erythrocytes by fractionation and found that most of the drug was bound with FK506 binding protein (FKBP), exhibiting a molecular weight of ~10 kDa (Nagase et al., 1994). The follow-up study by incubating this protein with cyclosporine A, another widely used immunosuppressant, did not show a significant binding, suggesting tacrolimus-FKBP interaction is specific and is likely the major reason responsible for the significant distribution of tacrolimus in erythrocytes in human blood.

Due to the high association of tacrolimus with erythrocytes, tacrolimus concentration is 4 to 114 times higher when using blood samples as a comparison with corresponding plasma in transplant patients (Venkataramanan et al., 1991; Bäckman et al., 1994; Jusko et al., 1995). There is a huge difference in the volume of distribution when using plasma and blood concentration, which are 30 L/kg and 1 L/kg, respectively (Tamura et al., 1987; Wallemacq and Verbeeck, 2001). Considering physiological relevance and also the sensitivity of the assay, monitoring tacrolimus concentration and exposure using blood samples are more favorable than using plasma samples. Currently, available methods either apply the immunology approach (ELISA and MEIA) or LC-MS/MS (Dietemann et al., 2001). The blood to plasma ratio of tacrolimus exhibits a huge inter- and intra-individual variability. And it is largely dependent on tacrolimus concentration and one's hematocrit level. For example, the ratio varies from 2.9 to 134.8 over a blood concentration ranging from 3 to 28.7 ng/ml (Jusko et al., 1995; Chow et al., 1997). A positive correlation was observed between the hematocrit level and the percentage of tacrolimus associated with erythrocytes (r^2 = 0.47) (Zahir et al., 2004).

1.1.4. Metabolism

Tacrolimus is mainly eliminated from the body through metabolism. As discussed before, tacrolimus shows extensive first-pass metabolism in the gut. And the liver is the major metabolizing organ that removes tacrolimus from systemic circulation. *In vitro* incubation of tacrolimus with human hepatic and intestinal microsomes indicated the major metabolizing pathways are through *O*-demethylation and hydroxylation (Shiraga et al., 1994; Shiraga et al., 1999). In total, eight metabolites were identified, including mono-demethylated, di-demethylated, hydroxylated, demethylated, and hydroxylated

metabolites (Shiraga et al., 1999). Notably, 13-*O*-demethylated tacrolimus is the major metabolite found from *in vitro* microsonal incubation and human blood after oral administration (Vincent et al., 1992; Gonschior et al., 1996; Chitnis et al., 2013). To determine the enzymes responsible for metabolizing tacrolimus, tacrolimus was incubated with lysates from Hep G2 cells expressing different human CYPs (1A2, 2A6, 2B6, 2C8, 2C9, 2D6, 2E1, 3A3, 3A4, and 3A5). And the result showed that CYP3A4 and CYP3A5 are the major metabolizing enzymes in terms of total metabolism, as well as the production of 13-*O*-demethylated tacrolimus (Shiraga et al., 1999). Examination of its immunosuppressive activity showed less than 10% of the original activity of tacrolimus (Iwasaki et al., 1995).

It has been showed that CYP3A5 polymorphism plays a significant role in determining metabolizing phenotype and clearance of tacrolimus. The *1 allele (A) and *3 allele (G) account for 23.7% and 76.3% of transplant patients, respectively (Goto et al., 2004). *3 allele codes for a non-functional protein, thus leading to poor metabolizing activity (Larriba et al., 2010). Human liver microsomes carrying the CYP3A5*1 allele (expressor) showed 1.5 to 2.7-fold higher metabolizing activity than CYP3A5*3/*3 genotype (non-expressor) (Dai et al., 2006; Picard et al., 2011). Patients who express CYP3A5*1/*1 and CYP3A5*1/*3 exhibit 2-fold and 1.7-fold greater clearance of tacrolimus as compared to CYP3A5*3/*3 carriers (non-expressor), which leads to significantly lower drug exposure (Barry and Levine, 2010). Choi *et al.* reported that the expressors showed 2.5-fold higher blood AUC as compared to non-expressors after oral administration of 1 mg tacrolimus (Choi et al., 2007). As a result, expressors typically require 1.5 to 2 times the recommend dose to achieve the same therapeutic concentration (Birdwell et al., 2015).

In addition to CYP3A5 polymorphism, the hematocrit level is another important factor that affects tacrolimus clearance and dosing. As described above, tacrolimus shows extensive binding with erythrocytes; such interaction largely minimizes the amount of free drug available for hepatic metabolism. Thus, although tacrolimus is rapidly eliminated *in vitro* by microsomes, hepatic extraction (4%) in the human body is a slow process (Jusko et al., 1995). Hematocrit level was found highly variable in transplant patients. Patients usually have low hematocrit levels after transplantation, which increase from 33% at the first month of post-transplantation to 40% after 12 months' recovery (Mix et al., 2003; Størset et al., 2014). In a clinical study, a negative correlation between hematocrit level and the ratio of dose/trough concentrations of tacrolimus in blood was found from liver transplant patients (R = −0.53) (Minematsu et al., 2004). Zahir et al. also reported a 46% higher blood clearance of tacrolimus in patients with a low hematocrit (< 35%) than patients with higher hematocrit levels (Zahir et al., 2005). Together, these studies indicate both CYP3A5 polymophism and hematocrit level are critical in determining extent of tacrolimus metabolism and therapeutic dose.

1.1.5. Elimination

Tacrolimus is mainly excreted through bile to feces after hepatic metabolism. In a human study, $92.6 \pm 30.7\%$ of the radioactivity was recovered in feces over an 11-day period after oral administration of ^{14}C-labeled tacrolimus (Moller et al., 1999). Urinary excretion, on the other hand, is only responsible for excreting 2.3% of the drug. While the majority of radioactivity in the blood was from unchanged tacrolimus, it was only at trace levels in both urine and feces, indicating extensive metabolism (Moller et al., 1999).

1.1.6. A potential role of gut bacteria in tacrolimus disposition

Recent studies suggest a role of gut bacteria in tacrolimus elimination and oral drug exposure. For example, orally administered antibiotics with minimal effects on CYP3A4/5 and P-gp expression/activity, such as levofloxacin increased tacrolimus exposure by ~25% in kidney transplant recipients (Federico, Carrano et al. 2006). John R. Lee's group compared kidney transplant patients (N=60) taking antibiotics and those who do not during the first 30 days of transplantation (N=200). The result showed a significant increase in tacrolimus trough concentration over tacrolimus dosage (C/D) on day 7 (p=0.001) and 15 (p=0.07) after receiving antibiotics (Zheng et al., 2019). As compared to the immediate-release formulation, sustained-release formulation retains the drug in the GI tract for a longer time, and more drug may reach the lower intestinal tract where has more bacteria. In theory, a drug that is liable to bacterial metabolism will likely show more significant metabolism when using extended-release formulation. Many studies showed higher doses were required in kidney transplant patients who took Advagraf (once-daily sustained-release formulation) than Prograf (twice-daily traditional formulation) to achieve the same therapeutic concentration (Crespo et al., 2009; de Jonge et al., 2010). In a study of 284 human subjects, kidney transplant patients who switched from Prograf to Advagraf on a 1:1 on a milligram basis showed a significant decrease in trough blood concentration, and about 30% of patients required more than a 20% dose increase (de Jonge et al., 2010). Moreover, analysis of the gut microbial composition in kidney transplant patients revealed that the fecal abundance of *F. prausnitzii* in the first week of transplantation is positively correlated with the tacrolimus dose required to achieve therapeutic concentrations (Lee et al., 2015). Together, these data suggest that gut bacteria may play a significant role in metabolizing tacrolimus and determining tacrolimus oral exposure.

1.2. Gut bacteria in reductive drug metabolism

1.2.1. Introduction.

The human gut harbors around 100 trillion bacteria, whose genomes are predicted to contain about 100 times more protein-encoding genes than the human genome (Gill et al., 2006; Sender et al., 2016). Such richness in the gene contents likely reflects extremely diverse catalytic reactions that can be mediated by gut bacteria, and unsurprisingly, gut bacteria have repeatedly been identified to metabolize small xenobiotic molecules including therapeutic drugs (Scheline, 1973; Sousa et al., 2008b; Spanogiannopoulos et al., 2016; Clarke et al., 2019). Gut, either small or large intestine, provides an environment with low redox potentials and with no to little oxygen available (Celesk et al., 1976; Circu and Aw, 2011; Espey, 2013; Friedman et al., 2018). Such anaerobic and reducing conditions in the gut likely position resident gut bacteria to readily mediate the reductive metabolism of incoming xenobiotics such as therapeutic drugs. This review is focused on drugs undergoing reductive metabolism by gut bacteria. Depending on chemically distinct groups, xenobiotics may undergo one or more types of six major reductive metabolisms: azo (-N=N-), nitro ($-NO_2$), alkene (-C=C-), ketone (-C=O), N-oxide (-N-O), and sulfoxide (-S=O) (Scheline, 1973; Sousa et al., 2008b; Spanogiannopoulos et al., 2016; Clarke et al., 2019). We have provided select examples of drugs in six chemically distinct groups, for which gut bacteria are known or suspected to mediate the reduction (Table I).

Table I. Gut bacteria identified to mediate reductive metabolisms.

Reductive metabolism	Drug	Gut bacteria identified	Cecal/intestinal contents/feces tested
Azoreduction	Prontosil	Many gut bacterial species	Rat cecal contents (Gingell et al., 1969a)
	Sulfasalazine	*Bacteroides fragilis; Clostridium perfringens; Corynebacterium acnes; Fusobacterium sp.; Streptococcus faecium; Streptococcus faecalis; Escherichia coli; Lactobacillus sp.* (Peppercorn and Goldman, 1972a)	
Nitroreduction	Chloramphenicol	*Escherichia coli* (Merkel and Steers, 1953a; Holt, 1967a);*Haemophilus influenza* (Smith et al., 2007; Crofts et al., 2019); *Neisseria meningitides* (Smith et al., 2007); *Bacteroides fragilis* (Onderdonk et al., 1979)	
	Nitrobenzodiazepines	*Escherichia coli* (Linwu et al., 2009b); *Clostridium leptum* (Rafii et al., 1997)	
Alkene reduction	Deleobuvir	N/A	Rat feces; human feces (McCabe et al., 2015)
	Digoxin	*Eggerthella lenta* (Saha et al., 1983b)	Human feces (Lindenbaum et al., 1981)
Keto- reduction	Nabumetone	*Escherichia coli; Lactobacillus casei; Lactobacillus plantarum; Parabacteroides distasonis* (Jourova et al., 2019)	

	Doxorubicin	*Raoultella planticola; Escherichia coli* (Yan et al., 2018)	11
Sulfoxide reduction	Sulindac	*Escherichia coli* (Etienne et al., 2003)	Human intestinal contents (Duggan, 1981); Human feces (Duggan et al., 1977a)
	Sulphinpyrazone	*Escherichia coli; Enterobacter sp.; Prote us sp.; Providencia sp.; Kle bsiella sp.; Citrobacter sp.; Pseudomonas sp.; Enteroc occus sp.; Bacteroides sp.; Fusobacterium sp.; Clostridi um sp.* (Strong et al., 1987)	Rat feces (Renwick et al., 1982a); Human feces (Strong et al., 1987)
N-Oxide reduction	Nicotine	N/A	Rat intestinal and cecal contents (Dajani et al., 1975a)
	Loperamide	N/A	Rat intestinal and cecal contents (Lavrijsen et al., 1995a)
	Ranitidine	N/A	Human feces (Basit and Lacey, 2001)

1.2.2. Enzymes for reductive metabolisms

Enzymes that catalyze oxidation and reduction reaction belong to oxidoreductase family (EC 1). Reactions can be expressed as $A^- + B \rightarrow A + B^-$, where oxidoreductases are responsible for the transmission of electrons from a donor (e.g., Alcohol, Aldehyde, alkyl, amine, NAD(P)H) to an acceptor (e.g., Oxygen, Fe^{3+}, $NAD(P)^+$) (Robinson, 2015). A typical reaction requires the consumption of cofactors, and NAD(P)H dependent (i.e., NAD(P)H or NAD(P)+) enzymes are most common that account for 80% of the oxidoreductases (Paul et al., 2019). The nucleotide binding domains, such as rossmann fold, is a structurally similar motif shared by many NAD(P)H dependent oxidoreductases (Hanukoglu, 2015). It recruits NAD(P)H and allow C4 carbon atom of the nicotinamide ring serves as the acceptor/donor of a proton. The catalytic domains, on the other hand, are more variable that are related to substrate specificity (Sellés Vidal et al., 2018).

Oxidoreductases are found in all the living organisms including animals, plants and bacteria, et al. They play crucial roles in variety of biological functions including chemical synthesis and detoxification. For example, many facultative anaerobic bacteria expressing nitrate/nitro reductases that can catalyze nitrate/nitro reduction to produce ammonium: $NO^{3-} \rightarrow NO^{2-} \rightarrow NH^{4+}$ (Bryant and DeLuca, 1991; Kamp et al., 2015). This provides nitrogen resource for synthesizing proteins and nucleic acids in bacteria (Kamp et al., 2015). In terms of bacteria mediated drug metabolism, oxidoreductases can catalyze various actions and change drug activity. Studies have been show antibiotic resistance in some pathogenic bacteria can be explained by expression of a certain

oxidoreductase. For example, oxidoreductase NfsB from gut bacterium *Haemophilus influenza* was found metabolize chloramphenicol to less active metabolites (Crofts et al., 2019). On the other hand, bacterial oxidoreductases may also activate prodrugs through metabolism. More details related to specific oxidoreductases will be discussed along with individual drugs.

1.2.3. Reductive drug metabolism

1.2.3.1. Azoreduction

Azo compounds are a group of organic chemicals (R-N=N-R′), in which "-N=N-" is the azo bond, and R or R′ is either alkyl or aryl (aromatic) group (Chung, 2016). Azo compounds with alkyl groups are colorless, whereas those (azo dyes) containing aromatic groups give characteristic colors. Because azo dyes are the most common coloring agents used in the textile, paper, cosmetics, food, and pharmaceutical industries, their (potentially toxic) metabolism in animals and humans, as well as their degradation in the environment, have been important health-related research subjects (Feng et al., 2012; Chung, 2016). Earlier studies have well established that azo dyes are metabolized in the body via both oxidative and reductive reactions, with the former mediated by the host and the latter mainly by intestinal bacteria (Levine, 1991).

1.2.3.1.1. Prontosil

The azo dye prontosil (Figure 2) was identified as an anti-infective agent active against Streptococcal infections in mice (Domagk, 1957). Prontosil exhibited its efficacy only *in vivo* mouse infection models, with no apparent antibacterial activity against Streptoccci *in vitro*. Because p-aminobenznesulfonamide (sulfanilamide) (Figure 2),

which can be generated upon the reductive cleavage of the azo bond of prontosil, was as effective as prontosil for controlling *Streptococcal* infections, prontosil was proposed to be reductively metabolized in the body into the active component sulfanilamide (Colebrook et al., 1936; Fuller, 1937). As was the case for many other azo dyes (Radomski and Mellinger, 1962; Ryan et al., 1968), prontosil was shown to be reduced by intestinal bacteria in rats and humans (Gingell et al., 1969b; Gingell and Bridges, 1971). Moreover, antibiotic treatments of rats receiving oral prontosil reduced the excretion of sulfanilamide significantly in urine further suggesting that gut bacteria play a critical role in cleaving the azo bond and producing the active component of prontosil (Gingell et al., 1971). With the finding of prontosil as a pro-drug that is converted to the active metabolite by gut bacteria, the azo linkage has been extensively employed in the development of in particular colon-specific pro-drugs that are activated by gut bacteria (Ali et al., 2018).

1.2.3.1.2. Sulfasalazine

Sulfasalazine (salazopyrin; salicylazosulfapryridine) is a compound synthesized by combining between 5-aminosalicylic acid and sulfapyridine (Figure 2). Since sulfasalazine was identified to be active in ulcerative colitis and introduced into clinical practice in 1941(Svartz, 1942), it has been used as the main treatment of ulcerative colitis (Hauso et al., 2015). Using conventional and germfree rats and gut bacteria, sulfasalazine was shown to be reductively metabolized by gut bacteria, the result of which is the generation of 5-aminosalicylic acid and sulfapyridine (Peppercorn and Goldman, 1972b; Schroder and Gustafsson, 1973). A later study determined that 5-aminosalicylic acid is the therapeutically active component (Das et al., 1973). Because the colon is the site where 5-aminosalicylic acid exerts its therapeutic effect and most of the 5-aminosalicylic acid

liberated from sulfasalazine by gut bacteria in the colon is not absorbed for systemic circulation (Azadkhan et al., 1982), it is not surprising that antibiotic treatments affect the clinical outcomes of sulfasalazine treatments. For example, in healthy volunteers (taking sulfasalazine for three days, 6-day break, ampicillin (250 mg four times daily) for five days followed by three days of sulfasalazine (2 g twice daily), the plasma concentration of sulfapyridine was significantly lower in posttreatment than in pretreatment with ampicillin, indicating that ampicillin treatment impairs the azo reduction of sulfasalazine by gut bacteria and the amount of liberated 5-aminosalicylic acid is reduced (Houston et al., 1982).
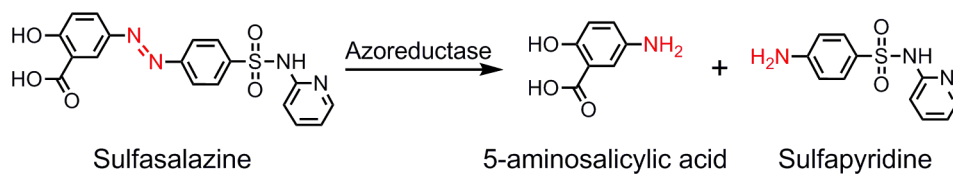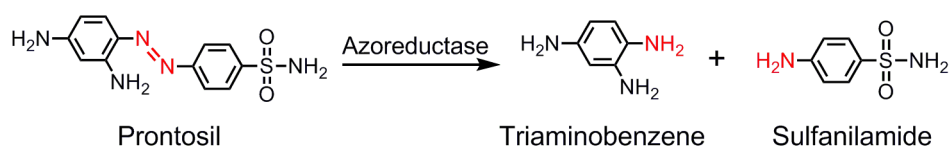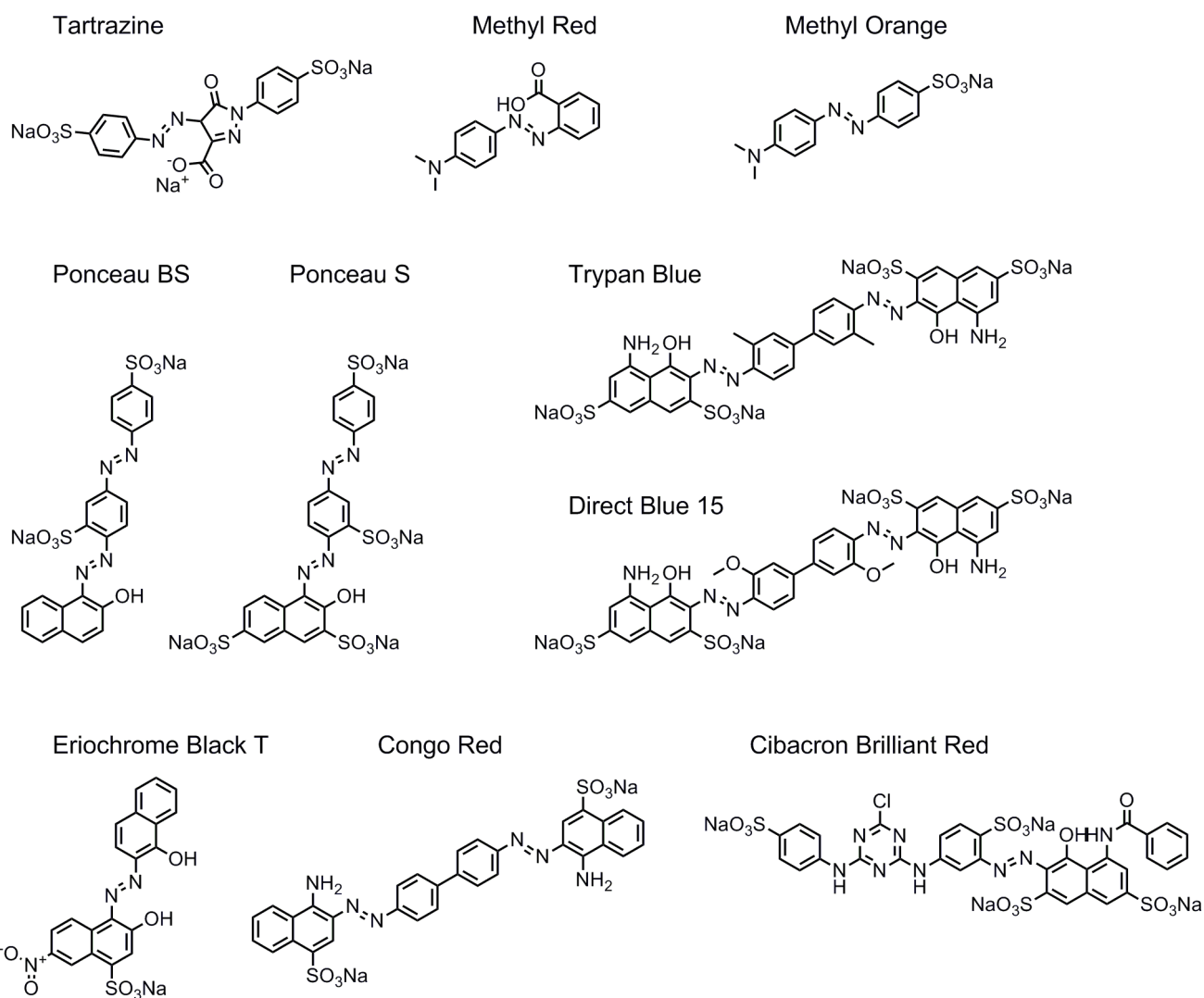
Figure 2. **Azoreduction by gut bacteria.** Drugs (A) and dyes (B) that undergo azoreduction by gut bacteria are shown. See text for details.

1.2.3.1.3. Azoreductases

Many earlier studies that investigated the reduction of azo dyes led to the identification of bacterial enzymes collectively called azoreductases (Mahmood et al., 2016). The majority of these enzymes are identified in aerobic bacteria, a few azoreductases are characterized in facultative anaerobic bacteria, and only one enzyme is known in obligate anaerobic bacteria. Phylogenetic analysis based on primary amino acid sequences classifies most of the known and putative azoreductases into four distinct clades (I-IV), while the AzoC azoreductase in the strict anaerobic gut bacterium Clostridium perfringens is phylogenetically separated from these clades (Suzuki, 2019).

Facultative and obligate anaerobic gut bacteria belonging to major phyla present in the human intestine appear to possess one or more (un)characterized azoreductases (Chung et al., 1978; Brown, 1981; Rafii et al., 1990; Xu et al., 2010). However, the physiological role of azoreductases in gut bacteria is unclear. Since the substrates of azoreductases, i.e., aromatic azo compounds, are extremely rare in nature (Blair and Sperry, 2013), it is difficult to imagine that these gut bacterial enzymes have evolved to catalyze azo reduction specifically. There is evidence that may suggest that azo reduction is an off-target activity of certain reductases; some azoreductases can catalyze the reduction of different types of substrates. For example, AzoR, the azoreductase of the facultative anaerobic gut bacterium *Escherichia coli*, catalyzes quinone (menadione) reduction with higher specific activity than the azo reduction of Methyl Red (Nakanishi et al., 2001), and it is also able to catalyze the reduction of nitro compounds (Prosser et al., 2010; Mercier et al., 2013). Moreover, a ΔazoR mutant

exhibits an aerobic growth defect in the presence of quinones (Liu et al., 2009). More work will be required to define better the physiological roles of azoreductases in gut bacteria.

As mentioned above, AzoC in C. perfringens is the only azoreductase characterized in strictly anaerobic bacteria (Morrison et al., 2012; Morrison and John, 2015). Though a physiological role of AzoC is not well defined, a study suggests that it might be involved in resistance to certain toxic azo dyes. It was shown that wild-type *C. perfringens ATCC 3626* grows slower in the presence than the absence of an azo dye such as tartrazine, Methyl Red, Methyl Orange, Ponceau BS, Ponceau S, Trypan Blue, or Direct Blue 15 (Figure 2).(Morrison and John, 2016) The growth inhibitory effects of these azo dyes appear to be specific since no such effects were observed with other azo dyes such as Eriochrome Black T, Congo Red, and Cibacron Brilliant Red (Figure 2). Interestingly, a ΔazoC mutant was partially or completely resistant to the growth inhibitory effects of Ponceau BS, Ponceau S, Trypan Blue, and Direct Blue 15, suggesting that the AzoC-mediated reductive cleavage products of these azo dyes might be responsible for the impaired growth. Moreover, the ΔazoC mutant displayed a similar growth defect to the wild type in the presence of tartrazine, Methyl Red, and Methyl Orange, suggesting the existence of additional azoreductase(s) (Morrison and John, 2016). Our unpublished search for AzoC homologs in gut microbial metagenomes using MetaQuery (Nayfach et al., 2015) indicate that gut bacteria in all major phyla possess AzoC homologs (>70% coverage, >30% identity, e-value >1e-5; data not shown) This gut microbiome search result, together with the reported phenotype of the ΔazoC mutant in C. perfringens, raises an intriguing question about the effects of azo dyes on gut microbiota. Tartrazine is one of the FDA-approved azo dyes for use as food additives. The fact that both the wild-type C. perfringens and ΔazoC mutant strains show similar growth defects when grown in the

presence of tartrazine might suggest the existence of as-yet-unknown azo reductase(s) that mainly mediates the azo reduction of tartrazine. To the best of our knowledge, studies investigating the effects of azo dyes on the composition and diversity of gut microbiota have not been reported. However, since AzoC homologs are present in all major gut bacterial phyla, short- or long-term intake of certain azo dyes as food additives may have profound effects on the relative abundance and/or function of gut microbiota, consequently affecting host physiology.

1.2.3.2. Nitroreduction

Similar to azo dyes, numerous aromatic compounds that contain nitro groups (-NO_2) have been synthesized for a variety of industrial purposes such as the synthesis of plastics, dyes, explosives, and drugs. Nitroaromatics also include nitrated-polycyclic aromatic hydrocarbons formed by (photo)chemical transformation of polycyclic aromatic hydrocarbons in air and during combustion processes (Ju and Parales, 2010). Since many nitroaromatic compounds have been found to have mutagenic and/or tumorigenic activity, their contamination in the environment and toxic effects on humans have been investigated extensively (Rosenkranz and Mermelstein, 1983; Peres and Agathos, 2000; Ju and Parales, 2010). The mutagenicity and/or tumorigenicity of nitroaromatic compounds have been proposed to be due to nitroso and hydroxylamine reactive intermediates that are generated during the reduction of nitro groups to amines by enzymes collectively termed nitroreductases (Roldan et al., 2008). A large number of studies about nitroreduction have been directed toward the identification and characterization of (an)aerobic environmental bacteria, with their potential applications in biodegradation of nitroaromatic compounds (Rieger et al., 2002; Symons and Bruce, 2006;

Ju and Parales, 2010). However, nitroaromatic compounds also include therapeutic drugs used in the treatment of a variety of human diseases, and nitroreduction by intestinal bacteria has been implicated in modulating the efficacy and/or toxicity of some nitroaromatic drugs.

1.2.3.2.1. Chloramphenicol

Chloramphenicol is a natural nitroaromatic compound (Figure 3) that was isolated from the culture of the soil Gram-positive bacterium *Streptomyces venezuela* as an antibacterial agent active against Gram-positive and Gram-negative bacteria (Ehrlich et al., 1947). Although effective in treatment of certain bacterial infections, the clinical utility of chloramphenicol is limited due to side effects such as neurotoxicity and hematological toxicity (Dinos et al., 2016), The mechanism of hematological toxicity is unclear, but a potential involvement of an amine metabolite of chloramphenicol (Figure 3) has been suggested based on the association of the toxicity with the oral (but not intravenous) route of chloramphenicol administration (Holt, 1967b). Commensal gut and pathogenic bacteria can reduce chloramphenicol to the amine metabolite *in vitro* (Smith and Worrel, 1950; Smith and Worrel, 1953; Onderdonk et al., 1979; Smith et al., 2007; Crofts et al., 2019); and in animal models of anaerobic infections, the anaerobic gut bacterium *Bacteroides fragilis* was shown to metabolize chloramphenicol via nitroreduction.(Onderdonk et al., 1979) Because the amine metabolite of chloramphenicol exhibits very weak, if any, antibacterial activity as compared to the parent compound (Smith et al., 2007), nitroreduction has been suggested to be one of the bacterial mechanisms for chloramphenicol resistance (Merkel and Steers, 1953b; Smith et al., 2007). This notion is supported by a recent finding that overexpression of a nitroreductase of *Hemophilus*

influenza in *E. coli* increased chloramphenicol resistance. Of note, a mutant strain with deletion of a nitroreductase has not yet been tested for susceptibility to chloramphenicol in any gut bacterial species; and the contribution of nitroreduction to intrinsic and/or inducible chloramphenicol resistance in gut bacteria is unclear (Crofts et al., 2019).

1.2.3.2.2. Nitrobenzodiazepines

Nitrobenzodiazepines (clonazepam, flunitrazepam, and nitrazepam) are sedative-hypnotic drugs that are widely used to treat sleeping disorders and relieve anxiety-related symptoms (Pinder et al., 1976; Mattila and Larni, 1980). Although safe at therapeutic doses, an accidental or intentional overdose of nitrobenzodiazepines may cause adverse effects such as reproductive and hepatic toxicities (Takeno and Sakai, 1991; Gidai et al., 2010). These toxic effects have been suggested to be due at least in part to the amino metabolites of nitrobenzodiazepines (Figure 3).

The reduction of a nitro group of nitrobenzodiazepines to an amino group has been well demonstrated to be mediated by intestinal bacteria *in vitro* and *in vivo*. For example, incubation of nitrobenzodiazepines with rat's cecal contents or individual gut bacteria *in vitro* was shown to produce the amine metabolites (Golovenko et al., 1977; Hewick and Shaw, 1978; Colburn et al., 1980; Levin and Dent, 1982; Elmer and Remmel, 1984; Robertson and Drummer, 1995; Rafii et al., 1997). In animal experiments, the levels of nitroreduction metabolites of nitrobenzodiazepines were significantly lower in germfree and antibiotic-treated rats as compared to conventional rats (Elmer and Remmel, 1984; Takeno and Sakai, 1991). The nitroreduction can also be catalyzed by host enzymes such as NADPH-cytochrome P450 reductase (Peng et al., 2004), but its contribution to total amounts of amino metabolites produced *in vivo* appears to be minimal, and the

nitroreduction by gut bacteria is suggested to be a main determinant for nitrazepam-induced teratogenicity (Takeno and Sakai, 1991).

Despite the observation that the gut bacterial conversion of nitrazepam to its amino metabolite is an essential step for the toxicity, only a few nitroreductases in gut bacteria have been identified and characterized to mediate the nitroreduction. To date, the NfsB protein of the facultative anaerobe *E. coli* and its homologous proteins (NfnB and NfsI) in closely-related enteric bacteria are the only nitroreductases experimentally shown to catalyze the nitroreduction of nitrobenzodiazepines to amino metabolites (LinWu et al., 2009a). An earlier study, however, has shown that obligate anaerobic gut bacteria such as *B. fragilis* and *C. perfringens* can catalyze the nitroreduction of nitrobenzodiazepines at rates 50-70 times higher than that by *E. coli* (Robertson and Drummer, 1995). In this respect, it is notable that four proteins have been purified from *B. fragilis* and determined to be nitroreductases (Kinouchi and Ohnishi, 1983), although they have not been tested for the nitroreduction of nitrobenzodiazepines. In *C. perfringens*, no nitroreductase(s) has been identified, but an as-yet-uncharacterized azoreductase is shown to possess nitroreductase activity.(Rafii and Cerniglia, 1993) A study also indicates the presence of other anaerobic gut bacteria *Clostridial* and *Eubacterium* species with nitroreductase activity (Rafil et al., 1991).

It is clear from these studies that major nitroreductase(s) in gut bacteria that catalyzes the nitroreduction of nitrobenzodiazepines has not yet been identified. To better understand the role of gut bacteria in modulating the adverse effects of nitrobenzodiazepines, identification of responsible nitroreductase(s) and determination of their distribution in gut bacteria will be required.
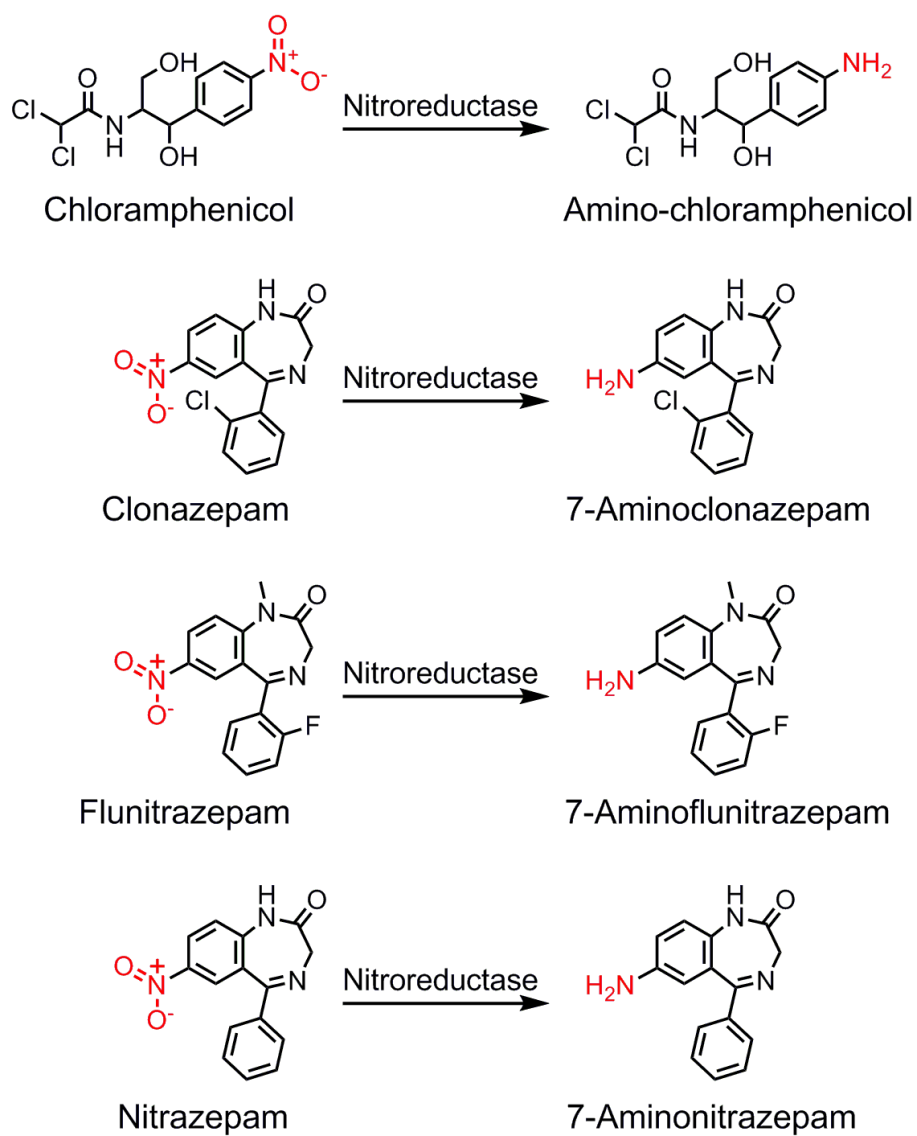
Figure 3. Nitroreduction by gut bacteria. Gut bacterial nitroreduction of chloramphenicol and nitrobenzodiazepines is shown. See text for details.

1.2.3.3. *N*-Oxide reduction

Gut microbial metabolism of xenobiotics containing N-oxide was first reported for the pyrrolizidine alkaloid heliotrine N-oxide in plant Heliotropium europaerum (Dick et al., 1963). The plant was known to cause chronic liver diseases in sheep after multiple seasons of grazing pastures. The pyrrolizidine alkaloids in the plant exist mostly as N-oxides. Considering relatively low levels of acute liver toxicity observed in sheep that grazed on the plants for only one season, potential inactivation of toxic plant compounds before intestinal absorption was postulated. The idea was tested by incubating the major alkaloid heliotrine N-oxide with sheep rumen contents, which revealed the production of an N-oxide reduction metabolite heliotrine (Figure 4). *In vivo*, heliotrine appeared to be further metabolized to 7-hydroxy-1-methylene pyrrolizidine in sheep rumen.

1.2.3.3.1. Nicotine

N-oxides can be produced from nitrogenous compounds such as nicotine by the host as oxygenated metabolites. Nicotine is converted to multiple metabolites, including nicotine N-oxide by hepatic flavin monooxygenase (Cashman et al., 1992). When nicotine N-oxide was orally administered to humans or conventional rats, significant amounts of nicotine were excreted in the urine (Beckett et al., 1970; Dajani et al., 1975c), suggesting conversion of nicotine N-oxide to nicotine *in vivo*. Interestingly, oral administration of nicotine N-oxide to germ-free rats also led to nicotine excretion into the urine (Dajani et al., 1975c), indicating the presence of host enzymes that can reduce nicotine N-oxide. Indeed, multiple microsomal and cytosolic enzymes in different tissues such as liver, small intestine, and kidney have been shown to reduce nicotine N-oxide under anaerobic

conditions (Dajani et al., 1975b). The presence of both oxygenating and reducing enzymes in the host tissues has been shown to cause "metabolic cycling" for amine drugs, through repetitive oxidations/reductions that potentially extend the residence time of drugs in the body (Ziegler, 1988). The potential contribution of gut bacterial N-oxide reduction to metabolic cycling and residence time for N-oxide forming drugs is underexplored.

1.2.3.3.2. Loperamide

Loperamide is an antidiarrheal agent that activates the opioid receptor in the large intestine (Stanciu and Gnanasegaram, 2017). Considering that N-oxide metabolites are more hydrophilic (i.e., less likely to be absorbed in the small intestine), loperamide N-oxide was developed as a colon-targeting pro-drug of loperamide, as well as to limit systemic availability and occasional central nerve side effects of loperamide. After oral administration of loperamide N-oxide to dogs, the pro-drug was converted through reduction to loperamide, exhibiting significant loperamide plasma exposure (~50% of exposure observed after administering an equal oral dose of loperamide itself) (Lavrijsen et al., 1995b). Furthermore, the mass balance of the metabolites, as well as the excretion pattern, were similar to those obtained after the oral dose of loperamide, indicating almost complete conversion of loperamide N-oxide to loperamide in the body. Incubation of the pro-drug with small intestinal or cecal contents of rats and dogs revealed significant N-oxide reductase activities in gut microbiota. The N-oxide reductase activity was heat- and oxygen-sensitive (i.e., >95% and ~90% drops in activities upon boiling or air exposure of gut contents). Interestingly, a significant amount of loperamide N-oxide was also reduced by small intestinal contents of germ-free rats under anaerobic conditions, suggesting potential non-enzymatic N-oxide reduction and/or involvement of host enzymes.

Consistently several host enzymes such as cytochrome P450s and xanthine oxidase were shown to mediate N-oxide reduction (Damani, 1991; Kitamura et al., 1999). However, the gut microbial enzymes catalyzing N-oxide reduction of loperamide N-oxide remain to be identified.

1.2.3.3.3. Ranitidine

Ranitidine is a histamine H2-receptor antagonist that is used to decrease gastric secretion and for treating gastrointestinal ulcers (Morgan and Ahlawat, 2019). In earlier pharmacokinetic studies of orally administered ranitidine, apparent "second peak" on concentration vs. time profile was observed for the majority of subjects (i.e., the first and second peak concentrations at 0.5-1.5 and 3-4 h after an oral dose) (Woodings et al., 1980). A similar phenomenon was also found for cimetidine, another H2-receptor antagonist developed and marketed before ranitidine (Bodemar et al., 1979). Considering minimal enterohepatic recycling of these drugs (Klotz and Walker, 1990), it was postulated that discontinuous intestinal absorption of these drugs along the gastrointestinal tract might explain the second peak. To determine the origin of the second peak, ranitidine was injected directly into the stomach, jejunum, or cecum via a nasoenteric tube in healthy volunteers, and blood samples were collected for drug analysis (Williams et al., 1992). There was no difference in pharmacokinetic parameters or the presence of second peaks between gastric and jejunal dosing. On the other hand, ranitidine exposure after cecal administration was less than 15% of that after gastric or jejunal administration, suggesting that absorption windows for ranitidine may be located between jejunum and cecum. While the reason for the second-peak phenomenon remained unclear, the low bioavailability after cecal administration raised the possibility of colonic ranitidine metabolism. Indeed,

incubation of ranitidine with human feces revealed extensive disappearance of the drug over time, which was saturated at high drug concentrations (Basit and Lacey, 2001). The major metabolite was identified as a product of oxygen loss at the diaminonitroalkene moiety and proposed to be an N-oxide reduction product of ranitidine tautomer. Similar metabolism by gut microbiota was observed for nizatidine, an H2-receptor antagonist that shares the same structural moiety of diaminonitroalkene as ranitidine, but not for cimetidine and famotidine that do not have the chemical moiety (Basit et al., 2002). Of note, the N-oxide reduction metabolites of ranitidine and nizatidine have not been identified in the systemic circulation, suggesting that the contribution of the metabolic pathway to overall ranitidine disposition may be minor. The clinical significance of ranitidine metabolism by gut microbiota remains to be determined.
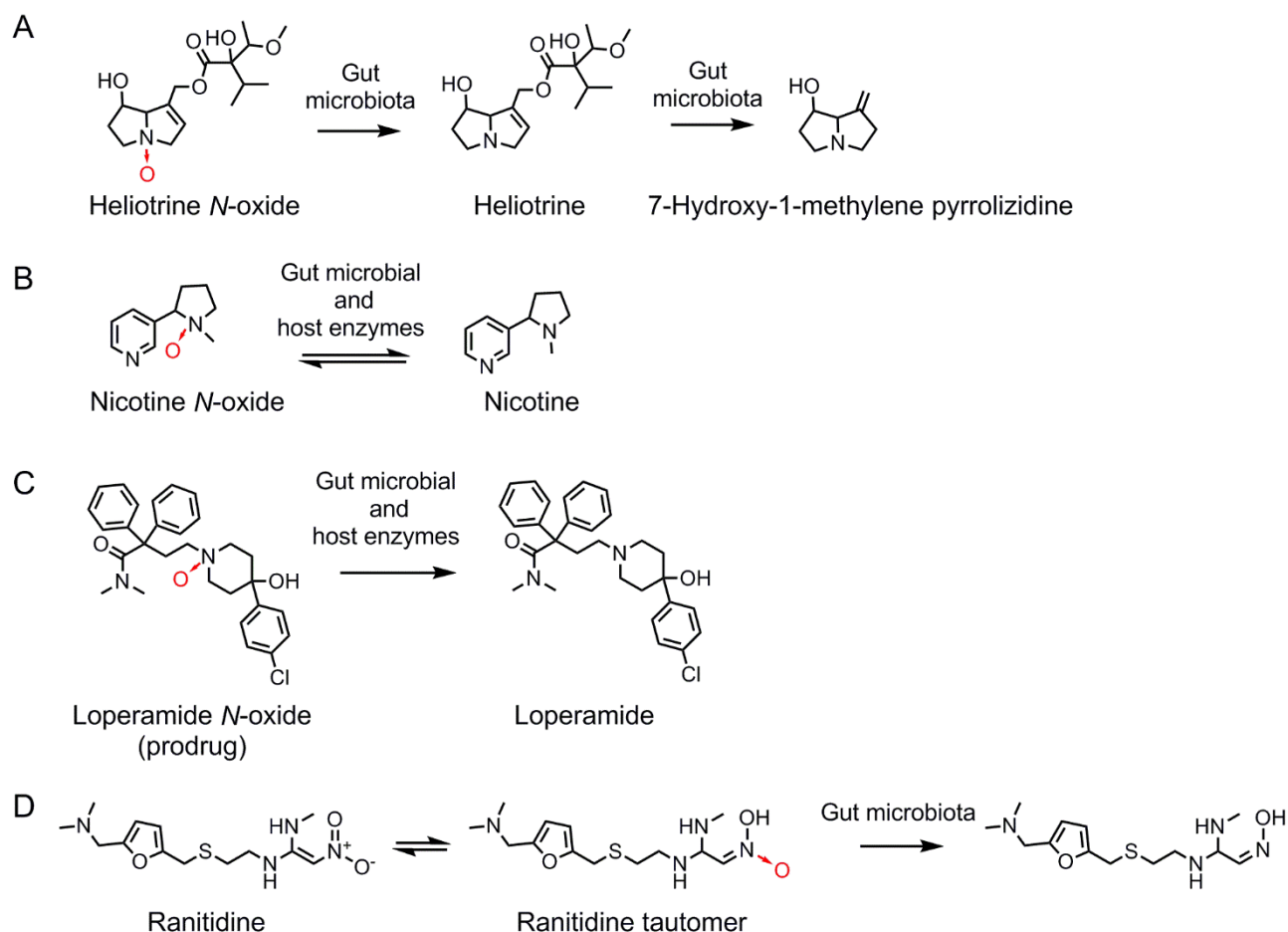
Figure 4. N-oxide reduction by gut contents. A plant alkaloid heliotrine N-oxide (A) and drugs (B-D) that potentially undergo N-oxide reduction by gut contents are shown. See text for details.

1.2.3.4. Alkene reduction

Alkene reduction by gut microbiota was best characterized through studies of cinnamic acid derivatives (Figure 5), common components in diet (Perez-Silva et al., 1966; Scheline, 1968; Scheline and Midtvedt, 1970). Dehydrogenation of cinnamic acid derivatives such as caffeic acid was shown to occur specifically in the gut microbiota community; antibiotic (neomycin) pre-treatment or germ-free condition significantly

decreased or abrogated urinary excretion of dehydrogenated products in rats (Perez-Silva et al., 1966; Scheline and Midtvedt, 1970). The reaction was mediated by several bacteria *Pseudomonas sp.*, *Lactobacillus sp.*, and *Clostridium sp.* isolated from rat feces or cecal contents(Perez-Silva et al., 1966; Soleim and Scheline, 1972), as well as *Clostridium sporogenes* (Dodd et al., 2017). An enzyme, acyl-CoA dehydrogenase mapped to a conserved gene cluster for the reductive metabolism of aromatic amino acids, was shown to catalyze the reaction in *C. sporogenes* (Dodd et al., 2017), suggesting the involvement of a gut bacterial metabolic pathway in the reductive metabolism of cinnamic acid derivatives.

1.2.3.4.1. Deleobuvir

Deleobuvir (Figure 5) is an NS5B RNA polymerase inhibitor used for the treatment of hepatitis C virus infection (Cheng et al., 2014). A study using radio-labeled deleobuvir in healthy volunteers revealed that the maximum plasma concentration of deleobuvir is reached at 3.5-5 h after oral administration (Chen et al., 2015). The alkene reduction product (CD 6168, 10-fold lower antiviral activity than deleobuvir) and acyl glucuronide conjugate of deleobuvir were shown to be two major circulating metabolites, representing ~15% and ~20% of the total radioactivity in the blood, respectively. Excretion into feces was the major route of elimination such that >95% of the dose was found in the fecal samples after the oral dose, and CD 6168 and its hydroxylated metabolites in the fecal samples accounted for a major portion of the dose (~60%). On the other hand, the amount of CD 6168 excreted into bile was minimal (less than 3% of the dose) in rats (McCabe et al., 2015), suggesting that CD 6168 may be produced mainly in the gastrointestinal tract. The *in vitro* incubation of deleobuvir with rat or human fecal samples (but not with human

liver tissue homogenates) resulted in CD 6168 production, indicating that CD 6168 is a gut microbial metabolite of deleobuvir (McCabe et al., 2015). Consistently, in rats pretreated with antibiotics (streptomycin and neomycin), the plasma exposure of CD 6168 decreased 9-fold as compared to control rats after oral administration of deleobuvir. In the antibiotic-treated rats, most of the deleobuvir dose was found in feces as unmodified while only 26% of the dose was found as the parent drug in the control group, further suggesting the role of gut bacteria in determining the disposition of deleobuvir and its metabolites. To better define potential interactions of deleobuvir with other drugs, the gut bacterial enzymes responsible for the alkene reduction of deleobuvir will need to be identified and their distribution in gut bacteria determined.

1.2.3.4.2. Digoxin

Digoxin (Figure 5) is a cardiac glycoside that has been used to treat heart failure and atrial fibrillation for over 200 years (Ehle et al., 2011). Digoxin is poorly water-soluble and its oral bioavailability varies among different individuals, ranging from 50% to 90% (Winter, 2004). Digoxin has a narrow therapeutic window (0.6 to 1.2 nM); supra-therapeutic concentrations may cause fatal cardiac arrhythmia (Smith and Haber, 1970; Vamos et al., 2015).

In the late 1960s, Luchi et al. reported a case of a patient who required an unusually high dose of digoxin (to control atrial fibrillation) which was accompanied by the presence of a large quantity of dihydrodigoxin, a ~20-fold less active metabolite of digoxin, in the urine (Luchi and Gruber, 1968). Later studies demonstrated large inter-individual variations in the extent of urinary excretion of dihydrodigoxin (Clark and Kalman, 1974; Peters et al., 1978). For example, in 100 patients receiving digoxin, the fraction of

dihydrodigoxin in the lipid-extractable cardiac glycosides in the urine ranged from 2% to 52%, and the fraction was greater than 30% in ~10% of the patients (Peters et al., 1978). The urinary excretion of dihydrodigoxin exhibited an inverse relationship with digoxin bioavailability; it is greatest after a poorly absorbed tablet was ingested, and least after intravenous administration, suggesting that colonic gut microbiota is involved in dihydrodigoxin formation. Indeed, incubation of digoxin with stool samples from dihydrodigoxin "excretors" (i.e., subjects who excreted >15% dihydrodigoxin in the urine) showed the production of dihydrodigoxin, whereas the same metabolite was not observed upon incubation with non-excretor's stool samples.(Lindenbaum et al., 1981) Furthermore, the administration of antibiotics (e.g., erythromycin, tetracycline, or clarithromycin) virtually eliminated the urinary excretion of dihydrodigoxin, with a concomitant (up to 4-fold) increase in serum digoxin concentrations (Lindenbaum et al., 1981; Hirata et al., 2005).

Growth of human fecal bacteria in digoxin-containing media led to the identification of the gut *Actinobacterium Eggerthella lenta*, which mediates digoxin reduction to dihydrodigoxin but exhibits strain-level differences (Saha et al., 1983a). For example, 18 out of 28 *E. lenta* strains tested were able to produce dihydrodigoxin *in vitro*. Interestingly, the fecal abundance of dihydrodigoxin-forming *E. lenta* was found to be similar between excretors and non-excretors, indicating that the mere presence of the bacterium in the gut does not account for dihydrodigoxin production in an individual. Arginine, which is known to stimulate *E. lenta* growth, was found to repress dihydrodigoxin formation in the bacterium, explaining the discrepancy above and suggesting that diet is a critical modulator of dihydrodigoxin production by *E. lenta* (Saha et al., 1983a). Using gene expression profiling, Haiser et al. found the expression of a gene, named cardiac

glycoside reductase (*cgr*), is upregulated in the presence of digoxin in dihydrodigoxin-producing *E. lenta* (Haiser et al., 2013a). The *cgr* gene was present only in *E. lenta* strains capable of catalyzing dihydrodigoxin formation, and the fecal abundance of *cgr* was higher in individuals highly producing dihydrodigoxin (as compared to low producers) (Haiser et al., 2013a). Furthermore, arginine repressed *cgr* expression in *E. lenta in vitro*; and in gnotobiotic mice mono-colonized with *E. lenta* and fed protein-rich diet, digoxin concentrations in serum significantly increased, further demonstrating the role of *E. lenta* in determining digoxin exposure.

The *cgr* locus is a two-gene operon (*cgr*1 and *cgr*2), and heterologous expression of *cgr*2 in another Actinobacterium *Rhodococcus erythropolis* L88, which cannot mediate digoxin reduction, is sufficient for digoxin reduction (Koppel et al., 2018). The *Cgr2* protein was found to be an oxygen-sensitive flavin- and [4Fe-4S] cluster-dependent reductase with narrow substrate specificity for cardenolides (including digoxin). The *cgr2* gene was detected in over 70% of fecal samples collected from >150 individuals, and a significant correlation was observed between fecal *cgr2* and *E. lenta* abundances (rho = 0.725). While *cgr2* was highly conserved among *E. lenta* strains carrying it, a naturally occurring genetic polymorphism (Y333N) was found to account for decreased digoxin reduction. As a result, these studies identify the *cgr2* gene and demonstrate the role of *cgr2* in digoxin reduction to dihydrodigoxin in *E. lenta*. In general, these studies illustrate multiple layers of factors modulating drug metabolism by gut microbiota, namely gut bacterial composition, bacterial gene regulation, strain-level genome variations, genetic polymorphisms, the nutritional milieu in the gut, and diet (Haiser et al., 2013a; Koppel et al., 2018).
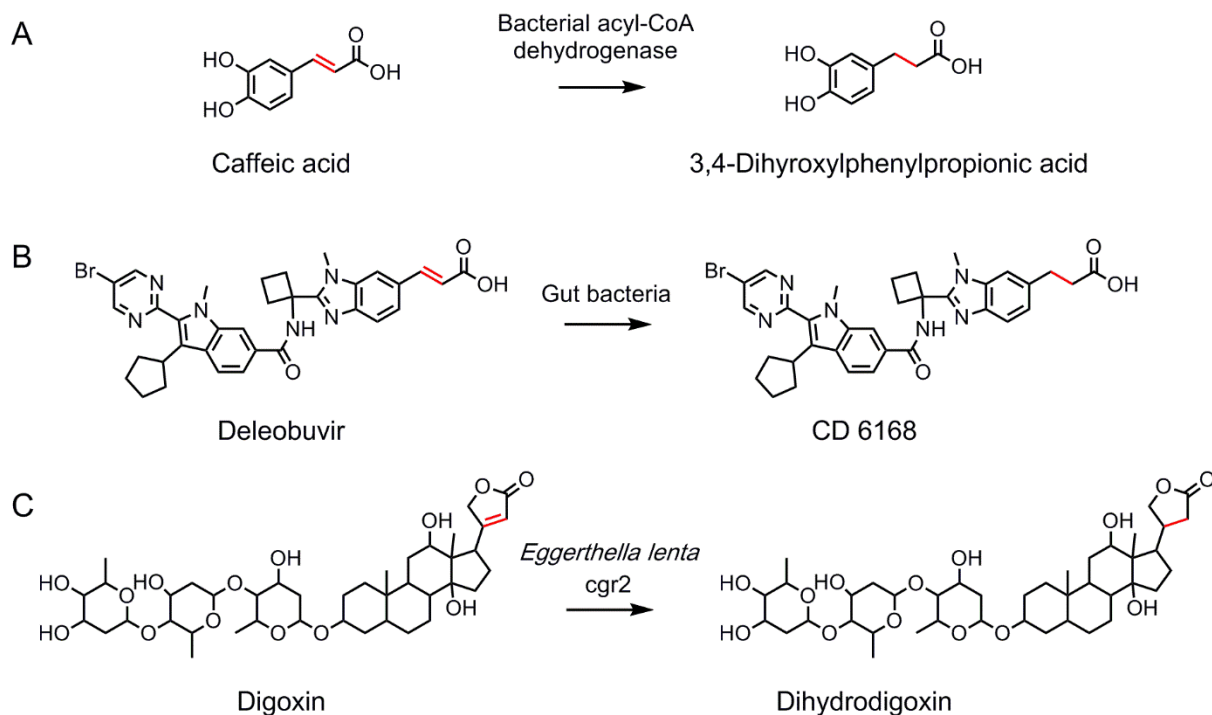
Figure 5. Alkene reduction by gut bacteria. Gut alkene reduction of dietary compound caffeic acid (A) and drugs including deleobuvir (B) and digoxin (C) is shown. See text for details.

1.2.3.5. Ketone reduction

The conversion of carbonyl groups to alcohol by host enzymes including carbonyl reductases (CBRs) and aldo-keto reductases (ABRs) has been relatively well characterized (Hoffmann and Maser, 2007; Barski et al., 2008). However, gut bacterial enzymes functionally equivalent to the host CBRs and ABRs are underexplored, and only a few examples of the keto-reduction of drugs by gut bacteria have been reported.

1.2.3.5.1. Nabumetone

Nabumetone (Figure 6) is a non-steroidal anti-inflammatory drug used for the management of arthritis and rheumatoid diseases to reduce pain and inflammation (Hedner et al., 2004). Orally administered nabumetone is completely metabolized with minimal detection of the parent drug in the blood (Hedner et al., 2004). The major circulating nabumetone metabolite (accounting for ~35% of the dose) is the pharmacologically active 6-methoxy-2-naphtylacetic acid (6-MNA) whose formation is catalyzed by hepatic cytochrome P450 (CYP) 1A2 (Turpeinen et al., 2009). In rats treated with the broad-spectrum antibiotic imipenem, the plasma exposure of 6-MNA was not significantly altered, suggesting that the extent of gut microbiota-mediated elimination of nabumetone is minimal. Earlier studies have also found a minor pharmacologically inactive metabolite [4-(6-methoxy-2-naphthyl)-butan-2-ol], which is produced by the keto-reduction of nabumetone and is present in the urine samples at a low amount (~1% of total nabumetone metabolites excreted into the urine).(Davies, 1997) Microsomal and cytosolic fractions of human livers, as well as host CBRs and AKRs, were shown to produce the keto-reduction metabolite (Skarydova et al., 2013). In a recent study, gut bacteria such as *E. coli* were also shown to mediate the keto-reduction of nabumetone under aerobic and anaerobic conditions *in vitro* (Jourova et al., 2019). However, the significance of this gut bacterial metabolism in nabumetone exposure is unclear.

1.2.3.5.2. Doxorubicin

Doxorubicin (Figure 6) is an anticancer agent that belongs to anthracycline antibiotics. Anthracyclines inhibit cancer cell growth via multiple mechanisms, including DNA cross-linking and free radial formation (Gewirtz, 1999). Doxorubicin is administered

intravenously and about half of the dose is eliminated into feces after biliary excretion (Speth et al., 1988). The major circulating metabolite is doxorubicinol, the C7-reduction product of doxorubicin, produced by host CBRs and AKRs (Jacquet et al., 1990; Piska et al., 2017). Doxorubicinol is less cytotoxic than the parent drug, but it inhibits the calcium pump at cardiac muscle sarcoplasmic reticulum, potentially responsible for dose-limiting cardiotoxicity of doxorubicin (Olson et al., 1988; Piska et al., 2017). Considering significant biliary excretion of doxorubicin, a screen for gut bacteria that may inactivate doxorubicin was conducted and identified the gut bacterium *Raoultella planticola*. This bacterium deglycosylates doxorubicin and produces 7-deoxydoxorubicinone, which is further metabolized to 7-deoxydoxorubicinol via keto-reduction (Yan et al., 2018). Further, by screening a collection of *E. coli* defined mutants, authors have identified a group of mutants inactivated for genes encoding molybdoenzymes. An earlier study has reported that the liver can convert doxorubicin to 7-deoxydoxorubicinol, as demonstrated in the isolated perfused rat liver (Ballet et al., 1987). The extent to which gut bacterial enzymes contribute to the overall keto-reductive metabolism of doxorubicin *in vivo* remains to be determined.

1.2.3.5.3. α-keto amides

The α-keto amide structure is a key frame of many biological active compounds with wide therapeutic applications in treating cancer, viral infection and inhibiting immune system (Muthukumar et al., 2018). One of the noteworthy features of α-keto amides is the presence of electrophilic carbonyl center that exhibits a strong electron withdrawing functionality. This makes α-keto amide much more reactive than a common carbonyl system. Representative drugs include tacrolimus, isatin, telaprevir, boceprevir and

plitidepsin (Figure 6C). Among these compounds, isatin is the most well studied for metabolism by microorganisms. Isatin was incubated with extract of sewage sludge anaerobically, followed by extraction using ethyl-acetate and separation by thin layer chromatography. The subsequent LC-MS and NMR analysis showed the formation of dioxindole, indicating a reduction reaction (Madsen and Bollag, 1988). Willian et al. identified multiple marine-derived fungi, including *Cladosporium sp. CBMAI 1237*, *Westerdykella sp. CBMAI 1679* and *Aspergillus sydowii CBMAI 935*, are capable of converting insatin to dioxindole, with a conversion from 2% to 89% after seven days' incubation (Birolli et al., 2017). Kohji et al. reported the same metabolism can also be catalyzed by yeast *Saccharomyces cerevisiae*. And an NADPH-dependent α-keto amide reductase with a mass of 36 kDa was identified as the metabolizing enzyme (Ishihara et al., 2004). They further examined the substrate specificity of this enzyme and found that it can metabolize many α-keto amides and α-keto esters but not substrates with β-keto esters or a single carbonyl group. Although bacterial metabolism of α-keto amide and bacterial α-keto amide reductase has not been discovered yet, dioxindole was found in human urine, suggesting a potential role of bacteria in reducing endogenous isatin and potentially other α-keto amides such as tacrolimus (Usami et al., 2001).
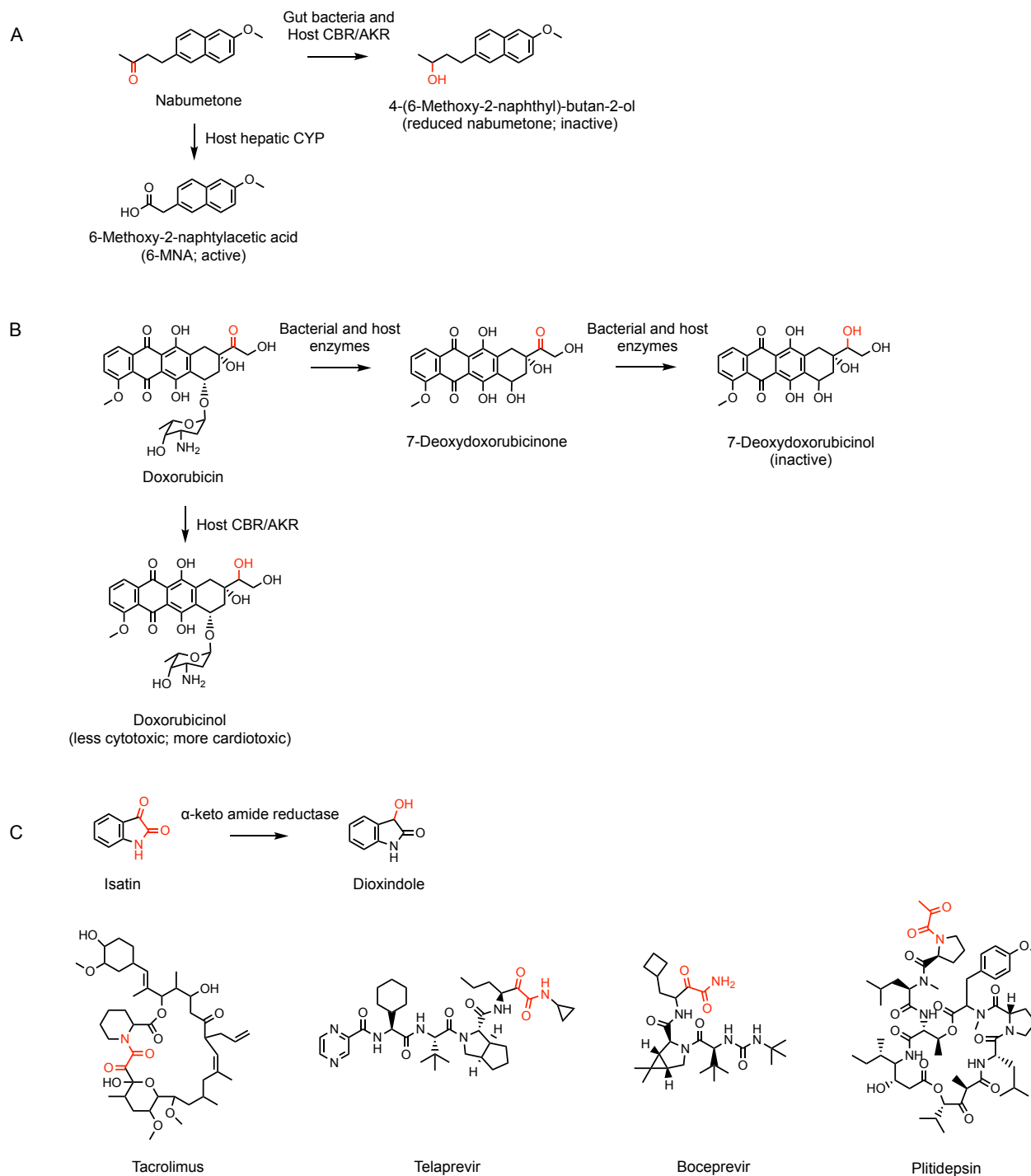
Figure 6. Keto-reduction by gut bacteria. Keto-reduction of nabumetone (A) and doxorubicin (B) is mediated by gut bacteria as well as host enzymes. CBR, carbonyl reductases; ABR, aldo-keto reductases (C) α-keto amides

1.2.3.6. Sulfoxide reduction

Gut bacterial reduction of the sulfoxide group was most extensively studied for sulphinpyrazone and sulindac (Figure 7). Gut bacterial metabolism of other compounds containing sulfoxide group such as the proton pump inhibitor omeprazole (Figure 7C) in the colon has also been reported (Watanabe et al., 1995); aerobic incubation of omeprazole with rat cecal or colonic contents led to ~50% decrease in amounts within 30 min. However, based on the large body of supporting evidence, our discussion of gut bacteria-mediated sulfoxide reduction will be focused on sulindac and sulphinpyrazone.

1.2.3.6.1. Sulindac

Sulindac (Figure 7A) is a non-steroidal anti-inflammatory drug used to treat inflammatory diseases such as rheumatoid arthritis and osteoarthritis (Duggan, 1981). Mass balance studies using radiolabeled sulindac in humans have demonstrated that sulindac is extensively and rapidly absorbed after oral administration; ~90% of the dose is absorbed with the maximum plasma concentration reached within one hour (Duggan et al., 1977a). Sulindac metabolites, sulindac sulfone (called "SSone" hereafter) and sulindac sulfide (called "SSide" hereafter) (Figure 7A), appear in the systemic circulation, providing similar plasma exposures as that of the parent drug sulindac. Upon intra-articular injection into the inflamed synovial fluid space, SSide was shown to be >60-fold more active as an anti-inflammatory agent than sulindac whereas SSone is inactive (Duggan et al., 1977b). After ingestion, sulindac (but not SSide) undergoes significant enterohepatic recycling as unmodified or conjugated form (acyl glucuronide), exhibiting prominent double peaks on plasma concentration vs. time profiles (Duggan et al., 1977a;

Dobrinska et al., 1983). Interestingly, cumulative recovery analysis found significant amounts of SSide but not the parent drug in human fecal samples, raising the possibility that sulindac may be converted to SSide in the gut. Consistent with this idea, when sulindac was incubated *in vitro* with rat cecal contents or human fecal samples, it was rapidly and completely converted to SSide (Duggan et al., 1977a).

In addition to putative gut microbial enzymes, host enzymes also appear to catalyze the reduction of sulindac to SSide. After intravenous administration of sulindac or SSide in rats, sulindac was readily converted to SSide or vice versa in the body (Duggan et al., 1977b). Animal tissue samples, including hepatic microsomes, mitochondria, and cytosol fractions, were shown to convert sulindac to SSide under aerobic and anaerobic conditions (Kitamura et al., 1980; Tatsumi et al., 1983; Etienne et al., 2003). Consistent with these *in vitro* results, both patients with ileostomies (where the colon is bypassed in drug elimination process into feces) and healthy control groups exhibited similar plasma exposures to SSide up to 12 h after oral administration of sulindac (Strong et al., 1985). On the other hand, SSide exposure after 12 h (which constitutes 55% of the total AUC in healthy subjects) decreased drastically in the ileostomy patients, suggesting that about half of the circulating SSide originates from the colonic metabolism of sulindac in healthy individuals. Supportive of the notion, incubation of sulindac with ileostomy effluent showed negligible SSide production, whereas extensive Sside formation was observed when sulindac was incubated with the fecal samples of healthy subjects (Strong et al., 1985).

Reactive nitrogen or oxygen species can cause chemical modifications of biological molecules. For example, the oxidation of the amino acid methionine produces methionine sulfoxides with altered biological activities (Moskovitz et al., 1998; Achilli et al.,

2015). Most, if not all, eukaryotic and prokaryotic cells have methionine sulfoxide reductases that can reduce proteinous methionine sulfoxide residues back to methionine in a thioredoxin-dependent manner. Methionine sulfoxide reductases, MsrA in *E. coli* and MsrB1 in the rat liver, were also shown to catalyze sulindac reduction to SSide under aerobic conditions (Etienne et al., 2003; Brunell et al., 2011). On the other hand, microsomal enzymes such as flavin-containing monooxygenases in the human liver and kidney catalyzed the oxidation of SSide back to sulindac (Hamman et al., 2000), and hepatic CYP P450 enzymes further oxidized sulindac to SSone (Brunell et al., 2011). These findings suggest that multiple host enzymes and (putative) gut bacterial enzymes govern the extent of host exposure to bioactive SSide.

1.2.3.6.2. Sulphinpyrazone

Sulphinpyrazone (Figure 7B) is a uricosuric and anti-platelet agent (Margulies et al., 1980). The major circulating metabolites of sulphinpyrazone after oral administration are sulphinpyrazone sulfide and sulfone (Figure 7B), which represent 13% and 6% of total sulphinpyrazone metabolites, respectively. Similar to sulindac, the sulfide metabolite of sulphinpyrazone appears to be produced mainly by gut bacteria and exhibits more potent anti-platelet activity than the parent drug. However, unlike sulindac that is also reduced to sulindac sulfide by host enzymes, sulphinpyrazone does not appear to be the substrate of host enzymes (Dieterle et al., 1980; Wallis, 1983). Anaerobic incubation of sulphinpyrazone with rat or rabbit liver and kidney homogenates showed minimal production of the sulfide metabolite (Renwick et al., 1982b; Strong et al., 1984). Furthermore, after oral administration of sulphinpyrazone, the sulfide metabolite was not detected in the blood and cecal contents of germ-free rats or rats treated with a cocktail

of antibiotics (bacitracin, neomycin, and tetracycline) (Renwick et al., 1982b). In addition to the difference between sulindac and sulphinpyrazone as being the substrates of host enzymes, gut bacteria and their enzymes for catalyzing sulphinpyrazone and sulindac reduction appear to differ. When sulphinpyrazone or sulindac was incubated anaerobically with one of over 200 bacterial strains isolated from human feces, sulphinpyrazone sulfide production was observed mainly with aerobic bacteria, whereas sulindac sulfide production was observed with both anaerobic and aerobic bacteria (Strong et al., 1987). Sulphinpyrazone is discontinued from the US market due to its renal side effects and unfavorable pharmacological interactions with other drugs (Strilchuk et al., 2019). However, a large body of information available on sulphinpyrazone reduction to the sulfide metabolite provides a rare opportunity to investigate and compare different substrates that are also subjected to sulfoxide reduction by gut bacteria.
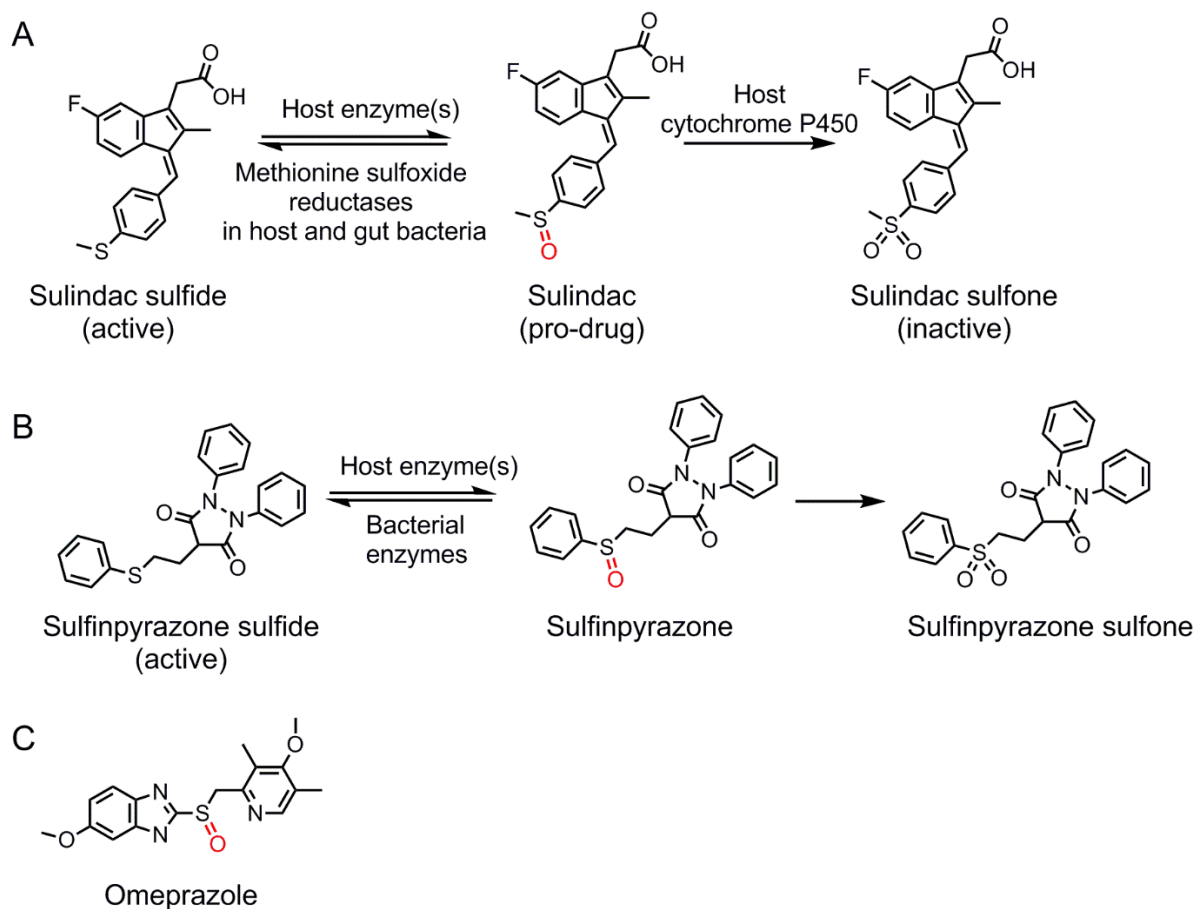
Figure 7. Sulfoxide reduction by gut bacteria. Sulindac (A) and sulfinpyrazone (B) are known to undergo sulfoxide reduction by gut bacteria as well as host enzymes. Omeprazole (C) is a potential substrate of bacterial sulfoxide reductase. See text for details.

1.3. Summary and research aims

Previous studies reveal the complexity of tacrolimus disposition, and the currently known contributing factors, including CYP3A4/5 metabolism and P-gp mediated efflux, cannot fully explain extensive gut extraction and low oral exposure. Lack of knowledge of other factors constitutes a substantial gap in optimizing tacrolimus dosage regimen and improving graft outcomes in transplant recipients.

Xenobiotic metabolism by gut microbiota has been reported over decades and supported by a large body of evidence encompassing drugs in diverse chemical classes and therapeutic areas. In this thesis research, we aimed to study the role of gut microbiota in tacrolimus disposition. Our central hypothesis is that gut bacteria metabolize tacrolimus and decrease systemic drug exposure. Specifically, I will (1) characterize bacterial metabolism of tacrolimus and its impact on tacrolimus disposition, (2) identify and characterize bacterial tacrolimus metabolite, and (3) identify tacrolimus metabolizing enzymes in gut bacteria.

CHAPTER 2. THE ROLE OF GUT BACTERIA IN TACROLIMUS DISPOSITION

Part of this chapter was previously published as

[1] Guo, Y., Crnkovic, C. M., Won, K. J., Yang, X., Lee, J. R., Orjala, J., ... & Jeong, H. (2019). Commensal gut bacteria convert the immunosuppressant tacrolimus to less potent metabolites. Drug Metabolism and Disposition, 47(3), 194-202.

[2] Guo, Y., Lee, H., Edusei, E., Albakry, S., Jeong, H., & Lee, J. R. (2020). Blood Profiles of Gut Bacterial Tacrolimus Metabolite in Kidney Transplant Recipients. Transplantation Direct, 6(10).

2.1. Introduction

Tacrolimus is a commonly used immunosuppressant for kidney transplant recipients as well as patients with glomerular diseases like membranous nephropathy and focal segmental glomerulosclerosis. However, due to its narrow therapeutic index, under-exposure or over-exposure to tacrolimus in kidney transplant recipients increases the risks for graft rejection or drug-related toxicity, respectively (Staatz and Tett, 2004). Maintaining therapeutic blood concentrations of tacrolimus has been difficult in part because its low and variable bioavailability, exhibiting an average of 25% (ranges from 5 to 93% (Staatz and Tett, 2004). And the major reason is due to a significant drug loss in the gut after oral drug administration, which was reported as 85% and 74% in healthy and liver transplant patients, respectively (Jusko et al., 1995; Hebert et al., 1999). Tacrolimus is highly cell permeable and being completely absorbed in human, which was

demonstrated by *in vitro* Caco-2 study and negligible parent drug recovery (i.e., 0.5%) from stool (Moller et al., 1999; Gertz et al., 2010). Thus, the significant drug loss is likely due to extensive gut metabolism. However, inhibiting known tacrolimus disposition enzymes including CYP3A4/5 and P-glycoprotein by co-administration of ketoconazole orally did not fully prevent drug loss, more than 50% of tacrolimus still did not reach the systemic circulation (Floren et al., 1997; Tuteja et al., 2001). This suggest other contributing factors are yet to be well defined. A better understanding of the factors responsible for the variability is crucial for maintaining target therapeutic concentrations of tacrolimus and improving kidney transplant outcomes.

The human gut is home to over trillions of microbes that can influence multiple aspects of host physiology (Schroeder and Backhed, 2016). In particular, intestinal bacteria can mediate diverse chemical reactions such as hydrolysis and reduction of orally administered drugs, ultimately affecting the efficacy and/or toxicity of drugs (Wallace et al., 2010; Haiser et al., 2013; Koppel et al., 2017). For example, digoxin is converted to the pharmacologically inactive metabolite, dihydrodigoxin, by the gut bacterium *E. lenta* (Haiser et al., 2013). However, for most clinically used drugs, the detailed roles of gut bacteria in their metabolism and/or disposition remain unknown.

F. prausnitzii is one of the most abundant human gut bacteria (10^8-10^9 16S rRNA gene copies/g mucosal tissue in ileum and colon), taxonomically belonging to the Clostridiales order (Qin et al., 2010; Arumugam et al., 2011). Because of its anti-inflammatory effects, *F. prausnitzii* has been investigated as a potential preventative and/or therapeutic agent for dysbiosis (Miquel et al., 2015; Rossi et al., 2016). We have recently shown that in 19 kidney transplant patients, fecal *F. prausnitzii* abundance positively correlates with oral tacrolimus doses required to maintain therapeutic blood

concentrations, independent of gender and body weight (Lee et al., 2015). It remains unknown, however, whether *F. prausnitzii* is directly involved in tacrolimus elimination in the gut. Herein, we tested a hypothesis that gut bacteria, including *F. prausnitzii*, metabolize tacrolimus and decrease drug exposure.

2.2. Methods

2.2.1. Bacterial strains and growth

F. prausnitzii A2-165 was obtained from DSMZ (Deutsche Sammlung von Mikroorganismen und Zellkulturen GmbH). *F. prausnitzii* VPI C13-20-A (ATCC 27766), and *F. prausnitzii* VPI C13-51 (ATCC 27768) were from American Type Culture Collection (ATCC). Other gut bacteria were from Biodefense and Emerging Infections (BEI) Research Resources Repository. Unless stated otherwise, all the bacterial strains were grown anaerobically (5% H_2, 5% CO_2, 90% N_2) on YCFA agar or broth at 37ºC in an anaerobic chamber (Anaerobe Systems, Morgan Hill, CA), and colonies from the agar plate were inoculated into pre-reduced YCFA broth for preparation of overnight cultures. Optical density at 600 nm (OD_{600}) was measured for estimation of bacterial concentration.

2.2.2. Tacrolimus metabolism by gut bacteria

To examine tacrolimus metabolism by gut bacteria, cells of a bacterial strain grown as described above were incubated with tacrolimus. Typically, tacrolimus (100 µg/ml) was incubated with bacterial cells in the anaerobic chamber at 37ºC for 24-48 h. Reaction was terminated by adding the same volume of ice-cold acetonitrile. After vortexing for 30 sec, samples were centrifuged at 16,100×g for 10 min, and the supernatant was collected for HPLC/UV analysis as described below.

2.2.3. M1 detection

The reaction mixture was analyzed by using HPLC (Waters 2695) coupled with a UV detector (Waters 2487). Typically, 50 µl of a sample was injected and resolved on a C8 column (Eclipse XDB-C8;4.6 x 250 nm; 5 µm) using water (0.02 M KH_2PO_4, pH 3.5; solvent A) and acetonitrile (solvent B) as mobile phase with the following gradient: 0-12 min (50% B), 12-17 min (50%-70% B), 17-23 min (70% B), 24-30 min (90% B), and 30-40 min (50% B). Eluates were monitored at 210 nm.

For further verification of M1 production by gut bacteria, the supernatant was also analyzed by HPLC tandem mass spectrometry (HPLC/MS/MS), Agilent 1200 HPLC interfaced with Applied Biosystems Qtrap 3200 using an electrospray ion source. The mobile phase consisted of water with 0.1% formic acid and 0.1% ammonium formate (v/v; solvent A) and MeOH (solvent B), and the following gradient was used: 0-2 min (40% B), 2-6 min (95% B), and 6-12 min (40% B). The separation was performed on an Xterra MS C18 (2.1 x 50mm, 3.5 µm; Waters) column at a flow rate of 0.3 ml/min, and M1 was detected at m/z 828.5/463.5 in the multiple reaction monitoring mode.

2.2.4. Healthy volunteers' stool samples

Fresh stool samples from healthy adults (100 mg wet weight/ml) were suspended in pre-reduced PBS. After centrifuge at 500 g for 5 min, the supernatant containing stool bacteria was incubated with tacrolimus (100 µg/ml) anaerobically for 48 h at 37°C. As controls, the stool samples were boiled for 10 min and then incubated with tacrolimus. The incubation mixtures were analyzed by HPLC/UV as described above. The study

protocol for human stool sample collection was approved by the Institutional Review Board at the University of Illinois at Chicago (protocol number 2018-0810).

2.2.5. Purification of the metabolite M1

F. prausnitzii cells were harvested from 1 L of an overnight culture grown in YCFA media and resuspended in 500 ml PBS containing 50 mg of tacrolimus. After anaerobic incubation at 37°C for 4 days, cells were removed by centrifugation and supernatant was collected. The supernatant was extracted twice each with 500 ml of ethyl acetate. The upper organic layer was collected and evaporated using a rotary evaporator. Dried extracts were then dissolved in 1 ml of MeOH and loaded on SPE column (HyperSep™ C18 Cartridges 5000 mg; Cat: 60108-702). The column was washed by 40 ml water, 40 ml 30% ACN / 70% water, and followed by sample elution using 100% ACN. After evaporation, dried extracts were then dissolved in 800 µl of MeOH and the metabolite M1 was purified using a semi-preparative HPLC coupled with PDA detector (Waters 996) and equipped with a Microsorb 60-C8 Dynamax column (Agilent- R00083311C; 250 x 10 mm). The mobile phase consisted of water (solvent A) and acetonitrile (solvent B), and the following gradient was used: 0-12 min (60% B), 12-17 min (60%-70% B), 17-23 min (70% B), 23-25 min (70%-100% B), 25-35 min (100% B), 35-40 min (100%-60% B), and 40-50% min (60% B). A peak at 19.5 min corresponding to M1 was collected, dried, and subjected to structure determination.

2.2.6. Mass spectrometry (MS) for M1 identification

Experiments were performed on a Shimadzu ultra performance liquid chromatography mass spectrometry (UPLCMS)-IT-TOF. Samples were run on a C18

column (Phenomenex Kinetex; 50 × 2.1 mm; 1.7 µm) at a flow rate of 0.5 ml/min with water/0.1% formic acid (solvent A) and acetonitrile/0.1% formic acid (solvent B) as mobile phase. The gradient program was set from 20% to 100% B for 7 min, held at 100% for 1 min, and returned to initial conditions for re-equilibration. High-resolution mass spectrometry (HRMS) spectra were acquired in both positive and negative modes with a scanning range from 150 to 2000 m/z, detector voltage at 1.7 kV, nebulizing gas (N2) flow at 1.5 L/min, drying gas (N_2) pressure at 130 kPa, CDL temperature at 200°C, and block heater temperature at 200°C. Tandem MS (MS/MS) fragmentation was performed with collision energy (CID) and collision gas set to 50% and frequency set to 45 kHz. Additional MS/MS analyses were performed on an impact II QTOF (Bruker) with a scanning range from 50 to 1500 *m/z*, capillary voltage at 4.5 kV, nebulizer gas pressure (N2) at 4 bar, drying gas flow at 12 L/min and temperature at 225°C. The three most intense ions per MS1 were selected for MS2, with active exclusion after three spectra. Each spectrum is an average of 65-100% stepping with CID set at 70 eV.

2.2.7. Infrared (IR) and nuclear magnetic resonance (NMR) spectroscopy

IR spectra were acquired on neat samples using a Thermo-Nicolet 6700 with Smart iTRTM accessory. One dimensional (1D) and 2D NMR spectra were obtained on a Bruker AVII 900 MHz spectrometer equipped with a 5 mm TCI cryoprobe. NMR chemical shifts were referenced to residual solvent peaks (CDCl$_3$ δ_H 7.26 and δ_C 77.16). NMR experiments included ^{1}H NMR, Distorsionless Enhancement by Polarization Transfer Quaternary (DEPTQ), Homonuclear [1]H-[1]H Correlation Spectroscopy (COSY), Heteronuclear Single Quantum Coherence Spectroscopy (HSQC), Heteronuclear

Multiple Bond Correlation Spectroscopy (HMBC), and ^{1}H-^{13}C HSQC-Total Correlated Spectroscopy (^{1}H-^{13}C HSQC-TOCSY).

2.2.8. Tacrolimus metabolism by hepatic microsomes

Human hepatic microsomes (purchased from Corning Life Sciences; 3 mg microsomal protein/ml) were incubated with tacrolimus (100 µg/ml) in a reaction mixture (1 mM NADP+, 5 mM MgCl$_2$, 0.2 U/L isocitrate dehydrogenase, and 5 mM isocitric acid) at 37°C for 2 h aerobically. The reaction was terminated by adding the same volume of ice-cold acetonitrile, followed by centrifugation at 16,100×g for 10 min, and the supernatant was used for Met ID using IT-TOF as described above.

To determine the microsomal stability of tacrolimus and M1. Tacrolimus or M1 (1 µM) was incubated with human hepatic microsome (0.5 mg/ml) in a reaction mixture (1 mM NADPH, 5 mM MgCl$_2$) at 37 °C aerobically. The reaction was stopped at 0, 20, 40, and 90 min by adding two times the volume of ice-cold acetonitrile with ascomycin as an internal standard. After centrifugation at 16,100 g for 10 min, the supernatant was analyzed for loss of parent compound by LC-MS/MS method as described above.

2.2.9. Kidney transplant recipients' stool samples.

Stool samples were collected from ten kidney transplant recipients during the first month after transplantation at Weill Cornell Medicine and sent to us for analysis. Tacrolimus dosing in each patient was adjusted to achieve a target therapeutic level of 8 to 10 ng/ml. The study protocol for kidney transplant stool sample collection was approved by the Institutional Review Board at Weill Cornell Medicine (protocol number 1207012730).

For the measurement of baseline levels of tacrolimus and M1 in stool samples, an aliquot of stool samples was suspended in pre-reduced PBS (final concentration 20 mg/ml). Also, to measure the capacity of stool samples to produce M1, an aliquot of stool samples was suspended in pre-reduced PBS (10 mg/ml) and incubated with tacrolimus anaerobically for 24 h at 37°C. These samples were mixed with five volumes of acetonitrile containing ascomycin as an internal standard. An aliquot (10 μl) was injected into Agilent 1290 UPLC coupled with Applied Biosystems Qtrap 6500. The mobile phase consisted of water with 0.1% formic acid and 10 mM ammonium formate (solvent A) and MeOH (solvent B), and the following gradient was used: 0-2 min (20% B), 2-5 min (90% B), and 5-8 min (20% B). The separation was performed on an Xterra MS C18 column (2.1x50 mm, 3.5 μm: Waters) at a flow rate of 0.3 ml/min, with the column temperature set at 50°C. M1, tacrolimus, and ascomycin were detected at *m/z* 828.5/463.4, 821.6/768.6, and 809.5/756.5, respectively, in the multiple reaction monitoring mode. Standard curves (2–100 ng/ml for both tacrolimus and M1) were prepared by spiking tacrolimus or M1 into the stool samples of healthy volunteers.

2.2.10. Kidney transplant recipients' blood samples.

A serial of blood samples was taken from kidney transplant patients (n=10) after oral administration of Prograf (tacrolimus). For the sample preparation, 1 ml blood was mixed with 2 ml water/MeOH (v/v, 30/70, 1 M $ZnSO_4$) containing an internal standard (5 ng/ml ascomycin). The samples were vortexed for 1 minute and centrifuged at 2000 *g* for 3 min. The supernatant was taken and drawn through a C18 extraction column pre-treated with 2 ml ACN and 2 ml water (pH=3 adjusted by sulfuric acid) by applying -5 Hg vacuum.

The column was washed with 2 ml water and then eluted with 2 ml ACN. Samples were then evaporated on a Speed Vac and reconstituted in 100 µl of ACN. 10 µl of sample was injected into ACQUITY UPLC BEH C18 Column (1.7 µm, 2.1 mm X 100 mm), running at a flow rate of 0.35 ml/min with 90% MeOH and 10% water (0.1% ammonium format and 0.1% formic acid), with column temperate at 60°C. Tacrolimus, M1, and internal standard were analyzed by LC-MS/MS (Agilent 1200 HPLC interfaced with an Applied Biosystems Qtrap 5500) at mass-to-charge (*m/z*) ratio 821.8/768.8, 828.5/463.5, and 809.5/756.6, respectively.

2.2.11. Determination of blood to plasma ratio for tacrolimus and M1

A blood sample from a healthy donor was obtained from a blood bank (Vitalant, IL) and used within a week after initial collection. Plasma was prepared by centrifuging at 4000×g for 15 min, and the hematocrit level (i.e., H) was calculated. Tacrolimus or M1 was added to 500 µl of blood or plasma (REF PL) to make a final concentration of 5 nM or 50 nM, and incubated at 37°C for 1 h. After the incubation, the blood was centrifuged at 4000×g for 15 min to obtain plasma (PL). And 200 µl of PL or reference PL were taken and mixed with 400 µl of iced ACN containing ascomycin as the internal standard. The samples were vortexed for 1 minute and centrifuged at 16000×g for 15 min. 10 µl of supernatant was analyzed by HPLC/MS/MS (Agilent 1200 HPLC interfaced with Applied Biosystems Qtrap 3200) using the method as described above. The blood to plasma ratio ($K_{RBC/PL}$) was calculated by the equation: $K_{RBC/PL} = \frac{1}{H} \times \left(\frac{I_{REF\ PL}}{I_{PL}} - 1 \right) + 1$

where the $I_{REF\ PL}$ and I_{PL} represent the area ratio between the substrate (i.e., tacrolimus or M1) and internal standard in REF PL and PL, respectively (Yu et al., 2005).

2.2.12. Immunosuppressant activity.

The immunosuppressant activity of tacrolimus and M1 was determined by measuring the proliferation of human blood mononuclear Cells as previously described (Messele et al., 2000) with a slight modification. Briefly, cryopreserved PBMCs were stabilized in RPMI1640 medium containing 10% heat-inactivated fetal bovine serum at 37°C and 5% CO_2 for 24 h. Cells were seeded at 1×10^6 cells/ml in 96-well round-bottom plates. After incubation for 24 h, cells were pretreated with tacrolimus, M1, or vehicle for 1 h, followed by treatment with PHA (5 µg/ml) and BrdU (20 µM) for 48 h. Cells were centrifuged at $1000 \times g$ for 5 min, washed with PBS, and fixed with 4% paraformaldehyde for 15 min. The fixed cells were permeabilized with 0.4% Triton X-100 for 5 min and incubated with 2 N HCl at 37°C for 30 min. After washing with PBS, the cells were incubated with 100 mM borate buffer (pH 8.0) for 10 min and washed again with PBS. After blocking with 2% BSA for 1 h, cells were incubated with horseradish peroxidase (HRP)-conjugated BrdU antibody (BU1/75, ICR1) for 1 h at room temperature. Cells were then washed with PBS and incubated with 3,3',5,5'-Tetramethylbenzidine (TMB) (a HRP substrate) for 30 min. The reaction was stopped by adding 2 N HCl. The absorbance was measured at 450 nm on a plate reader (BioTek, Winooski, VT).

2.2.13. Antifungal assay.

The antifungal activity of tacrolimus and M1 was examined as previously described (Ianiri et al., 2017). Briefly, *Malassezia sympodialis* M1154/77 (a gift from Dr. Joseph Heitman, Duke University) grown overnight in modified Dixon (mDixon) medium at 37°C was plated on mDixon agar. After 1 h incubation, an aliquot (3 µl) of tacrolimus or M1 at

different concentrations was spotted on top of the agar and incubated at 37°C for 2 days. The agar plates were visually inspected, and the images were taken using a camera.

2.2.14. Estimation of the extent of tacrolimus metabolism by intestinal bacteria.

F. prausnitzii was grown overnight in YCFA medium. The overnight culture typically reaches an optical density at 600 nm (OD_{600}) of ~2, which corresponds to ~1.6×108 *F. prausnitzii* cells/ml. Cells were harvested by centrifugation at 2,000 × *g* for 5 min resuspended in PBS, and serially diluted in PBS (OD_{600} 0.02, 0.2, 0.4, 0.8, 1.6, and 2). To determine the relationship between the number of bacterial cells and the extent of M1 formation, the cell suspensions at different densities were incubated with tacrolimus (10 µg/ml) at 37°C for 2 h under anaerobic conditions. The reaction was stopped by adding 4 volumes of ice-cold acetonitrile containing ascomycin as an internal standard. After vortexing (1 min) and centrifugation at 16,100×g (10 min), the supernatant (2 µl) of each sample was injected into HPLC/MS/MS (Agilent 1200 HPLC interfaced with Applied Biosystems Qtrap 3200) and M1 concentrations were determined as described above. To examine the relationship between incubation time and M1 formation, *F. prausnitzii* cells (OD_{600} 0.8, equivalent to 6.3×10^7 cells/ml) in PBS were incubated with tacrolimus (10 µg/ml) for different time (0.5, 1, 2, 4, 8, and 24 h), and M1 formation was determined as described above. To examine the relationship between tacrolimus concentrations and M1 formation, tacrolimus at different concentrations (2, 10, 20, 40, and 50 µg/ml) was incubated with *F. prausnitzii* cells (OD_{600} 0.8) for 1 h, and M1 formation was determined as described above. Assuming that the capabilities of bacteria in human small intestine to produce M1 are similar to that of *F. prausnitzii* cells in PBS, the total amount of M1

formed in the small intestine was estimated as previously reported (McCabe et al., 2015) with modifications:

M1 formation rate *in vitro* (μg/cells/h) = $\dfrac{\text{Amount of M1 formed (μg)}}{\text{bacterial cell number} \times \text{incubation time (h)}}$ (eq. 1)

Amount of M1 formed in the human small intestine

= M1 formation rate *in vitro* × total number of bacterial cells × small intestinal transit time

(h) (eq. 2)

The value of 4×10^{10} cells was used as the total number of bacteria in the small intestine (Sender et al., 2016), and 3.3 h was used as small intestine transit time (Yu et al., 1996).

2.2.15. Mouse PK study

Adult male C57BL/6 mice (9 weeks; male; 20-28 g body weight) were purchased from Jackson Laboratory (Sacramento, CA) and acclimated for one week. To start the experiment, mice (N=6-7/group) were either given regular water (control group) or water containing 0.5 mg/mL vancomycin and 0.1mg /mL polymyxin B (antibiotics group) for 24 h. After 4 h fasting, tacrolimus (Prograf injection, 2 mg/kg) was given to both groups through oral gavage. Ten μl of blood was collected from the saphenous vein at 5, 30, 120, 300, 480, 1440 min post-drug administration. Blood samples were extracted by adding 100 μl MeOH/water (v/v, 20/1, 0.12 mM $ZnSO_4$) containing internal standard (5 ng/ml ascomycin), and vortexed for 1 min and centrifuged at 16,000 *g* for 20 min. Ten μl of the supernatant was injected into LC-MS/MS for measuring tacrolimus using the method described above. An additional group of mice (N=4/group) was used to examine the effect of antibiotics in bacterial abundance and expression of known tacrolimus disposition

enzymes. After giving drinking water w/wo antibiotics, livers, small intestines were collected. Stool samples were also collected before and after antibiotics treatment.

2.2.16. Measurement of fecal bacterial abundance

Bacterial genomic DNA was extracted from the stool samples using QIAamp DNA Stool Mini Kit, and the DNA concentration was measured by Nanodrop. To assess bacteria abundance, bacterial DNA was diluted 5-fold using ddH2O, and bacterial 16S rDNA was amplified by qRT-PCR using universal bacterial primers (Forward: 5'-AAACTCAAAKGAATTGACGG-3'; Reverse: 5'-CTCACRRCACGAGCTGAC-3') (Zahir et al., 2001). The reaction mixture contained 5 µl master mix, 0.5 µl primers, and 4.5 µl of bacterial DNA. Relative bacterial abundance was calculated using ΔΔCt method by normalizing to the weight of stool. The standard curve was generated by diluting DNA from one of the samples for 10, 100, 1000, and 10000 times, where the linearity between Ct value and the amount of bacterial DNA was examined.

2.2.17. Measurement of M1 formation by mouse stool

Fresh stool samples from mice (50 mg wet weight/ml) before and after antibiotictreatment (which antibiotics at what concentration) were incubated with tacrolimus (100 µg/ml) anaerobically for 24 h at 37 °C. The incubation mixtures were analyzed by HPLC/UV as described previously.

2.2.18. mRNA extraction and qPCR

Total RNA was extracted from mouse liver (5 mg) and intestine (5 mg) using TRIzol. cDNA was synthesized from RNA by PCR using High Capacity cDNA Archive Kit

(ThermoFisher Scientific). Using the cDNA as template, qRT-PCR was performed using the primers from Integrated DNA Technologies (California, USA): Cyp3a11 (Forward: 5'-AGTAGCACACTTTCCTTCACC-3'; Reverse: 5'-CCATCTCCATCACAGTATCATAGC-3'); Abcb1a (Forward: 5'-GAAAAGAAACCAGCAGTCAGTG-3'; Reverse: 5'-TCATGTCACCAAAGATCAGCA-3'); Abcb1b (Forward: 5'-TGTTGGTCTATGCGTCTTATGC-3'; Reverse: 5'-CTGGTTTGTGTCCCTTGGTT-3'). Relative gene expression of Cyp3a11, Abcb1a, and Abcb1b was calculated using ΔΔCt method by normalizing to Gapdh (Forward: 5'-AATGGTGAAGGTCGGTGTG-3'; Reverse: 5'-GTGGAGTCATACTGGAACATGTAG-3').

2.2.19. Small intestinal metabolism of tacrolimus in rodents

C57BL/6 mice (Jackson, N=2) or Sprague Dawley rats (Taconic, N=2) were sacrificed, and small intestinal content was collected by perfusing with 25 ml pre-reduced YCFA inside the anaerobic chamber. The small intestinal bacterial mixture was obtained by centrifuging the content at 100×g for 5 minutes to obtain the supernatant, followed by 4000×g for 15 min and resuspending the pellet in 1 ml YCFA for mouse and 3 ml for rat, respectively. Tacrolimus or positive control compounds (10 μM) was incubated with 250 μl of small intestinal content anaerobically at 37°C for 2 h, and the reaction was stopped by adding 250 μl of cold ACN. After vortexing for 1 min and centrifuging at 16000×g for 20 min, 10 μl of the supernatant was injected into LC-MS/MS to analyze the metabolite production. Of note, positive control compounds (i.e., compounds known to be metabolized by small intestinal bacteria) were different for mice and rats: L-dopa for rats and compound X for mice. The name of compound X was not disclosed due to unpublished information.

2.2.20. Cofactor dependency of M1 formation

F. prausnitzii was grown anaerobically overnight in YCFA media. Cells were harvested by centrifugation at 4000×*g* for 10 min at 4 °C and re-suspended in 10% of the original volume of BugBuster 10X Protein Extraction Reagent supplemented with EASYpack Protease Inhibitor Cocktail. The mixture was Incubate at 25 °C for 30 min on a shaker at 300 rpm, followed by centrifuge at 16000×*g* for 30 min to collect the supernatant as the protein lysate. The protein concentration was determined using Bicinchoninic Acid Assay. The protein extract was adjusted to 1 mg/ml using normal PBS or pre-reduced PBS. Protein extracts (200 µl) containing 1 mM of a cofactor (NAD, NADP, NADH, or NADPH) was pre-incubated anaerobically or aerobically for 10 min. The reaction was started by adding 2 µl tacrolimus (final concentration at 5 µg/ml) and the mixture was incubated anaerobically or aerobically for 24 h at 37 °C. 400 µl of cold ACN was added to stop the reaction and vortex for 1 minute. After centrifuging at 16000×*g* for 30 min, Two µl of the supernatant was injected into LC-MS-MS (Applied Biosystems Qtrap 5500) for measuring M1 production.

2.2.21. Analysis of *F. prausnitzii* genome

The GenBank file (NZ_CP022479.1) of *F. prausnitzii* A2165 genome and the list of protein-coding genes (n=2839) were downloaded from NCBI microbial genome database. Genes potentially encoding oxidoreductases were retrieved by searching for oxidoreductase, dehydrogenase, and reductase in the annotated function of proteins. Respective oxidoreductases (n=61) of *F. prausnitzii* were used as bait to BLAST search for homologs in the genomes of *E. coli* MG1655 K-12 and *B. subtilis* BD168 using

Geneious Prime (Version 2020.0.2). A cutoff for homologous genes was 90% overall

coverage and 35% identity in amino acids. Oxidoreductases of *F. prausnitzii* retrieving

homologs in either *E. coli* MG1655 K-12 or *B. subtilis* BD168 were excluded, as both *E.*

coli MG1655 K-12 and *B. subtilis* BD168 do not metabolize tacrolimus. The rest of

oxidoreductases were prioritized for expression based on functional annotation.
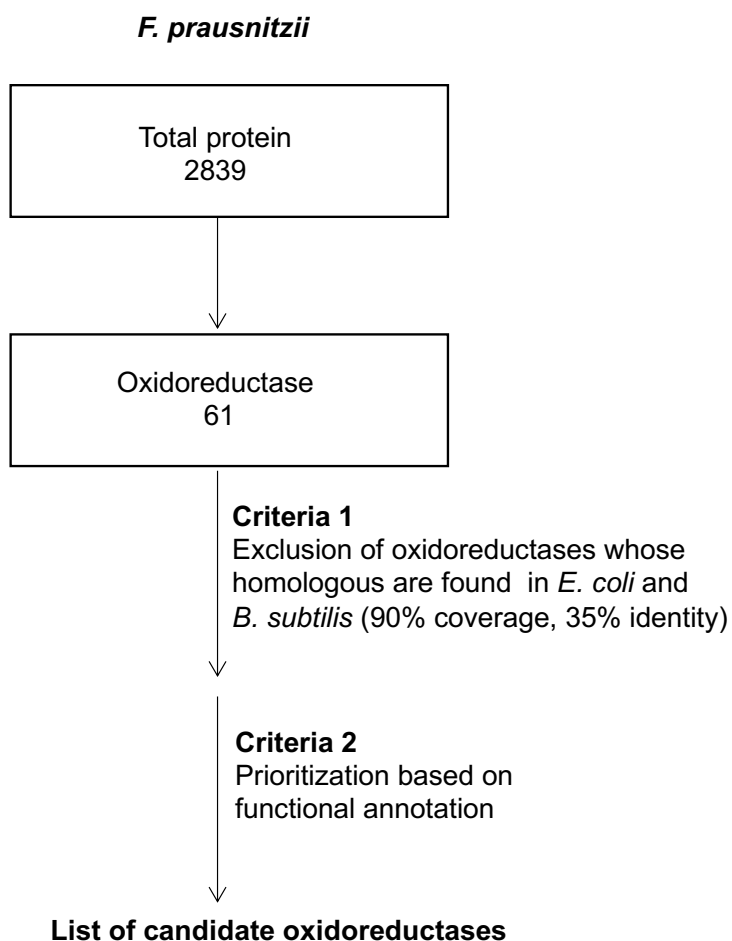
Figure 8. Work flow of selection of candidate enzymes.

2.2.22. Overexpresion of *F. prausnitzii* oxidoreductases in *E. coli*

F. prausnitzii A2-165 was grown overnight in the anaerobic chamber at 37°C. Genomic DNA was extracted using QIAamp DNA Mini Kit (Cat No: 51304). Respective oxidoreductase genes were amplified by PCR using primers listed in Table II. A PCR (50 µl) consists of 25 µl Q5 High-Fidelity 2X Master Mix, 2.5 µl each for forward and reverse primer (0.5 µM), and 200 ng genomic DNA as template. The PCR program starts with an initial denaturation at 98°C for 30 sec, followed by 25 cycles at 98°C for 10 sec, 62°C for 30 sec and 72°C for 40 sec; and a final extension at 72°C for 2 min. PCR products were cleaned up using QIAquick PCR Purification Kit (Cat No: 28104). *E. coli* containing plasmid pBAD22 was grown overnight at 37°C, and plasmids were extracted using PureYield Plasmid Miniprep System (Promega, A1222). pBAD22 plasmid carries L-arabinose-inducible promoter for overexpression of a downstream gene. Plasmid and PCR product were digested with NheI-HF (Cat No: R3131S) and HindIII-HF (Cat No: R3104S). Digested products were cleaned using QIAquick PCR Purification Kit. Ligation was performed at 25°C for 10 min and 65°C for 10 min. The quantity of PCR product was calculated based on 50 ng plasmids using NEBioCalculator, and 50 µl ligation mixture also contained 2 µl T4 DNA ligase buffer, 1 µl T4 DNA ligase and water. For transformation, 3 µl of the ligate was added to ice-cold cuvette containing electrocompetent *E.coli* LMG194 and electroporated at 1700 V, 200 Ω, and 25 µF. LB medium (700 µl) was added and grew the cells at 37°C for 45 min. An aliquote (80 µl) of culture was spread on LB agar supplemented with 100 µg/ml of ampicillin and incubated

overnight at 37°C. The next day, eight colonies were picked for colony-PCR to identify transformants carrying a recombinant plasmid (pBAD22-oxidoreductase). To verify correct cloning, plasmids were extracted from positive colonies and sent to UIC RRC Genome Research Core for Sanger DNA sequencing. Transformants containing sequence-verified recombinant plasmids were used for overexpression of a cloned oxidoreductase and tested for tacrolimus metabolism.

Table II. List of primer sequences used in this study

Label	Candidate enzymes	Primer	Sequence
1	2-dehydropantoate 2-reductase	Forward	CGGGCTAGCAGGAGGAGCAAGGAATGAAAATACAATCTGTTGCCATTT
		Reverse	GGCAAGCTTTTATTTTGCCCAGGTGGG
		Colony-forward	TTACGGAACACATTCAGGAA
2	Fe-S oxidoreductase	Forward	CGGGCTAGCAGGAGGAGCAAGGAATGGAAAACATCAAGAAAAACTTCG
		Reverse	GGCAAGCTTTTACTGCTTGTCAAATTCCG
		Colony-forward	TTCAACTATGTGGACTAC
3	ketopantoate reductase family protein	Forward	CGGGCTAGCAGGAGGAGCAAGGAATGAAGATTCTGGTATATGGTGC
		Reverse	GGCAAGCTTTCATTGCAGATACCTCCC
		Colony-forward	AAAATATAAGGTCGTTTACG
4	FAD-dependent oxidoreductase	Forward	CGGGCTAGCAGGAGGAGCAAGGAATGGAAAACATGATCCTGC
		Reverse	GGCAAGCTTTTACAGCTGGCAGGC
		Colony-forward	ATCGAGATGATGGACAAG
5	aldo/keto reductase	Forward	CGGGCTAGCAGGAGGAGCAAGGAATGGAATACAGAGCATGGAAAA
		Reverse	GGCAAGCTTTTACAGCTGATCCAGCTC
		Colony-forward	ATTATGGAGCCCATCAAG
6	SDR family oxidoreductase	Forward	CGGGCTAGCAGGAGGAGCAAGGAATGAAACCTGTCTGTGTGATTA
		Reverse	GGCAAGCTTTCAGCGGGAAAGGCC
		Colony-forward	AGTCAACATCAATGATGC
7	NAD(P)/FAD-dependent oxidoreductase	Forward	CGGGCTAGCAGGAGGAGCAAGGAATGGCAAAGGTGTTGATC
		Reverse	GGCAAGCTTTCAGAGGTGATTTGCAAAACT
		Colony-forward	AAAAATGTGACCCTGACC
8	flavin reductase family protein	Forward	CGGGCTAGCAGGAGGAGCAAGGAATGAGCAAACAGAGCTG
		Reverse	GGCAAGCTTTCATTTTTTCCGTTTTCCGG
		Colony-forward	ATCAACCTGCCCACTGAA
9	SDR family oxidoreductase	Forward	CGGGCTAGCAGGAGGAGCAAGGACTGAGCGATGAGGACAA
		Reverse	GGCAAGCTTTCAAATCACCAGGCCG
		Colony-forward	AGAAGCTGTTCACCGATAT

10	aldo/keto reductase	Forward	CGGGCTAGCAGGAGGAGCAAGGAATGGAAAACCTGAACATTGG
		Reverse	GGCAAGCTTTCAGGAAATGGCATCCA
		Colony-forward	TGGATGTCATTCAGGAAAA
11	FAD-dependent oxidoreductase	Forward	CGGGCTAGCAGGAGGAGCAAGGAATGGAAAAATACGATCTGATCATTG
		Reverse	GGCAAGCTTTCAGCACCCTTCCTTTTC
		Colony-forward	TTCAAGGAGAAGAAGAGC
12	SDR family NAD(P)-dependent oxidoreductase	Forward	CGGGCTAGCAGGAGGAGCAAGGAGTGGAAAAGAATGTTCTGAACA
		Reverse	GGCAAGCTTTCAGACACCAGAGTAGGC
		Colony-forward	ACACCGACAAGGAATTCT
13	aldo/keto reductase	Forward	CGGGCTAGCAGGAGGAGCAAGGAATGGATATGGTCACATTGG
		Reverse	GGCAAGCTTTTACACCTTGACTTCCCC
		Colony-forward	TATATTTCCGGTGAGCAG
14	NAD(P)/FAD-dependent oxidoreductase	Forward	CGGGCTAGCAGGAGGAGCAAGGAATGTCTAACATTGTGATCATCG
		Reverse	GGCAAGCTTTCATTTCCGCAGGGCTTT
		Colony-forward	TGCGATGCCTTTTTCTA
15	SDR family oxidoreductase	Forward	CGGGCTAGCAGGAGGAGCAAGGAATGTCAACCAAAACTGTCTG
		Reverse	GGCAAGCTTTCAGCCCAGCTTTTTCTT
		Colony-forward	AAAGCATACGTTGTCAG
16	NAD(P)-dependent oxidoreductase	Forward	CGGGCTAGCAGGAGGAGCAAGGAATGGCATTACACGTTCTGG
		Reverse	GGCAAGCTTTTATTTGACTTCCTGTTTGCC
		Colony-forward	TCAAGAACGAAGAGGGC
17	NADH:flavin oxidoreductase	Forward	CGGGCTAGCAGGAGGAGCAAGGAATGTACGACACCATCCTG
		Reverse	GGCAAGCTTTCAGATGCTGCCCTGT
		Colony-forward	TTCTCTTCCGCCATCTT
18	ketopantoate reductase family protein	Forward	CGGGCTAGCAGGAGGAGCAAGGAATGAGGATCTTGGTGTACG
		Reverse	GGCAAGCTTTTACTTCTTTCTGGGCAGG
		Colony-forward	TTTGGTTTCCAGAACAAT
19	D-2-hydroxyacid dehydrogenase	Forward	CGGGCTAGCAGGAGGAGCAAGGAATGAAAGCTGTCATTCTGGA
		Reverse	GGCAAGCTTTTATCTGTTGACGATGTGCT
		Colony-forward	ATTATGATACCCTGCTGA

20	3-phosphoglycerate dehydrogenase	Forward	CGGGCTAGCAGGAGGAGCAAGGAATGTTTACGATCAAGACCCTGAAC
		Reverse	GGCAAGCTTTTACAGGATGCGCACCCG
		Colony-forward	AAAAAGTTTGTGGGCAAC
21	mannitol dehydrogenase family protein	Forward	CGGGCTAGCAGGAGGAGCAAGGAATGAAGCTGTCTGATATCAAGAACGG
		Reverse	GGCAAGCTTTCAGCGGGCGACAACGTA
		Colony-forward	CATCCAGAAGATCGGTTAT
22	Gfo/Idh/MocA family oxidoreductase	Forward	CGGGCTAGCAGGAGGAGCAAGGAATGAAAAGAGCTGCGATCATTGG
		Reverse	GGCAAGCTTTCACGGAGCAACGGGATG
		Colony-forward	GTTGAACTGAAAAAGATCAT
23	Gfo/Idh/MocA family oxidoreductase	Forward	CGGGCTAGCAGGAGGAGCAAGGAATGGAAAAGACTGAAGGAAAGATTCG
		Reverse	GGCAAGCTTTTACTCGCGGACGGGGAA
		Colony-forward	GGTTTTCTCCAAGAACAT
24	Gfo/Idh/MocA family oxidoreductase	Forward	CGGGCTAGCAGGAGGAGCAAGGAATGAAACTAGGGATCCTGG
		Reverse	GGCAAGCTTTTATTTATCACAGGGAAATTTGA
		Colony-forward	ATGGAGTACAACAGCTTC
25	Zn-dependent alcohol dehydrogenase	Forward	CGGGCTAGCAGGAGGAGCAAGGAATGCTGACCTATACCTATGTTTCAG
		Reverse	GGCAAGCTTTCAGCACTCCACTGCCAC
		Colony-forward	AAAAAGGGCTTCGTGAA
		Colony-reverse	AGGCAAATTCTGTTTTATC

Note:
Forward: forward primer to amplify target gene
Reverse: reverse primer to amplify target gene
Colony-forward: forward primer to amplify recombinant plasmid
Colony-reverse: reverse primer to amplify recombinant plasmid; same for all the recombinant plasmid

2.2.23. Screening for M1 producing oxidoreductases

E. coli LMG194 that contains pBAD22 plasmid overexpressing a *F.prausnitzii* oxidoreductase was grown in LB medium (100 µg/ml ampicillin and 0.5% glucose) anaerobically at 37°C overnight. The next day, overnight culture was diluted 50-fold in fresh LB medium (100 µg/ml ampicillin). The culture was grown to OD_{600}~0.6, and L-(arabinose was added at a final concentration of 0.1% or water as a control. After 4 h of incubation, the culture was split in half. With one, bacterial cells were harvested by centrifugation, resuspended in 1X SDS-PAGE sample buffer (OD_{600} 20), and boiled for 10 min to lyse the cells. The overexpression of candidate enzymes was examined using gel electrophoresis followed by staining with Coomassie Brilliant Blue. For the other, tacrolimus at a final concentration of 5 ug/ml was added and incubated overnight anaerobically at 37°C. M1 production was analyzed using LC-MS/MS using the method described above.

2.3. Results

2.3.1. *F. prausnitzii* metabolizes tacrolimus.

A previous study has shown a positive correlation between fecal abundance of *F. prausnitzii* and oral tacrolimus dose to achieve therapeutic concentration in 19 kidney transplant patients. Hereby, we first examined whether *F. prausnitzii* is capable of metabolizing tacrolimus, cells of *F. prausnitzii* A2-165 strain grown overnight (in YCFA media) was incubated with tacrolimus (100 μg/ml; 124 μM) anaerobically at 37°C. After 48 h incubation, the mixture was resolved using HPLC and analyzed by a UV detector. The HPLC chromatogram of intact tacrolimus showed multiple peaks, demonstrating tautomer formation as previously reported (Namiki et al., 1993) (Figure 9A). For estimation of a concentration of intact tacrolimus, the area of the largest peak at retention time 19.7 min was used. After 24 h incubation with *F. prausnitzii*, the concentration of tacrolimus was decreased by ~50% (Figure 9B), which was accompanied by appearance of two new peaks (designated M1 and M2, Figure 9A). The M1 and M2 peaks were not observed when tacrolimus was incubated with boiled *F. prausnitzii* cells (Figure 9A), indicating that the production of M1 and M2 requires live bacterial cells. Similarly to strain *A2-165*, two additional strains of *F. prausnitzii* (*ATCC 27766* and *ATCC 27768*) were found to produce M1 and M2 (data not shown), suggesting that this function is likely conserved in different strains of *F. prausnitzii*.
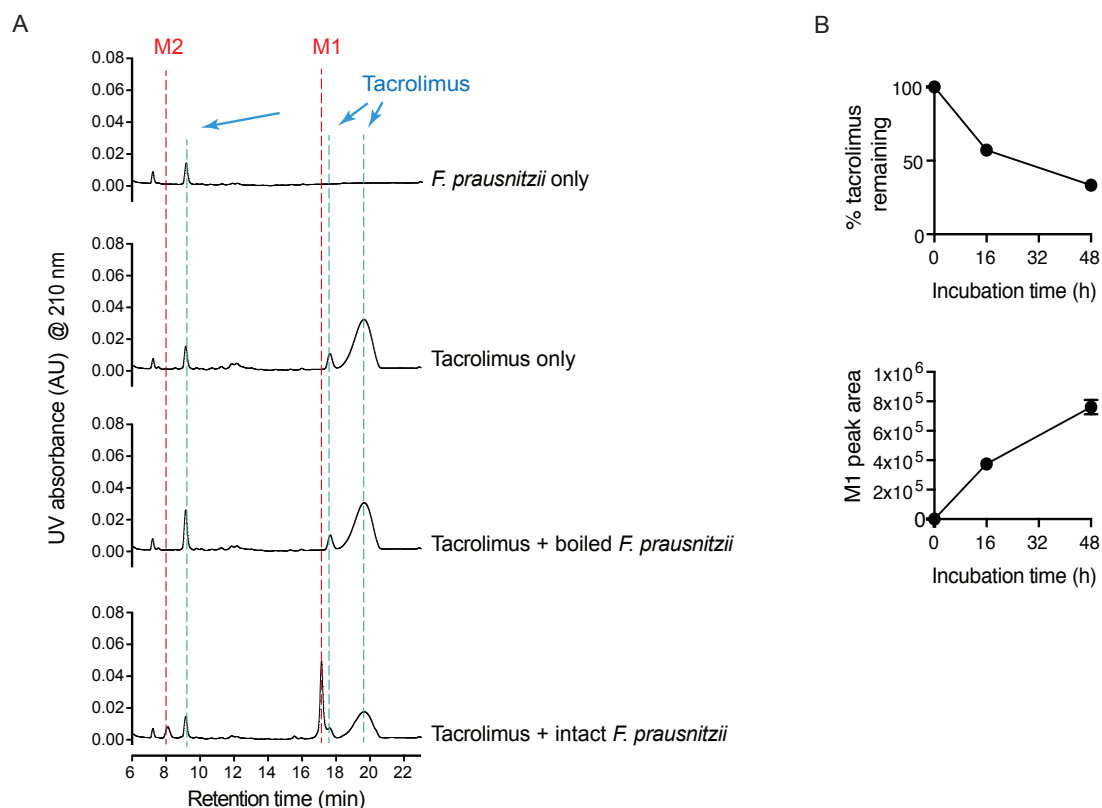
Figure 9. *F. prausnitzii* metabolizes tacrolimus. (A) *F. prausnitzii* A2165 (OD600 2.6) cultured in YCFA media was incubated with tacrolimus (100 μg/ml) anaerobically at 37°C for 48 h. The mixture was analyzed by using HPLC/UV. (B) Time profiles of tacrolimus disappearance and M1 appearance upon anaerobic incubation of tacrolimus (100 μg/ml) with *F. prausnitzii*.

2.3.2. Stool bacteria metabolize tacrolimus.

To examine whether such metabolism also occurs in complex bacterial community, we incubated tacrolimus with fresh stool samples from two healthy adults, and M1 production was assessed. Both stool samples produced M1, whereas the control stool samples that were boiled prior to tacrolimus incubation did not (Figure 10).
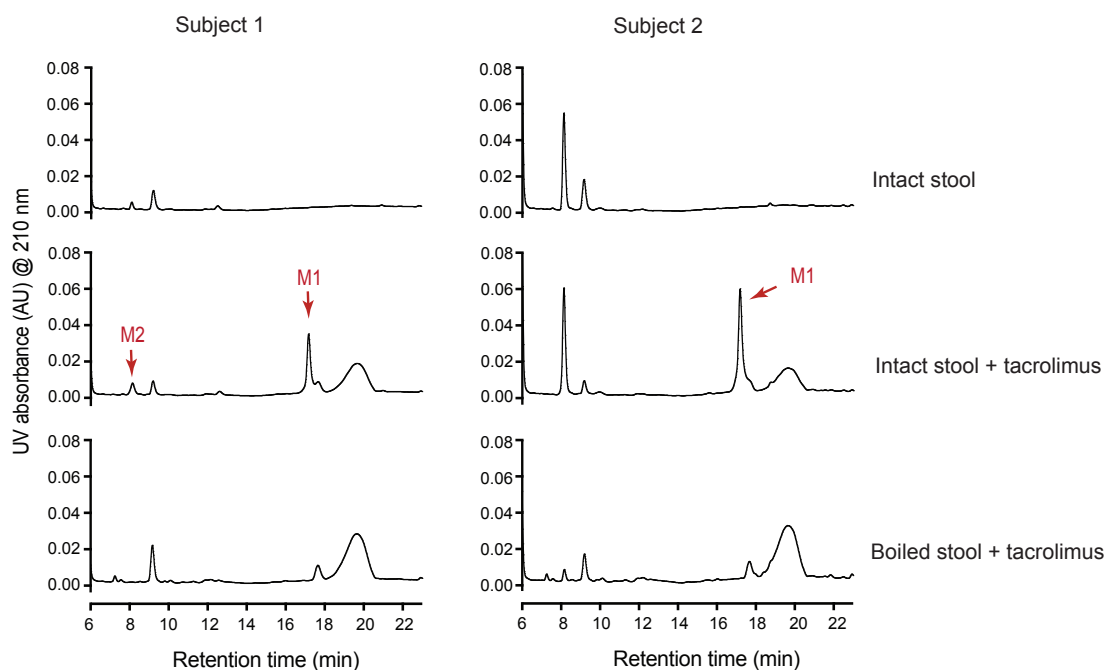
Figure 10. Human gut microbiota convert tacrolimus to M1. Tacrolimus (100 μg/ml) was incubated anaerobically with human stool samples from two different subjects (100 mg wet weight/ml) for 48 h at 37°C. A separate set of samples was boiled for 10 min before incubation with tacrolimus. The incubation mixtures were analyzed by HPLC/UV.

2.3.3. M1 is a C9 keto-reduction metabolite of tacrolimus.

For structural elucidation, we focused on the major product M1. M1 was mass produced by incubating large amounts of tacrolimus with F. prausnitzii. After liquid-liquid extraction using ethyl acetate and solid phase extraction, M1 was purified using preparative HPLC. The chemical structure of M1 was then determined using various spectroscopic methods. Of note, when the purified M1 was re-injected into HPLC/UV, it resolved into multiple peaks (including one corresponding to M2), indicative of isomerization and/or tautomerization of M1 into M2 (Figure 11).
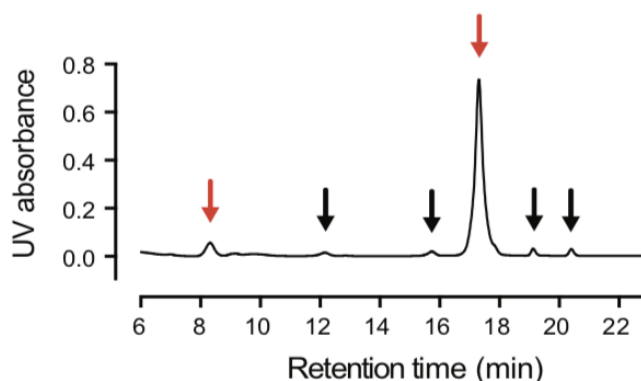
Figure 11. HPLC/UV chromatogram of purified M1. Tacrolimus (50 mg) was incubated with *F. prausnitzii A2-165* (OD ~2; 500 ml) for 96 h, followed by ethyl acetate extraction of the mixture. The fraction for M1 was isolated by using HPLC, combined, dried, and reconstituted in MeOH. An aliquot (1 μl) was analyzed by HPLC-UV. Red arrows denote the retention times for M2 and M1. Black arrows denote retention times for potential M1 isomers.

To further gain insight into the chemical identity of M1, high-resolution mass spectrometry (HRMS) was performed. The m/z value of M1 is [M+Na]$^+$ 828.4846, which is consistent with the formulas $C_{44}H_{71}NO_{12}Na$ (with a calculated mass of 828.4874 Da) for M1. The calculated formulas suggested M1 to be a reduction product of tacrolimus (i.e., the addition of 2H to the parent tacrolimus). The fragmentation pattern of M1 as compared to that of tacrolimus indicated that M1 is likely a keto-reduction product of tacrolimus (Figure 12). IR spectroscopy further supported that M1 is a product of a carbonyl reduction from tacrolimus. Major differences were observed in the C=O and O-H stretch regions of the IR spectra (Figure 13).
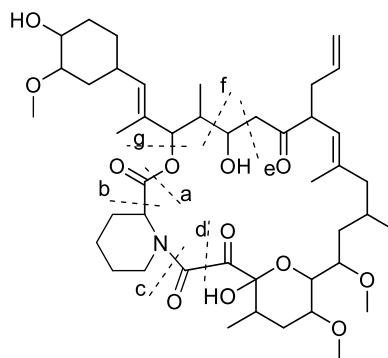
Tacrolimus fragmentation

[Ion + Na]⁺	Tacrolimus			M1		
	Calc. *m/z*	IT-TOF	QTOF	Calc. *m/z*	IT-TOF	QTOF
M	826.4717	826.4702	826.4692	828.4874	828.4846	828.4889
M-H₂O	808.4612	808.460	808.4589	810.4768	810.478	810.4645
M-2H₂O	790.4506	790.455		792.4663		
a-c	715.4033	715.403	715.4153	717.4190		717.4116
a-c-H₂O	697.3928	697.391	697.3919	699.4084	699.406	699.4103
a-c-2H₂O	679.3822	679.380	679.3885	681.3979	681.397	
g-d	671.4135	671.410		673.4292	673.425	
g-d-H₂O	653.4029	653.400	653.4029	655.4186	655.419	655.4230
g-d-2H₂O	635.3924	635.388	635.3983	637.4080	637.409	
f-g	616.3098	616.317	616.3092	618.3254	618.324	618.3274
f-a	598.2992	598.299	598.2940	600.3149	600.315	
f-b	572.3199	572.324	572.3102	574.3356	574.334	572.3380
f-c	487.2308	489.229	487.2259	489.2464	489.246	489.2615
f-d	461.2515	461.249	461.2524	463.2672	463.267	463.2670
f-d-H₂O	443.2410	443.239	443.2420	445.2566	445.255	445.2614
e-g	588.3149	588.315	588.3163	590.3305	590.351	590.3219
e-d	431.2410	431.239	431.2437	433.2566	433.254	433.2625
	433.2566	433.257	433.2556	435.2723	435.272	435.2743
	415.2460	415.246	415.2469	417.2617	417.261	417.2579
	371.2198		371.2194	371.2198		371.2145
	353.2093		353.2137	353.2093		353.2051
	261.1467		261.1431	261.1467		261.1449
[Ion + H]⁺						
Piperidine	84.0813		84.0803	84.0813		84.0794
Pipecolic acid	130.0868		130.0873	130.0868		130.0862

Figure 12. MS1 and MS2 fragments of tacrolimus and M1 obtained in IT-TOF and QTOF systems
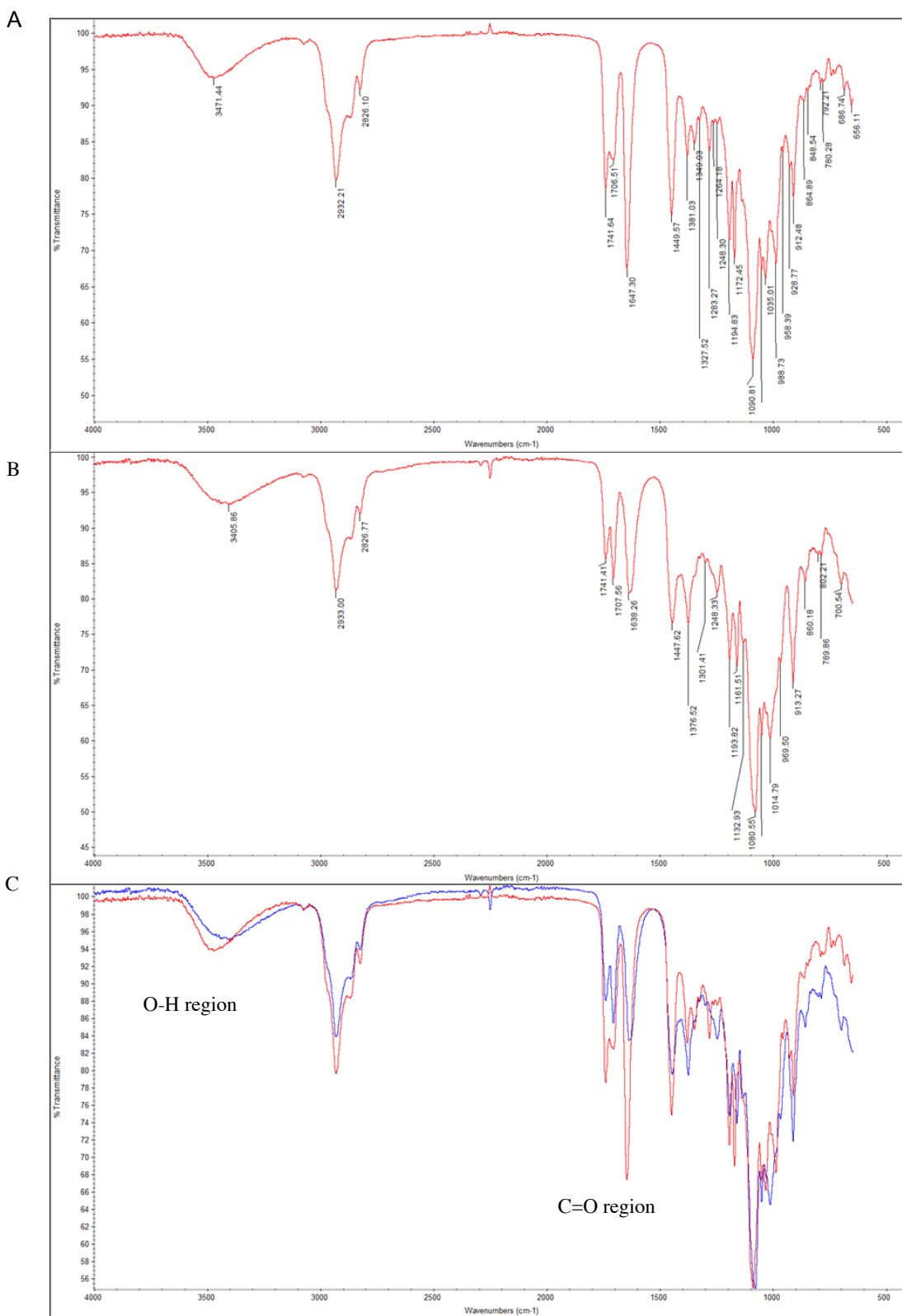
Figure 13. IR spectra of (A) tacrolimus, (B) M1, (C) overlay of tacrolimus (red) and M1 (blue) spectra

NMR was used to determine the exact modification site where two hydrogen atoms were added. The spectra showed three major isomers of M1 in $CDCl_3$ (Figure 14). Detailed analysis of 1D and 2D NMR spectra revealed the site of carbonyl reduction at C-9 and the identity of M1 to be 9-hydroxy-tacrolimus (Table III-V). In particular, analysis of the DEPTQ spectrum of M1 revealed the absence of the resonances associated with the carbonyl carbon C-9 found in tacrolimus (δC 196.3 for the major isomer, 192.7 for the minor isomer). Instead, three resonances consistent with the reduction of the carbonyl at C-9 to an alcohol were observed at δC 73.0 (isomer I), 68.4 (isomer II), and 69.7 ppm (isomer III). These resonances were associated with protons at δH 4.02, 4.51, and 4.37 ppm, respectively, in the HSQC spectrum. In turn, the latter resonances showed COSY correlations to exchangeable protons (δH 4.23, 3.21, and 3.58, respectively). HMBC correlations from H-9 to C-8 and C-10 were observed, supporting the assignment of M1 as 9-hydroxy-tacrolimus. These results establish the structure of M1 as the C-9 keto-reduction product of tacrolimus (Figure 15).

Figure 14. Expansions of the DEPTQ spectra (226 MHz, CDCl₃) of M1 (three major isomers assigned) and tacrolimus (two isomers)

Table III. NMR spectroscopic data of M1 (Isomer I), CDCl$_3$[a]

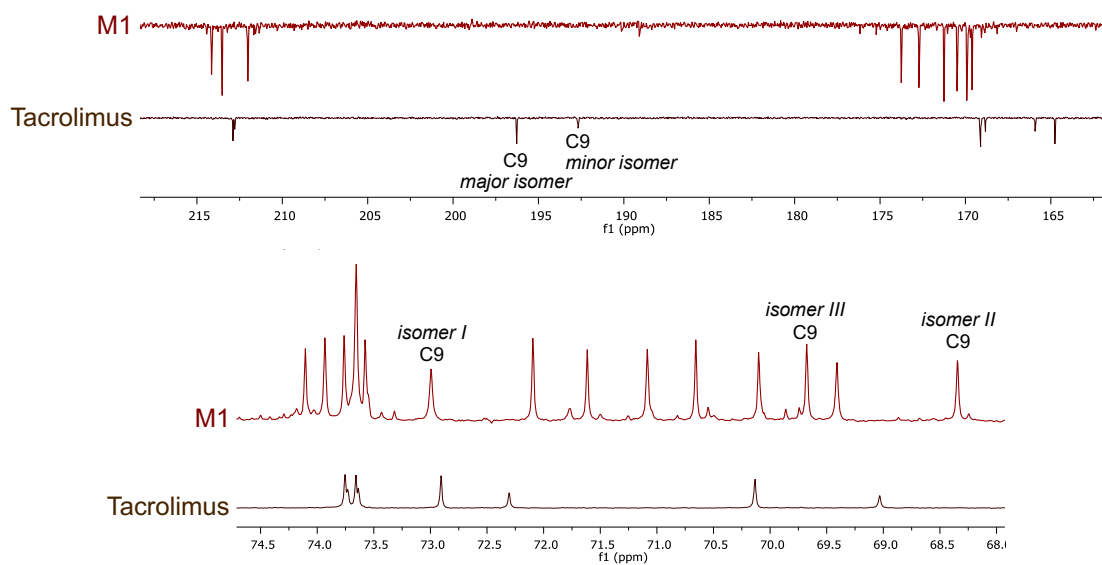| Position	δ$_C$, mult[b]	δ$_H$ (mult, *J* in Hz)[b,c]	COSY	HSQC-TOCSY (H→C)	HMBC (H→C)
1	169.6, C	-			
2	55.9, CH	5.39 (d, 4.5)	3, 6	3, 4, 5, 6	1, 3, 4
3	27.9, CH$_2$	2.26, 1.70	2, 4	2, 4, 6	5
4	21.3, CH$_2$	1.80, 1.40	3, 5, 6	2, 3, 5, 6	
5	25.1, CH$_2$	1.73, 1.70	4, 6	2, 3, 6	
6	41.0, CH$_2$	4.51, 2.85	2, 4, 5	2, 3, 4, 5	2, 4, 5, 8
8	171.3, C	-			
9	73.0, CH	4.02 (d, 6.5)	4.23		8, 10, 11
10	97.5, C	-			
11	35.7, CH	1.70	5.40, 12, 11-Me	12, 13, 11-Me	10, 11-Me
11-Me	16.4, CH$_3$	0.86 (d, 6.6)	11	11, 12, 13, 14	10, 11, 12
12	33.4, CH$_2$	1.96, 1.47	11, 13	14, 11-Me	10, 11, 13
13	73.7, CH	3.30	12, 14	11, 12, 14	15
13-OMe	56.3-56.4, CH$_3$	3.35-3.37			13
14	72.1, CH	3.74 (d, 9.8)	13, 15	12, 13, 11-Me	10, 12, 13
15	76.0, CH	3.53	14, 16	16, 17, 18, 17-Me	
15-OMe	57.6, CH$_3$	3.35			15
16	34.7, CH$_2$	1.48, 1.10 (d, 3.6)	15, 17	15, 17, 18, 17-Me	17, 18, 17-Me
17	25.8, CH	1.58	16, 18, 17-Me	17-Me	16, 18
17-Me	19.3, CH$_3$	0.80 (d, 6.5)	17	15, 16, 17, 18	16, 17, 18
18	48.9, CH$_2$	2.00, 1.91	17	17, 17-Me	17, 19, 17-Me
19	139.3, C	-			
19-Me	16.0, CH$_3$	1.64 (s)	20	20, 21	18, 19, 20, 22
20	122.2, CH	5.18 (d, 8.7)	21, 19-Me	21, 35, 36, 37, 19-Me	21, 22, 35
21	52.6, CH	3.45, (d, 8.2)	20, 35	20, 35, 36, 37	19, 20, 22, 35, 36
22	214.1, C	-			
23	44.1, CH$_2$	2.63 (d, 17.3), 2.43	24	24, 25-Me	22
24	69.4, CH	4.06 (dd, 10.3, 4.6)	3.41, 23, 25	23, 25, 25-Me	22, 26, 25-Me
25	40.3, CH	1.87	24, 26, 25-Me	24, 26, 25-Me	23, 24, 27, 25-Me
25-Me	10.3, CH$_3$	0.90	25	24, 25, 26	24, 25, 26
26	76.9, CH	5.13	25	25, 25-Me	1, 24, 25, 27, 28, 25-Me
27	132.1, C	-			
27-Me	14.5-14.6, CH$_3$	1.66	28	26, 28	26, 27, 28
28	128.8, CH	4.96	29, 27-Me	29/30, 31, 32, 33/34, 27-Me	26, 27, 29/30, 33/34, 27-Me
29	35.0, CH	2.30	28, 30, 34	28, 30, 31, 32, 33/34, 27-Me	
30	34.9-35.0, CH$_2$	2.01-2.04, 0.95	29, 31	28, 29, 31, 32, 33/34	31, 32
31	84.3, CH	3.00	30, 32	28, 29/30, 32, 33/34	32, 33, 31-OMe
31-OMe	56.7-56.8, CH$_3$	3.40			31
32	73.8, CH	3.39	31, 33	28, 29/30, 31, 33/34	31
33	31.3, CH$_2$	1.99, 1.35	32, 34	28, 29/30, 31, 32, 34	29/30, 31
34	30.7-30.8, CH$_2$	1.61, 1.04	29, 33	28, 29/30, 31, 32, 33	29
35	36.6, CH$_2$	2.44, 2.23	21, 36	20, 21, 36, 37	20, 21, 22, 36, 37
36	135.6, CH	5.71	35, 37	20, 21, 35, 37	21, 35
37	116.9, CH$_2$	4.98, 5.01	36	20, 21, 35, 36	35

Table IV. NMR Spectroscopic Data of M1 (Isomer II), CDCl$_3$

Position	δ$_C$, mult[b]	δ$_H$ (mult, J in Hz)[b,c]	COSY	HSQC-TOCSY (H→C)	HMBC (H→C)
1	170.5, C	-			
2	53.3, CH	5.20 (d, 5.5)	3, 6	3, 4, 5, 6	1, 3, 4, 6
3	26.4, CH$_2$	2.29, 1.74	2, 4	2, 4, 6	6
4	21.8, CH$_2$	1.77, 1.35	3	2, 6	
5	25.2, CH$_2$	1.64, 1.49	6	2, 3, 4, 6	
6	44.5, CH$_2$	4.10 (br d, 13.6), 2.99	2, 5	2, 3, 4, 5	2, 5, 8
8	172.7, C	-			
9	68.4, CH	4.51	3.21		8, 10
10	99.3, C	-			
11	33.0, CH	2.19	4.77, 12, 11-Me	13, 14, 11-Me	10, 11-Me
11-Me	16.4, CH$_3$	1.00 (d, 6.8)	11	11/12, 13, 14	10, 11/12
12	32.3, CH$_2$	2.04, 1.50	11, 13	13, 14, 11-Me	10
13	74.1, CH	3.39	12, 14	14, 11-Me	
13-OMe	56.3-56.4, CH$_3$	3.35-3.37			13
14	71.6, CH	3.68 (d, 9.6)	13, 15	13, 11-Me	10
15	77.1, CH	3.50	14, 16	14, 16, 17, 18, 17-Me	
15-OMe	57.6, CH$_3$	3.35			15
16	35.9, CH$_2$	1.56, 1.28	15, 17	15, 17, 18, 17-Me	14, 15, 17-Me
17	26.3, CH	1.55	16, 18, 17-Me	15, 18, 17-Me	18
17-Me	19.2, CH$_3$	0.76 (d, 6.3)	17	15, 16, 17, 18	16, 17, 18
18	48.0, CH$_2$	2.11, 1.75	17	17, 17-Me	17, 19, 17-Me
19	140.5, C	-			
19-Me	16.1, CH$_3$	1.71 (s)	20	20, 21	18, 19, 20, 22
20	122.7, CH	4.89 (d, 9.6)	21, 19-Me	21, 35, 36, 37, 19-Me	21, 22, 35, 36, 37
21	53.3, CH	3.39	20, 35	20, 35, 36, 37	19, 22, 35, 36
22	212.0, C	-			
23	43.7, CH$_2$	2.76, 2.23	24	24, 25-Me	22
24	70.1, CH	3.87	3.36, 23, 25	23, 25, 25-Me	23, 26
25	41.0, CH	1.85	24, 26, 25-Me	24, 26, 25-Me	23, 24, 27, 25-Me
25-Me	10.1, CH$_3$	0.92	25	24, 25, 26	24, 25, 26
26	78.3, CH	5.00	25	25, 28, 25-Me	1, 24, 25, 27, 28, 25-Me, 27-Me
27	132.5, C	-			
27-Me	14.5-14.6, CH$_3$	1.67	28	26, 28	26, 27, 28
28	130.1, CH	5.12 (d, 9.1)	29, 27-Me	29/30, 31, 32, 33/34, 27-Me	26, 27, 29/30, 33/34, 27-Me
29	35.0, CH	2.30	28, 30, 34	28, 30, 31, 32, 33/34, 27-Me	
30	34.9-35.0, CH$_2$	2.01-2.04, 0.95	29, 31	28, 29, 31, 32, 33/34	31, 32
31	84.2, CH	3.00	30, 32	28, 29/30, 32, 33/34	32, 33, 31-OMe
31-OMe	56.7-56.8, CH$_3$	3.40			31
32	73.7, CH	3.39	31, 33	28, 29/30, 31, 33/34	31
33	31.3, CH$_2$	1.99, 1.35	32, 34	28, 29/30, 31, 32, 34	29/30, 31
34	30.7-30.8, CH$_2$	1.61, 1.04	29, 33	28, 29/30, 31, 32, 33	29
35	34.9, CH$_2$	2.46, 2.23	21, 36	20, 21, 36, 37	20, 21, 22, 36, 37
36	135.6, CH	5.69	35, 37	20, 21, 35, 37	21, 35
37	116.7, CH$_2$	4.98, 5.01	36	20, 21, 35, 36	35

Table V. NMR Spectroscopic Data of M1 (Isomer III), CDCl$_3$[a]

Position	δ$_C$, mult[b]	δ$_H$ (mult, J in Hz)[b,c]	COSY	HSQC-TOCSY (H→C)	HMBC (H→C)
1	169.9, C	-			
2	53.5, CH	4.72 (d, 6.5)	3, 6	3, 4, 5, 6	1, 3, 4, 6, 8
3	26.2, CH$_2$	2.20, 1.79	2, 4	2, 4, 5	1
4	20.6, CH$_2$	1.72, 1.28	3	2, 6	
5	24.4, CH$_2$	1.74, 1.55	6	2, 3, 6	
6	43.5, CH$_2$	3.80 (br d, 13.3), 3.37	2, 5	2, 3, 4, 5	2, 4, 5
8	173.8, C	-			
9	69.7, CH	4.37 (d, 10.3)	3.58		8, 10, 11
10	97.8, C	-			
11	36.9, CH	1.78	12, 11-Me	13	10
11-Me	17.0, CH$_3$	1.09 (d, 6.7)	11	11, 12, 13	10, 11, 12
12	33.6, CH$_2$	1.99, 1.54	11, 13	14	10, 13
13	73.9, CH	3.39	12, 14	14, 11-Me	
13-OMe	56.3-56.4, CH$_3$	3.35-3.37			13
14	71.1, CH	3.68 (d, 9.6)	13	13, 11-Me	10
15	75.4, CH	3.59	16	16, 17, 18, 17-Me	17-Me
15-OMe	57.6, CH$_3$	3.35			15
16	35.9, CH$_2$	1.56, 1.28	15, 17	15, 17, 18, 17-Me	14, 15, 17-Me
17	26.2, CH	1.85	16, 17-Me	16, 18, 17-Me	
17-Me	20.5, CH$_3$	0.90	17	15, 16, 17, 18	16, 17, 18
18	49.4, CH$_2$	2.23, 1.72	17	17-Me	19
19	140.1, C	-			
19-Me	15.8, CH$_3$	1.66 (s)	20	20, 21	18, 19, 20, 22
20	122.6, CH	4.97	21	21, 35, 36, 37, 19-Me	21, 22, 36
21	52.4, CH	3.36	20, 35	20, 35, 36, 37	19, 20, 22, 35, 36
22	213.5, C	-			
23	42.6, CH$_2$	2.74, 2.22	24	24, 25-Me	22
24	70.7, CH	3.87	3.12, 23, 25	23, 25, 25-Me	23, 26
25	40.1, CH	1.91	24, 26, 25-Me	24, 26, 25-Me	23, 24, 27, 25-Me
25-Me	9.6, CH3	0.89	25	24, 25, 26	24, 25, 26
26	76.1, CH	5.32	25	25, 28, 25-Me	1, 24, 25, 27, 28, 25-Me, 27-Me
27	132.9, C	-			
27-Me	14.5-14.6, CH3	1.65	28	26, 28	26, 27, 28
28	129.0, CH	5.09 (d, 9.1)	29, 27-Me	29/30, 31, 32, 33/34, 27-Me	26, 27, 29/30, 33/34, 27-Me
29	35.0, CH	2.27	28, 30, 34	28, 30, 31, 32, 33/34, 27-Me	
30	34.9-35.0, CH$_2$	2.01-2.04, 0.95	29, 31	28, 29, 31, 32, 33/34	31, 32
31	84.3, CH	3.00	30, 32	28, 29/30, 32, 33/34	32, 33, 31-OMe
31-OMe	56.7-56.8, CH$_3$	3.40			31
32	73.6, CH	3.39	31, 33	28, 29/30, 31, 33/34	31
33	31.3, CH$_2$	1.99, 1.37	32, 34	28, 29/30, 31, 32, 34	29/30, 31
34	30.7-30.8, CH$_2$	1.61, 1.04	29, 33	28, 29/30, 31, 32, 33	29
35	34.9, CH$_2$	2.46, 2.11	21, 36	20, 21, 36, 37	20, 21, 22, 36, 37
36	135.8, CH	5.69	35, 37	20, 21, 35, 37	21, 35
37	116.7, CH$_2$	4.98, 5.01	36	20, 21, 35, 36	35

[a] Frequencies of 900 MHz for 1H and 226 MHz for ^{13}C
[b] A range of values (-) is indicated for chemical shifts that are interchangeable among isomers
[c] Peak multiplicity and coupling constants (J) are only reported for non-overlapping peaks on the ^{1}H spectrum
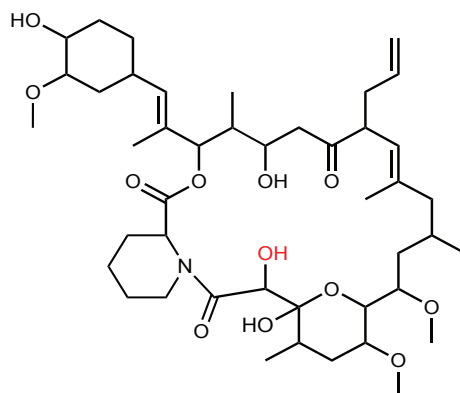
Tacrolimus
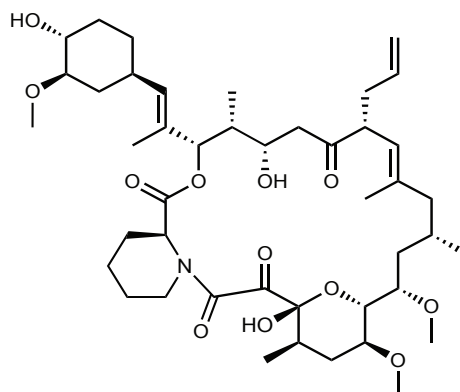
M1

Figure 15. Chemical structures of tacrolimus and *F. prausnitzii*–derived metabolite

M1. M1 structure was determined using mass and NMR spectroscopic methods.

2.3.4. Tacrolimus is metabolized by a wide range of commensal gut bacteria.

To determine whether other gut bacteria can metabolize tacrolimus, 25 human gut bacterial isolates were examined for their M1 producing ability. The tested bacteria include those belonging to major orders that are known to be highly abundant in the human gut (Qin et al., 2010; Arumugam et al., 2011). Bacteria grown overnight in YCFA media anaerobically were incubated with tacrolimus (100 μg/ml) for 48 h, and the mixtures were analyzed by HPLC/UV. Apparently, gut bacteria in the orders of *Clostridiales* and *Erysipelotrichales*, but not those in *Bacteroidales*, *Bacillales*, *Enterobacterales* and *Bifidobacteriales* produced M1 (Table VI). To further verify the results, the mixtures were re-analyzed by HPLC/MS/MS which exhibits higher sensitivity than HPLC/UV. M1 production by bacteria in *Clostridiales* was verified. M1 production by bacteria in *Bacteroidales* was detectable by HPLC/MS/MS at ~100-fold lower levels than that by bacteria in *Clostridiales*. M1 peak was not detected upon tacrolimus incubation with *B. longum*, *E. coli,* and *B. subtilis*.

Table VI. Screening gut bacteria for tacrolimus conversion to M1

Phylum	Class	Order	Bacterium	M1 production detected
Actinobacteria	*Actinobacteria*	*Bifidobacteriales*	*Bifidobacterium longum*	No
Proteobacteria	*Gammaproteobacteria*	*Enterobacterales*	*E. coli*	No
Bacteroidetes	*Bacteroidia*	*Bacteroidales*	*Bacteroides finegoldii*	Yes[a]
			Bacteroides cellulosilyticus	Yes[a]
			Bacteroides finegoldii	Yes[a]
			Bacteroides ovatus	Yes[a]
			Parabacteroides merdae	Yes[a]
			Parabacteroides johnsonii	Yes[a]
			Parabacteroides goldsteinii	Yes[a]
Firmicutes	*Bacilli*	*Bacillales*	*B. subtilis*	No
	Clostridia	*Clostridiales*	*Ruminococcaceae sp.*	Yes
			Anaerostipes sp.	Yes
			Dorea formicigenerans	Yes
			Clostridium clostridioforme	Yes
			Clostridium hathewayi	Yes
			Blautia sp.	Yes
			Clostridium aldenense	Yes
			Clostridium symbiosum	Yes
			Clostridium citroniae	Yes
			Coprococcus sp.	Yes
			Clostridium bolteae	Yes
			Clostridium cadaveris	Yes
			Ruminococcus gnavus	Yes
	Erysipelotrichia	*Erysipelotrichales*	*Erysipelotrichaceae sp.*	Yes
			Clostridium innocuum	Yes

[a]M1 production observed only when using sensitive HPLC-MS/MS for detection.

2.3.5. M1 is not produced by human liver microsomes

To determine if human enzymes also produce M1, tacrolimus was incubated with human liver microsomes in a NADPH regenerating system for 2 h. The reaction mixture was analyzed by IT-TOF. The major metabolites being observed are demethylated tacrolimus $[M + Na]^+$ 812.4550 as reported, while no M1 was formed (Figure 16). This data suggests that M1 is an unique bacteria-derived tacrolimus metabolite.
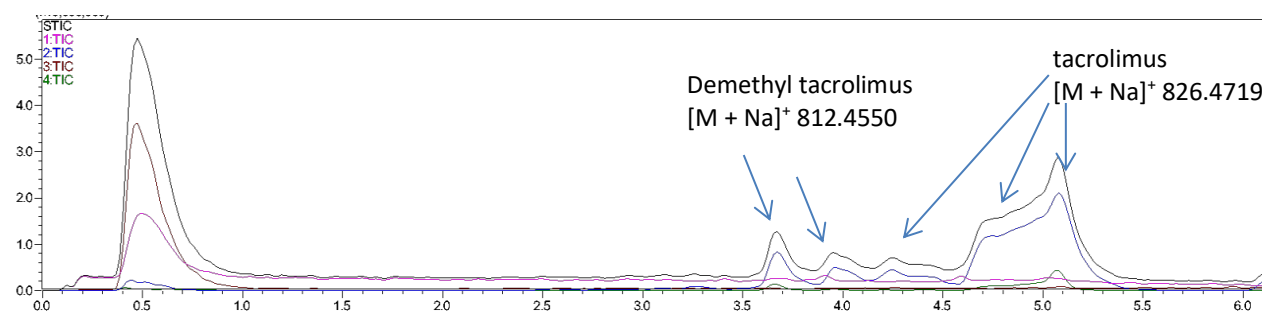

Figure 16. Human hepatic microsomes does not produce M1. Human hepatic microsomes (3 mg microsomal protein/ml) was incubated with tacrolimus (100 µg/ml) in a reaction mixture (1 mM NADP+, 5 mM $MgCl_2$, 0.2 U/L isocitrate dehydrogenase, and 5 mM isocitric acid) at 37°C for 2 h aerobically. The mixture was analyzed by using IT-TOF.

2.3.6. M1 is a less potent immunosuppressant than tacrolimus.

Structural change at C-9 position may alter the affinity of drug biding with FKBP-12. Herein, we compared the activities of M1 and tacrolimus by measuring PBMC proliferation after treatment with T-lymphocyte mitogen PHA (Messele et al., 2000). The 50% inhibitory concentration (IC50) of M1 was 1.97 nM whereas IC50 of tacrolimus was 0.13 nM, demonstrating that M1 was ~15-fold less potent than the parent tacrolimus in inhibiting T-lymphocyte proliferation (Figure 17).
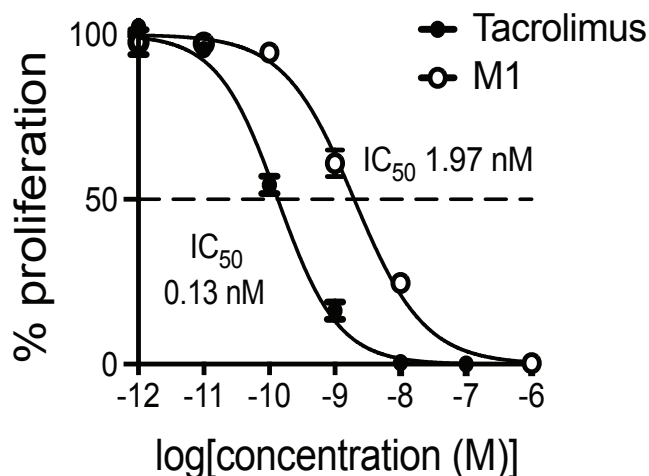
Figure 17. M1 is less potent than tacrolimus as an immunosuppressant. Immunosuppressant activities of tacrolimus and M1 were examined in PBMCs by measuring cell proliferation after treatment with a T-lymphocyte mitogen in the presence of tacrolimus or M1.

2.3.7. M1 is a less potent antifungal agent than tacrolimus.

Tacrolimus is known to exhibit antifungal activity via the same mechanism for immunosuppression (Steinbach et al., 2007). To further examine the pharmacological activity of M1, an antifungal assay was performed. An aliquot of M1 or tacrolimus was placed onto a lawn of the yeast *Malassezia sympodialis*, and their antifungal activities were estimated based on the size of halo formed. M1 was about 10 to 20-fold less potent than tacrolimus in inhibiting the yeast growth (Figure 18), consistent with the results obtained from the PBMC proliferation assay. Taken together, these results demonstrate that M1 is less potent as an immunosuppressant and antifungal agent than the parent drug tacrolimus is.
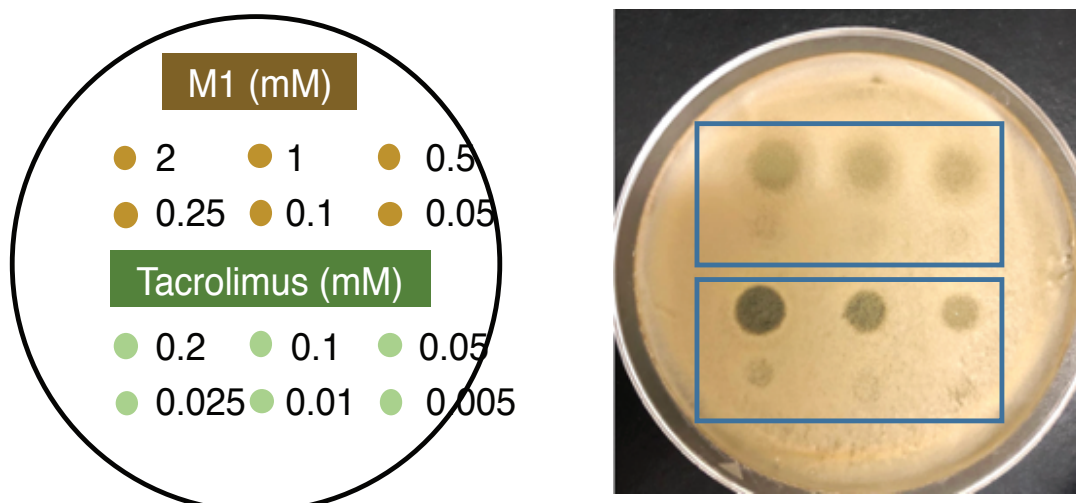
Figure 18. M1 is less potent than tacrolimus as an antifungal agent. Antifungal activities of tacrolimus and M1 were examined using Malassezia sympodialis. The yeast was inoculated on a modified Dixon agar plate. After 1 hour incubation, an aliquot of tacrolimus or M1 at different concentrations was placed on the plate, as shown in the left panel, and incubated at 37°C for 2 days.

2.3.8. M1 is detected in transplant patients stool samples.

F. prausnitzii is one of the most abundant human gut bacteria species (Qin et al., 2010; Arumugam et al., 2011), and its fecal abundance was shown to have a positive correlation with oral tacrolimus dosage (Lee et al., 2015). To explore a potential role of *F. prausnitzii* in tacrolimus metabolism in kidney transplant recipients, we evaluated 10 stool samples from kidney transplant recipients who were taking oral tacrolimus. Based upon the sequencing results of the V4-V5 hypervariable region of the 16S rRNA gene in stool samples, we selected 5 kidney transplant recipients whose stool samples had a relative gut abundance of *F. prausnitzii* greater than 25% (designated as "high *F. prausnitzii*"

group) and 5 kidney transplant recipients whose stool samples showed no to little (if any) presence of *F. prausnitzii* ("low *F. prausnitzii*" group). We first determined the baseline levels of tacrolimus and M1 in the stool samples from patients taking tacrolimus. We were able to measure baseline tacrolimus levels in eight of the ten stool samples, but we did not detect a significant difference in the baseline tacrolimus level between the high *F. prausnitzii* group and the low *F. prausnitzii* group (median 0.63 vs. 0.29 ng/mg, respectively, $p = 0.46$). We were also able to measure baseline M1 levels in five of the ten stool samples, but we did not detect a significant difference in the baseline M1 level between the high *F. prausnitzii* group and the low *F. prausnitzii* group (median 0.12 vs. <0.1 ng/mg, respectively, $p = 0.48$). Next, we tested the stool samples of both high and low *F. prausnitzii* groups for the capability of M1 production by incubating each of them with tacrolimus (10 μg/ml) for 24 h. M1 production was detected in all ten samples, but the amount produced was similar between the high and low *F. prausnitzii* groups (median 4.5 vs. 7.1 ng/mg, respectively, $p = 0.31$). The 16S rDNA sequencing analysis revealed that gut bacteria belonging to the *Clostridiales* order (a main group of bacteria that are expected to produce the majority of M1) were highly abundant in all ten samples (Table VII). However, the relative abundance of neither *F. prausnitzii* (Rho = -0.36, $p = 0.31$) nor *Clostridiales* (Rho = 0.44, $p = 0.20$) showed a significant correlation with M1 production. Oral tacrolimus doses (to maintain therapeutic blood concentrations) were similar between the high and the low *F. prausnitzii* groups (median 6 vs. 4 mg/day, respectively, $p = 0.34$) (Table VII).

Table VII. M1 levels in kidney transplant patients' stool samples.

Patient ID	Age (years)	Gender	Post-transplant Day	Tacrolimus oral dose[a] (mg/day)	Fecal abundance of *F. prausnitzii*	Fecal abundance of *Clostridiales*	Baseline tacrolimus level in stool samples (ng/mg stool)	Baseline M1 level in stool samples (ng/mg stool)	M1 production upon tacrolimus incubation (ng/mg stool)
1	45	Female	31	9	46%	86%	0.88	0.38	5.1
2	56	Male	18	3	39%	89%	BQL[c]	BQL[d]	3.5
3	61	Male	20	5	32%	71%	0.63	BQL[d]	4.5
4	59	Female	12	6	27%	76%	0.71	0.12	2.9
5	50	Male	32	10	26%	79%	0.37	0.41	6.4
6	52	Female	28	6	ND[b]	15%	0.29	BQL[d]	3.5
7	57	Male	15	3	ND[b]	44%	0.85	BQL[d]	4.1
8	71	Male	18	4	ND[b]	95%	BQL[c]	0.60	7.1
9	25	Male	27	4	ND[b]	74%	0.49	BQL[d]	12.6
10	52	Male	32	6	ND[b]	95%	0.14	BQL[d]	11.0

[a], at the time of stool collection
[b], not detected
[c], below the quantification limit (i.e., 0.1 ng/mg stool)
[d], below the quantification limit (i.e., 0.1 ng/mg stool)

2.3.9. M1 is detected in transplant patients blood samples

M1 is a novel metabolite of tacrolimus uniquely formed by gut bacteria, as hepatic microsomes do not produce M1. We further investigated whether M1 can be detected in human blood as an indication for gut bacterial metabolism of tacrolimus. We recruited 10 kidney transplant recipients at the time of transplantation and evaluated the pharmacokinetics of M1 after oral administration of tacrolimus. M1 and parent tacrolimus concentrations were determined by LC-MS/MS. The Weill Cornell IRB approved this study. The kidney transplant recipients had a median age of 50 and were male in 8 cases, were African American in 3 cases, and had deceased donor transplantations in 2 cases. Detection of M1 was observed in all patients within the first 4 h after oral administration, regardless of tacrolimus-naïve or tacrolimus-exposed patients (Figure 19). The result supports the concept of active metabolism of tacrolimus by gut bacteria. M1 levels were highly variable with some patients having at least 5% of parent tacrolimus concentration after oral administration (patient 1, 5, and 6).
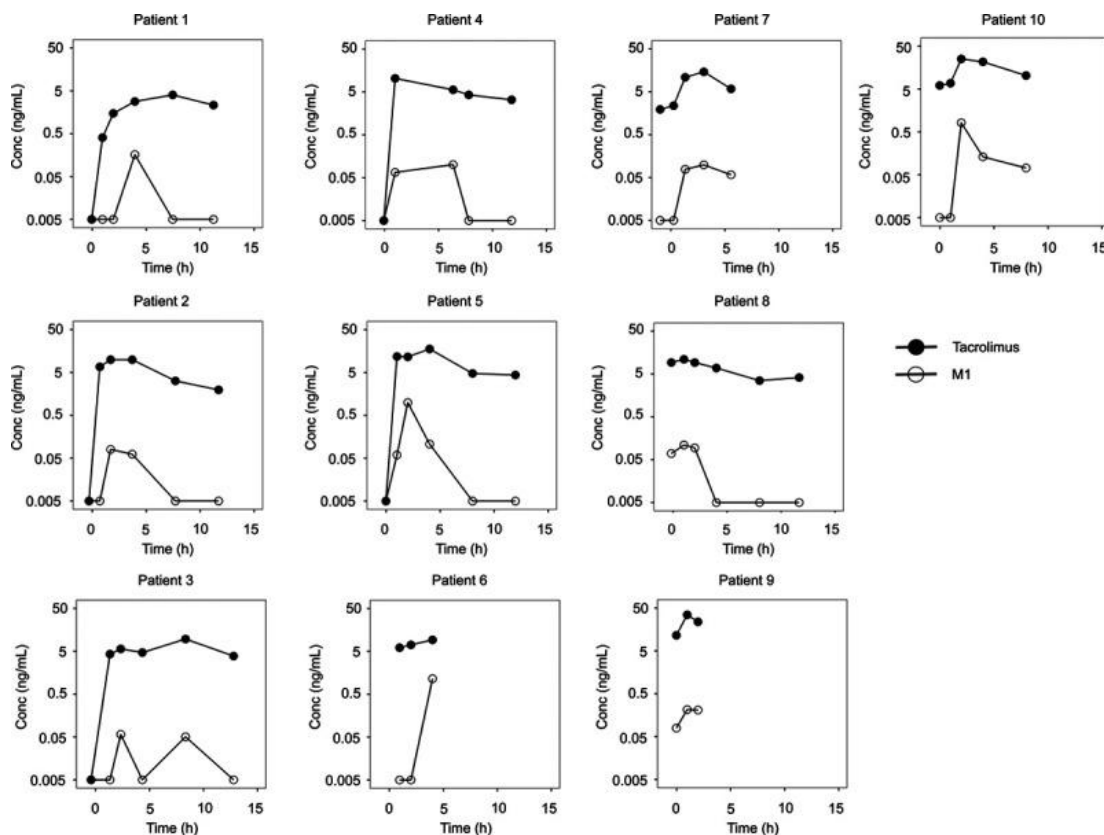
Figure 19. Pharmacokinetics of M1 and parent tacrolimus in kidney transplant recipients. Each graph represents a patient with the concentration of either M1 or parent tacrolimus on the y axis (logarithmic scale) and time in h on the x axis. Each point represents a time point when blood was drawn and analyzed for M1 (white points) and parent tacrolimus (black points). M1 values < 0.05, the lower quantification limit of the M1 assay, and tacrolimus values < 0.4, the lower quantification limit of the tacrolimus assay, were represented as 0.005 for plotting purposes on the graphs. Patients 1–6 were tacrolimus-naïve, and patients 7–10 were tacrolimus-exposed.

2.3.10. M1 and tacrolimus shows similar microsomal stability

To determine if low blood exposure of M1 is due to faster hepatic metabolism. M1 or tacrolimus (1 µM) was incubated with human hepatic microsomes (0.5 mg/ml) in a NADPH regenerative system, and drug loss was analyzed at 0, 20, 40 and 90 min using LC-MS/MS. The results showed that both M1 and Tacrolimus were rapidly eliminated by microsomes, with a half-life of 4 min and 3 min, respectively (Figure 20). This suggest M1 and tacrolimus exhibit similar metabolic stability.
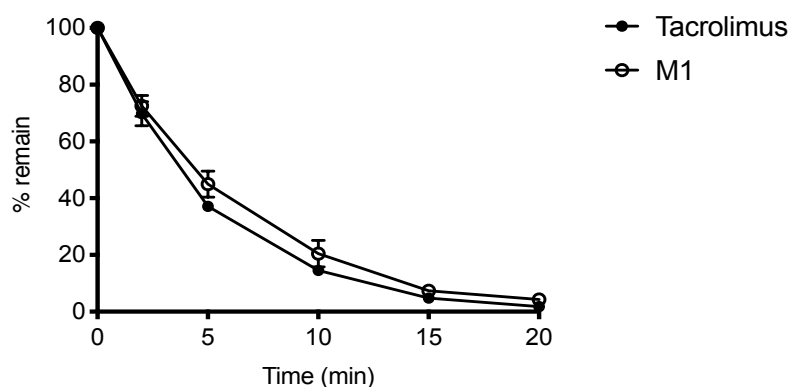

Figure 20. M1 and tacrolimus exhibit similar metabolic stability. Tacrolimus (1 µM) was incubated with human liver microsomes (0.5 mg/ml) for 0, 20, 40 and 90 min. The remaining of parent compound was measured using LC-MS/MS.

2.3.11. M1 exhibits low blood to plasma ratio

Tacrolimus is rapidly eliminated via *in vitro* microsomal incubation. However, hepatic extraction is only 4% in the body(Jusko et al., 1995). And extensive RBC binding due to interaction with FKBP is a known rate-limiting factor for tacrolimus elimination (Nagase et al., 1994; Minematsu et al., 2004). C-9 ketone on tacrolimus is an important functional group for FKBP binding, which was converted to hydroxyl group through

bacterial metabolism (Clackson et al., 1998). Thus, we hypothesized that M1 might exhibit insignificant RBC binding as compared to tacrolimus, thus may lead to faster elimination. To determine the extent of RBC binding of M1, we examined the blood to plasma ratio ($K_{RBC/PL}$) of M1. Tacrolimus or M1 was added to human blood or plasma and incubated at 37°C for 1 h, and concentration of the chemicals in two matrices were measured using HPLC/MS/MS (Agilent 1200 HPLC interfaced with Applied Biosystems Qtrap 3200). M1 shows $K_{RBC/PL}$ less than 1 at both concentrations; such value typically reflects an insignificant RBC binding (Emmons and Rowland, 2010). Moreover, a comparison of $K_{RBC/PL}$ between tacrolimus and M1 revealed the latter is about 4-fold lower (Table VIII). Thus, poor RBC binding of M1 may be responsible for rapid hepatic clearance and low blood exposure.

Table VIII. Comparison of blood to plasma ratio between tacrolimus and M1

Compounds	$K_{RBC/PL}$	Fold difference
Tacrolimus (5 nM)	3.27 ± 0.81	4.05
M1 (5 nM)	0.81 ± 0.26	
Tacrolimus (50 nM)	1.69 ± 0.61	4.39
M1 (50 nM)	0.39 ± 0.28	

Data were shown as mean±standard deviation.

2.3.8. Extensive tacrolimus metabolism may occur in the human small intestine.

For gross estimation of the extent of tacrolimus metabolism in human small intestine, M1 production kinetic profiles were obtained using *F. prausnitzii* as a model bacterium. M1 production increased linearly with the incubation time of up to 4 h (Figure 21A) and the amount of *F. prausnitzii* up to $1.2{\times}10^8$ cells/ml (Figure 21B). M1 production increased with the increasing concentrations of tacrolimus (Figure 21C) and did not reach a plateau at the highest concentration tested (50 µg/ml; a concentration attained when a typical tacrolimus oral dose 5 mg is dissolved in 100 ml water). Based on the assumption that bacteria in the human small intestine exhibit M1 production capabilities similar to that of *F. prausnitzii* in PBS, the extent of M1 production in the small intestine (at 50 µg/ml tacrolimus concentration) was estimated to be 1.9 mg.

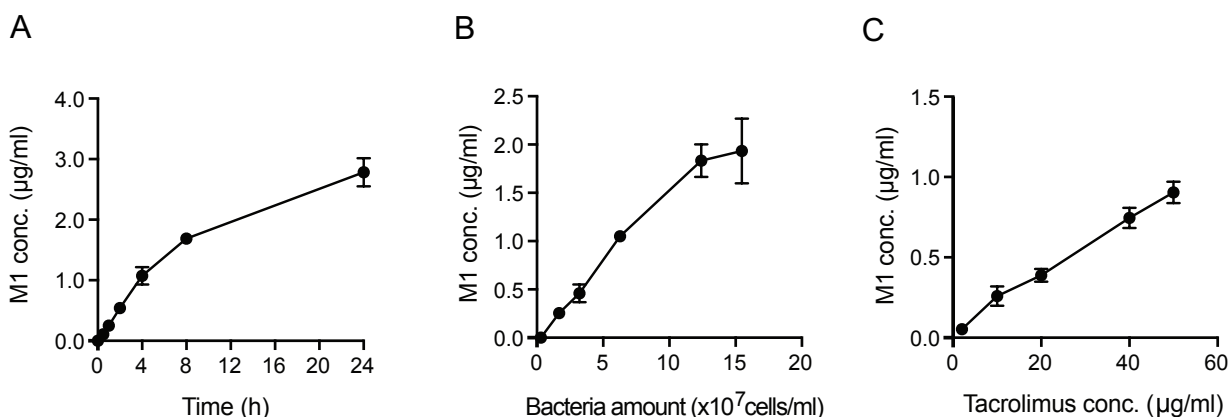**Figure 21. M1 formation by small intestinal bacteria may be extensive.** A, Tacrolimus (10 µg/ml) was incubated anaerobically with varying amounts of *F. prausnitzii* in PBS at 37°C for 2 h. B, Tacrolimus (10 µg/ml) was incubated with *F. prausnitzii* (6.3×107 cells/ml) for varying time. C, Tacrolimus at varying concentrations was incubated with *F. prausnitzii*

(6.3×107 cells/ml) for 1 h. M1 concentrations in the reaction mixtures were analyzed by LC-MS/MS.

2.3.12. One-day antibiotic treatment depletes gut bacterial abundance in mice

To further determine the extent of tacrolimus metabolism by bacteria, we attempted to deplete gut bacteria and examine its effects on tacrolimus pharmacokinetics in mouse model. 3-day antibiotics' treatment has been reported to alter expression of metabolizing genes and transporters (Kuno et al., 2016). We first determined whether short term antibiotics' treatment can decrease bacterial abundance in mice while not affecting hepatic and intestinal expression of tacrolimus disposition genes (i.e., Cyp3a11 and Abcb1) (Li et al., 2009; Vaidyanathan et al., 2016). Jejunum was selected to represent the small intestine because tacrolimus is mainly absorbed in jejunum in rodents (Watanabe et al., 1998). To this end, mice were given regular water (CON) or water containing vancomycin (0.5 mg/mL) and polymyxin B (0.1 mg /mL) (ABX) for one day. Measurement of fecal bacterial abundance after antibiotics' treatment showed a significant decrease to 3% of the pre-administration value (Figure 22A). Correspondingly, the bacterial metabolism, determined by M1 formation from ex-vivo incubation of tacrolimus with mouse stool, was also significantly decreased after one-day antibiotic treatment (Figure 22B). Meanwhile, there were no significant changes observed in hepatic and jejunum expression of Cyp3a11 and two isoforms of Abcb1 (i.e., Abcb1a and Abcb1b) (Figure 22C, 22D). This result indicated that one-day antibiotic treatment with vancomycin and polymyxcin B at given concentration is sufficient to deplete bacterial abundance without altering the expression of tacrolimus disposition genes.
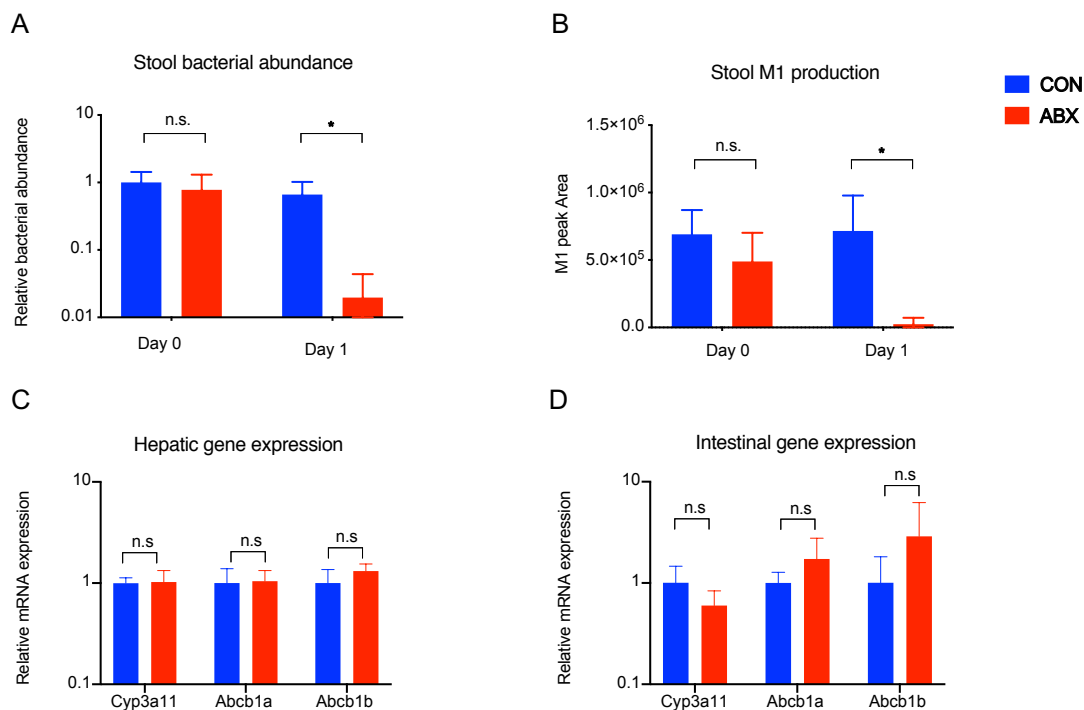
Figure 22. Antibiotic treatment reduces bacterial abundance in mice. C57BL/6J mice (n=4/group) were given drinking water with or without antibiotics (0.5 mg/mL vancomycin and 0.1mg /mL polymyxin B) for one day. Fecal samples were collected before and after antibiotics treatment. After 4 h of fasting, mice were sacrificed, and liver and small intestine were collected (A) Bacterial DNA was extracted from fecal pellet (30–70 mg) using QIAamp DNA Stool Mini Kit. Bacterial DNA was amplified by qPCR using universal bacterial 16S rDNA primer, and relative bacterial abundance was calculated using ΔΔCt method and normalized by weight of fecal pellet. (B) Tacrolimus (100 μg/ml) was incubated with mouse stool (50 mg/ml) anaerobically for 24 h at 37°C. M1 production was analyzed by HPLC-UV. Total RNA was isolated from mouse livers (50 mg) and Jejunum (50 mg/ml), (C) hepatic and (D) Jejunum expression of tacrolimus disposition genes was examined by qPCR and normalized by GAPDH.

2.3.13. Antibiotics do not alter tacrolimus PK in mice

To determine the extent of contribution of bacterial metabolism on tacrolimus oral exposure, we performed a pharmacokinetic study in CON and ABX mice. Tacrolimus (2 mg/kg) was given to mice through oral gavage, and a serial of blood was collected for measurement of tacrolimus concentration using LC-MS/MS. PK profiles of was subsequently plotted (Figure 23A). After oral administration, tacrolimus quickly reaches peak concentration (C_{max}). T_{max} occurred at 5 or 30 min in individual mice, indicating a rapidly absorption of tacrolimus from the intestine. Surprisingly, tacrolimus PK profile appears to be similar between control and antibiotic-treated mice, and the AUC (0-24 h) was not significantly different between two groups (Figure 23B). This result showed antibiotic treatment did not increase tacrolimus oral exposure in mice.
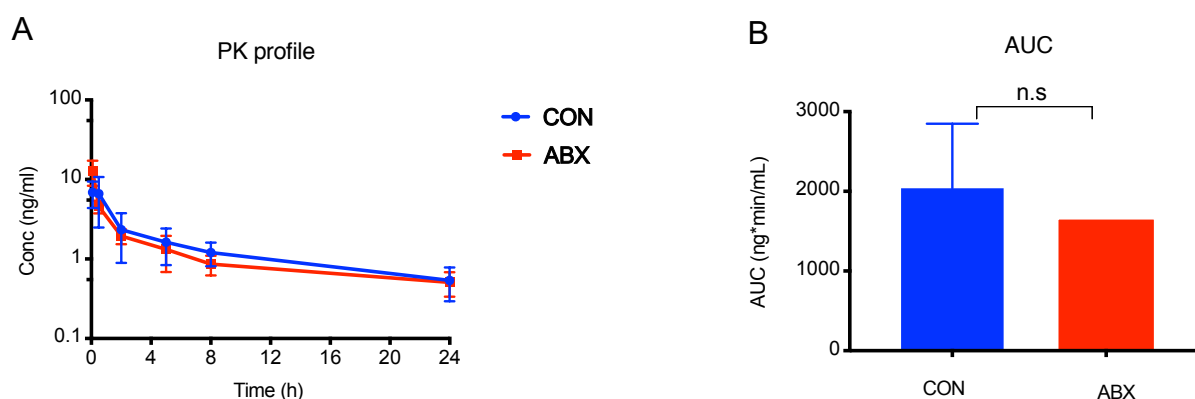
Figure 23. Antibiotic treatment does not alter tacrolimus oral drug exposure in mice. C57BL/6J mice (n=6-7/group) were given drinking water w/o antibiotics (0.5 mg/mL vancomycin and 0.1mg /mL polymyxin B) for 1 day. After 4 h fasting, tacrolimus (Prograf injection, 2 mg/kg) was given orally. Multiple blood sampling was performed at 5, 30, 120, 300, 480, 1440 min (10 µl / time point), tacrolimus concentration was measured by LC-MS/MS. (A) PK profile of tacrolimus (B) AUC

2.3.14. Rodents are not good models to study bacterial metabolism of tacrolimus

Antibiotic treatment depleted bacterial abundance without changing the expression of tacrolimus disposition genes in mice, yet no changes in PK were observed. Such an unexpected result leads to the hypothesis that tacrolimus metabolism by mouse gut bacteria may be insignificant at major drug absorption sites. Mouse small intestinal transit time is about 1-3 h (Padmanabhan et al., 2013). Considering tacrolimus is rapidly absorbed (tmax = 5 minute), most of the tacrolimus given orally is likely to be obsorbed in the small intestine and only contact with small intestinal bacteria. Therefore, we examined the extent of tacrolimus metabolism by mouse small intestinal bacteria. Mouse small intestinal content was collected by flushing the small intestine with pre-reduced YCFA. The bacterial mixture was prepared by centrifuging the content at 100×g for 5 minutes to obtain the supernatant, followed by 4000×g for 15 min and re-suspending the pellet in 1 ml pre-reduced YCFA broth. Tacrolimus (10 μM) was incubated with bacterial mixture anaerobically at 37°C for 2 h, and the reaction was stoped by adding same volume of ACN with ascomycin as the internal standard. After centrifuge at 16000×g for 30 minutes, the supernatant was analyzed using LC-MS/MS. Compound X was shown to be metabolized by mouse small intestinal bacteria through demethylation (Unpublished result from our lab), and therefore, it was used as a positive control drug. After 2-hour incubation, there was a negaligible M1 formation, while a significant metabolism was observed for compound X (22.1%) (Figure 24A). This result confirmed our hypothesis that mouse small intestinal bacteria play a negligible role in metabolizing tacrolimus, which potentially explains why there is no difference in tacrolimus oral exposure between CON and ABX mice. We further examined if a rat can be an alternative model. However,

incubation of rat small intestinal content with tacrolimus also showed negligible M1 production as compared to L-dopa to dopamine conversion (48%) (Figure 24B). L-Dopa was previously shown to be converted to dopamine by rat small intestinal bacteria (van Kessel et al., 2019) and used as a positive control drug. Thus, we conclude that rodents are not good models to study the contribution of tacrolimus metabolism by intestinal bacteria.
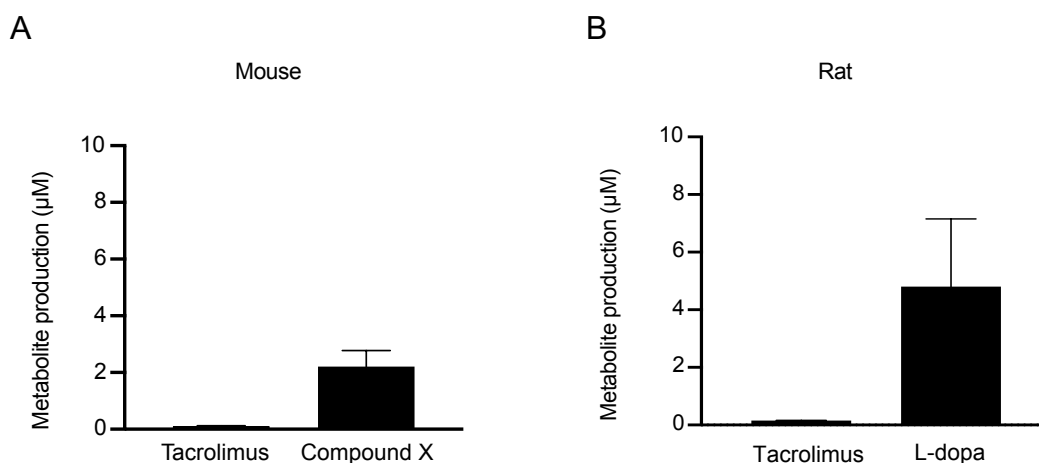
Figure 24. Rodents' small intestinal gut bacteria do not metabolize tacrolimus. Tacrolimus or a positive control compound (comopound X or L-dopa at 10 µM) was incubated with 250 µl of mouse (A) or rat (B) small intestinal content anaerobically at 37°C for 2 h, and the metabolite production was analyzed by LC-MS/MS.

2.3.15. M1 producing enzyme(s) is cofactor-dependent and oxygen-sensitive oxidoreductase

Conversion of tacrolimus to M1 is a reductive reaction, suggesting that enzyme(s) involved are likely to belong to oxidoreductases (EC 1). A noteworthy feature of oxidoreductases is their dependency on cofactors NADP(H) or NAD(H) to catalyze the

reaction (Sellés Vidal et al., 2018). Thus, to confirm if the tacrolimus metabolizing enzyme indeed belongs to oxidoreductases class, we characterized the dependency of M1 production on supplementation of NADP(H) or NAD(H). Tacrolimus was incubated with protein lysate of *F. prausnitzii* anaerobically at 37 °C, which was supplemented with major cofactors reported in microbial redox reactions (i.e., NAD, NADP, NADH, NADPH) (Geertz-Hansen et al., 2014). The same experiment was also performed aerobically to assess oxygen sensitivity of the reaction. The result showed that M1 formation was cofactor dependent, which requires one of the cofactors (i.e., NADH, NADPH) to serve as hydrogen donors (Figure 25). Moreover, M1 was only formed under the anaerobic condition that was independent of cofactor supplementation, suggesting the reaction is sensitive to the presence of oxygen (Figure 25).
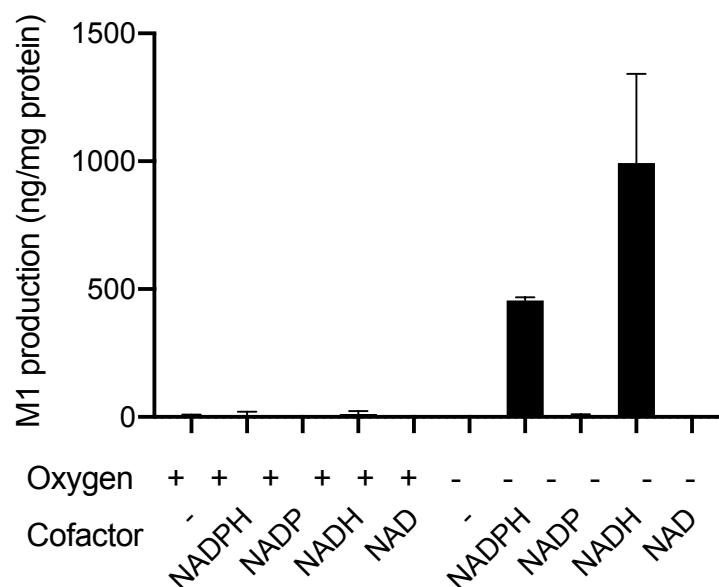

Figure 25. M1 formation is NAD(P)H-dependent and oxygen-sensitive. Tacrolimus was incubated aerobically or anaerobically with *F. prausnitzii* lysate (1 mg/ml protein) at 37°C for 24 h, supplemented with different cofactors. M1 formation was measured by LC-MS/MS.

2.3.16. Identification of four oxidoreductases of *F. prausnitzii* converting tacrolimus to M1

To identify *F. prausnitzii* oxidoreductases responsible for converting tacrolimus to M1, we selected candidate enzymes based on several criteria.   The genome of *F. prausnitzii* has 61 genes annotated to encode oxidoreductases. Of 61 oxidoreductases, we excluded those that have homologs in either *E. coli* MG1655 K-12 or *B. subtilis* BD168. Both *E. coli MG1655* and *B. subtilis BD168* are non-metabolizers that do not metabolize tacrolimus (Figure 26). Each of 61 oxidoreductases in *F. prausnitzii* was used as bait to BLAST-search in the genomes of the two non-metabolizers, and homologs were identified with the cutoff of 90% overall coverage and 35% amino acid sequence identity (Rost, 1999). As a result, a total of 17 homologs identified in non-metabolizers and excluded from further analysis (Table IX). Of the remaining 44, 21 enzymes were excluded as their functional annotations indicate that these enzymes mediate reactions other than ketone reduction (Table X). As a result, our final candidate list included 23 candidate oxidoreductases, six of which are enzymes predicted to catalyze ketone reduction and 16 of which have uncharacterized functions.
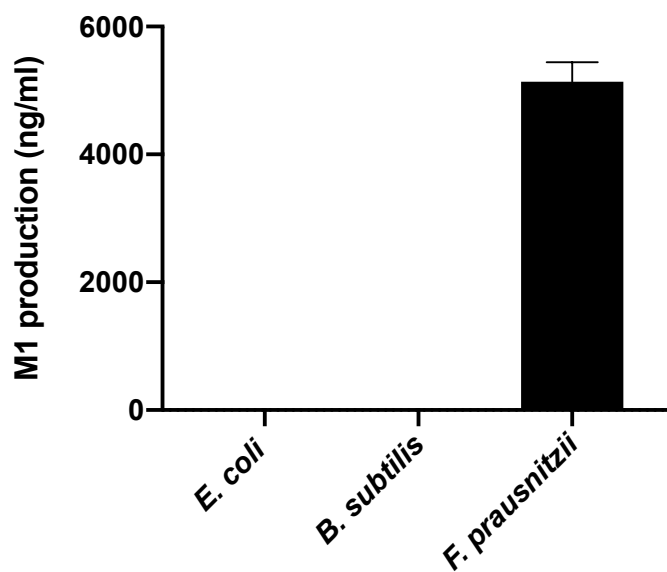
Figure 26. *E. coli* and *B. subtilis* does not metabolize tacrolimus. *F. prausnitzii* A2165, *E. coli MG1655* and *B. subtilis BD168* (OD_{600} 1) were incubated with tacrolimus (5 µg/ml) anaerobically at 37°C for 24 h. The mixture was analyzed for M1 formation using LC-MS/MS.

Table IX. Homologs of *F. prausnitzii* oxidoreductases in none-M1 producers

Annotated *F. prausnitzii* oxidoreductase	Locus tag	*E. coli*	*B. subtilis*
dTDP-4-dehydrorhamnose reductase	RS05945		✓
aldo/keto reductase	RS07915	✓	✓
SDR family NAD(P)-dependent oxidoreductase	RS08600		✓
iron-containing alcohol dehydrogenase	RS10360	✓	
3-oxoacyl-[acyl-carrier-protein] reductase	RS11265	✓	✓
pyrroline-5-carboxylate reductase	RS01835	✓	
glutamate-5-semialdehyde dehydrogenase	RS01845	✓	
NADP-specific glutamate dehydrogenase	RS02705	✓	
hydroxylamine reductase	RS02710	✓	
lactaldehyde reductase	RS04400	✓	
malate dehydrogenase	RS05985	✓	✓
pyruvate:ferredoxin (flavodoxin) oxidoreductase	RS08900	✓	
anaerobic ribonucleoside-triphosphate reductase	RS10810	✓	
tagaturonate reductase	RS12590	✓	✓
acyl-CoA dehydrogenase	RS01785		✓
UDP-N-acetylmuramate dehydrogenase	RS01105		✓
dihydroorotate dehydrogenase	RS06135		✓

Table X. List of enzymes mediating reactions other than ketone reduction

Annotated *F. prausnitzii* oxidoreductase	Locus tag	Reaction type
succinate dehydrogenase	RS05640	C=C $\rightleftharpoons$ C-C
trans-1,2-dihydrobenzene-1,2-diol dehydrogenase	RS02970	C=C $\rightleftharpoons$ C-C
sulfide/dihydroorotate dehydrogenase-like FAD/NAD-binding protein	RS14200	SH2$\rightleftharpoons$ S or C=C $\rightleftharpoons$ C-C
precorrin-6A reductase	RS11845	C=C $\rightleftharpoons$ C-C
NADP-dependent isocitrate dehydrogenase	RS07700	COOH $\rightleftharpoons$ CO2
prephenate dehydrogenase	RS07950	COOH $\rightleftharpoons$ CO2
4-hydroxy-3-methylbut-2-enyl diphosphate reductase	RS06200	OH $\rightleftharpoons$ H2O
4-hydroxy-tetrahydrodipicolinate reductase	RS01310	OH $\rightleftharpoons$ H2O
N-acetyl-gamma-glutamyl-phosphate reductase	RS08625	HPO4 $\rightleftharpoons$ PO4
nitroreductase	RS03455	NO2 $\rightarrow$ NH2
nitroreductase family protein	RS05380	NO2 $\rightarrow$ NH2
TlpA family protein disulfide reductase	RS04690	S-S $\rightleftharpoons$ SH+SH
methylenetetrahydrofolate reductase	RS05870	C-NH2 $\rightarrow$ CH3 + NH
saccharopine dehydrogenase family protein	RS04895	NH $\rightleftharpoons$ NH2
5,10-methylenetetrahydrofolate dehydrogenase	RS14370	C-N $\rightleftharpoons$ N=C
IMP dehydrogenase	RS01560	N=C $\rightarrow$ N=CO
xanthine dehydrogenase	RS01715	N=C $\rightleftharpoons$ N=CO
molybdopterin dehydrogenase	RS01755	N=C $\rightarrow$ C-N
phosphoadenosine phosphosulfate reductase	RS09510	SO4 $\rightarrow$ SO3
epoxyqueuosine reductase QueH	RS10995	C-O-C $\rightarrow$ C=C
homoserine dehydrogenase	RS02560	C-OH $\rightleftharpoons$ CHO

Table XI. List of oxidoreductases being cloned

Label	Annotated *F. prausnitzii* oxidoreductase	Locus tag	MW (Da)	Reaction type
1	2-dehydropantoate 2-reductase	RS01135	35	C=O ⇌ C-OH
2	Fe-S oxidoreductase	RS02070	42	Uncharacterized
3	ketopantoate reductase family protein	RS02885	34	C=O ⇌ C-OH
4	FAD-dependent oxidoreductase	RS03425	69	Uncharacterized
5	aldo/keto reductase	RS04850	43	Uncharacterized
6	SDR family oxidoreductase	RS05250	29	Uncharacterized
7	NAD(P)/FAD-dependent oxidoreductase	RS06215	47	Uncharacterized
8	flavin reductase family protein	RS06260	21	Uncharacterized
9	SDR family oxidoreductase	RS07735	29	Uncharacterized
10	aldo/keto reductase	RS07915	36	Uncharacterized
11	FAD-dependent oxidoreductase	RS08025	52	Uncharacterized
12	SDR family NAD(P)-dependent oxidoreductase	RS08600	30	Uncharacterized
13	aldo/keto reductase	RS09180	29	Uncharacterized
14	NAD(P)/FAD-dependent oxidoreductase	RS09290	28	Uncharacterized
15	SDR family oxidoreductase	RS09765	48	Uncharacterized
16	NAD(P)-dependent oxidoreductase	RS10445	41	Uncharacterized
17	NADH:flavin oxidoreductase	RS14490	36	Uncharacterized
18	ketopantoate reductase family protein	RS14585	38	C=O ⇌ C-OH
19	D-2-hydroxyacid dehydrogenase	RS03590	35	C=O ⇌ C-OH
20	3-phosphoglycerate dehydrogenase	RS06535	41	C=O ⇌ C-OH
21	mannitol dehydrogenase family protein	RS12675	59	C=O ⇌ C-OH
22	Gfo/Idh/MocA family oxidoreductase	RS01235	37	Uncharacterized
23	Gfo/Idh/MocA family oxidoreductase	RS01240	45	Uncharacterized
24	Gfo/Idh/MocA family oxidoreductase	RS12150	36	Uncharacterized
25	Zn-dependent alcohol dehydrogenase	RS03330	37	Uncharacterized

2.3.17. Identification of four oxidoreductases convering tacrolimus to M1

To identify the oxidorectase(s) responsible for M1 production in *F. prausnitzii*, 23 respective candidate genes were cloned into pBAD22 carrying L-arabinose-inducible promoter and each of the resulting plasmids was transformed into *E. coli LMG 194*. Despite multiple attempts, the RS10445 gene (No. 16 in Table XI) could not be cloned for unknown reason, while the rest of 22 candidate genes were successfully cloned and transformants were obtained. We also cloned two additional genes (RS07915 and RS08600; No. 10 and 12 in Table XI) as negative controls. These two genes were initially excluded based on our selection criteria but were randomly included to confirm our approach to selecting candidate oxidoreductase genes. As a result, a total of 24 genes were cloned, and transformants were obtained.

Each transformants was grown anaerobically and treated by 0.1% L- arabinose to induce the expression of a candidate oxidoreductase, and examined for capability of converting tacrolimus to M1. Cultures without induction were also examined for comparison. Overexpression of four candidate enzymes (No. 4, 9, 17, and 25) was not visible by Coomassie blue staining, and changing arabinose concentration to 0.01% or 1% did not improve overexpression (data not shown). The rest of the enzymes were shown to be well expressed under inducing conditions (Figure 27).

The results showed that four (No. 5, 8, 14, and 15 in Table XI) out 22 candidate oxidoreductases are capable of producing M1. Two randomly chosen oxidoreductases (NO. 10 and 12) did not show tacrolimus metabolism (Figure 28). Although No. 14 gave highest conversion of tacrolimus to M1, we did not conclude it has the highest activity due to lack of enzyme kinetics study.
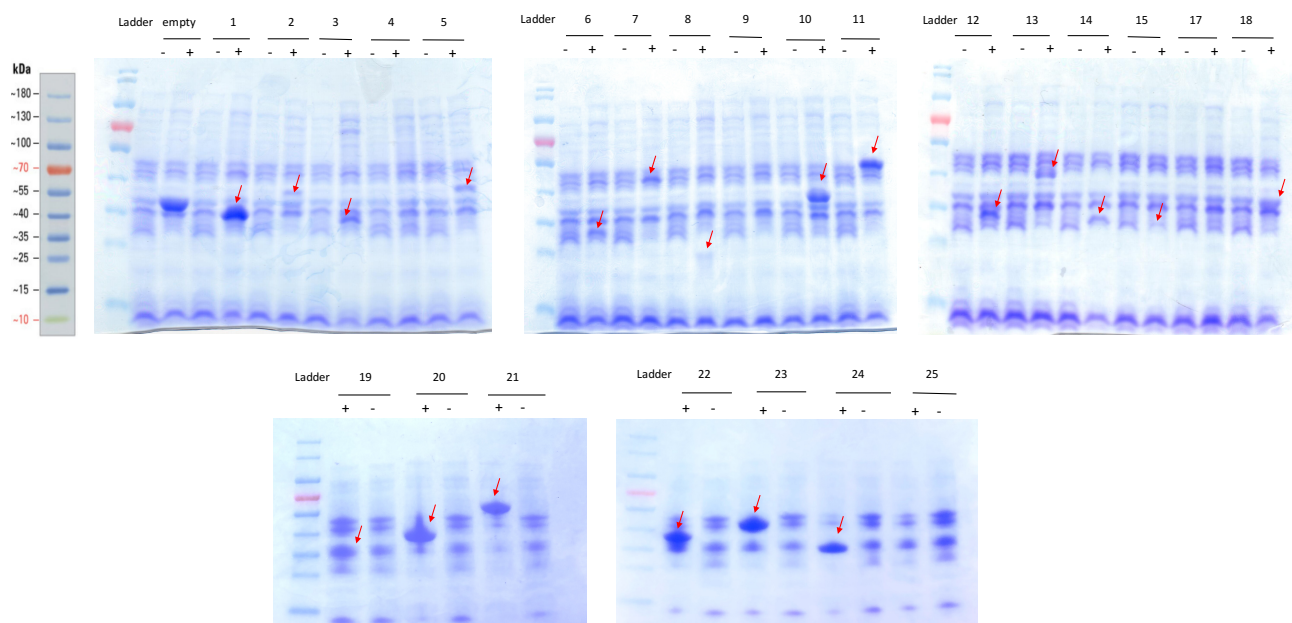
Figure 27. Overexpression of oxidoreductases. The transformants were treated with (+) and without (-) L- arabinose at final concentration of 0.1%. Bacteria cells were harvest after 4 h of induction. 1X SDS-PAGE sample buffer was added to and boiled at 100°C for 10 min to lyse the cells. The expression of candidate enzymes was examined using gel electrophoresis followed by Coomassie Blue staining. The red arrows indicate overexpressed enzymes.
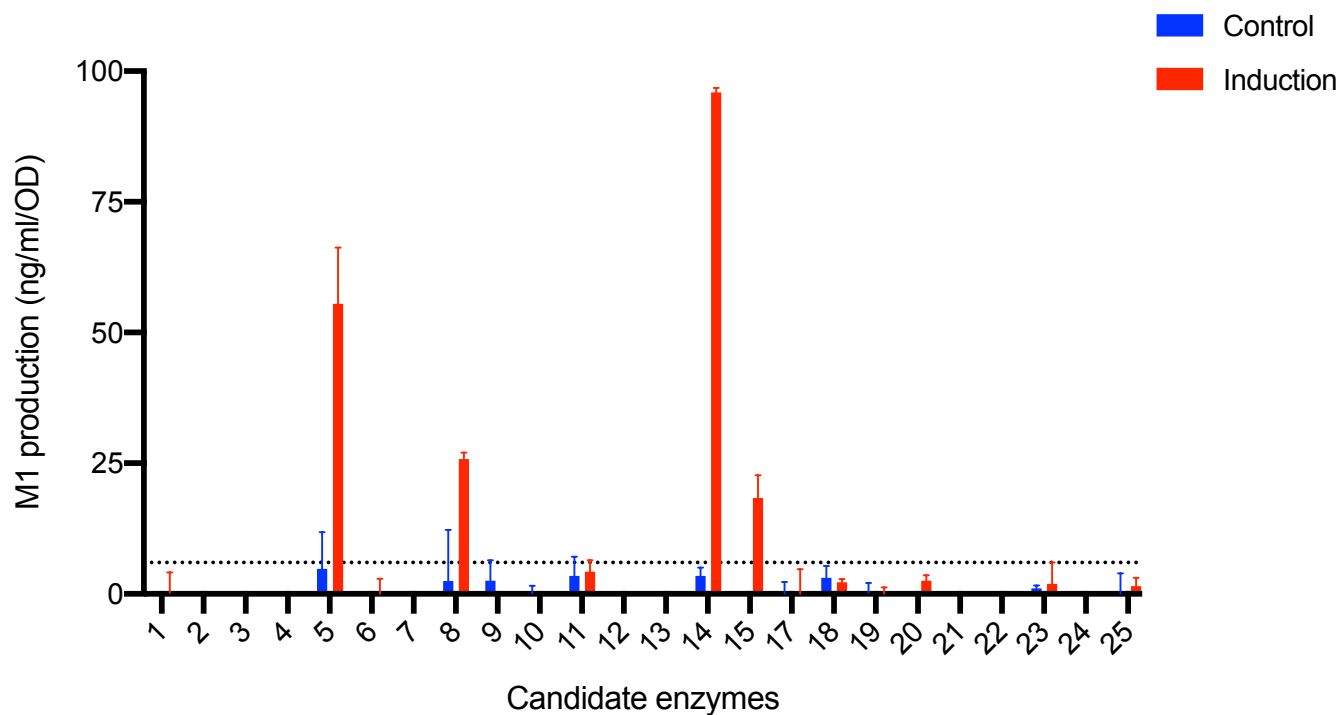
Figure 28. Multiple oxidoreductases are capable of producing M1. The tranformants were treated with (+) and without (-) L- arabinose at a final concentration of 0.1%. Cells were harvest after 4 h of induction. Bacterial culture was incubated with 5 µg/ml tacrolimus anaerobically at 37°C for 24 h. M1 production was measured using LC-MS/MS. The dash line represents 20% of the baseline M1 signal.

2.4. Discussion

In this project, we have demonstrated that a wide range of commensal gut bacteria can metabolize tacrolimus into a novel metabolite M1 (9-hydroxy-tacrolimus). To the best of our knowledge, this represents the first experimental evidence for commensal gut bacteria being involved in the metabolism of tacrolimus. M1 is ~15-fold less potent than tacrolimus in inhibiting both the proliferation of activated T-lymphocytes and the growth of the yeast *M. sympodialis*. This result is consistent with the currently available structure-activity relationships of tacrolimus analogs; modifications at the C-9 position affect the interaction of tacrolimus with its effector protein (i.e., FK506 binding protein 12) and lead to decreased immunosuppressant activities (Goulet et al., 1994).

In animals and humans, tacrolimus is eliminated mainly via biliary excretion as metabolites (IWASAKI et al., 1998a; IWASAKI et al., 1998b; Möller et al., 1999). However, only a few metabolites have been identified upon tacrolimus incubation with hepatic microsomes, with 13-*O*-demethyltacrolimus being the major product (Christians et al., 1991; Christians et al., 1992). Most tacrolimus metabolites remain unidentified (Iwasaki et al., 1993; Iwasaki, 2007), suggesting that unknown metabolic pathways (potentially mediated by gut bacteria) may be responsible for their production. Our data from clinical samples reveal that the bacterial M1 product is present in both human feces and blood, supporting the notion of active metabolism of tacrolimus by gut bacteria. M1 concentration was found much lower as compared to tacrolimus in the blood, which is consistent with results from previous tacrolimus disposition studies using a radiolabeled compound (Moller et al., 1999). Since M1 is 15-fold less immunosuppressive than parent tacrolimus, it is unlikely M1 contributes significantly to immunosuppressive effects on the host. Although tacrolimus and M1 are both cleared rapidly upon *in vitro* hepatic microsomal

incubation, M1 shows 4-fold lower RBC binding that is known as a rate-limiting factor for tacrolimus clearance. Thus, low exposure of M1 may be explained by fast elimination *in vivo*.

Multiple factors have been reported to contribute to the low and variable bioavailability of orally administered tacrolimus. These include differential expression and/or activity levels of cytochrome P450 enzymes (especially CYP3A5 polymorphism) and the drug transporter P-glycoprotein (P-gp) in the intestine and liver (Staatz and Tett, 2004). Previous pharmacokinetic studies in healthy volunteers and renal transplant recipients have shown that hepatic extraction of tacrolimus is very low (i.e., 4-8%) (Floren et al., 1997; Tuteja et al., 2001), suggesting that the low oral bioavailability of tacrolimus is mainly due to drug loss in the gut. P-gp-mediated drug efflux and intestinal CYP3A-mediated metabolism were proposed as major contributors to the loss. However, results from drug-drug interaction studies have shown that oral bioavailability of tacrolimus increases to at most ~30% when co-administered with ketoconazole, a potent inhibitor of CYP3As and P-gp (Floren et al., 1997; Tuteja et al., 2001); 50% of the oral dose is lost (not reaching systemic circulation) even when intestinal CYP3A and P-gp activities are blocked by ketoconazole.

Our results also revealed that multiple commensal gut bacteria are capable of metabolizing tacrolimus, suggesting that differences in gut bacterial composition may lead to differential tacrolimus exposure in kidney transplant recipients. Gut bacteria that extensively metabolized tacrolimus into M1 (including *F. prausnitzii*) belong to the *Clostridiales* order. On the other hand, bacteria in Bacteroidales were found to be weak producers of M1 (i.e., detectable only by sensitive HPLC/MS/MS), and *B. longum* in *Bifidobacteriales* did not produce detectable amounts of M1. A previous study has shown

that fecal abundance of *F. prausnitzii* (belonging to *Clostridiales* order) was positively correlated with oral tacrolimus dose in 19 kidney transplant patients (Lee et al., 2015). However, we observed no differences in M1 production between high and low *F. prausnitzii* groups of stool samples. Also, we did not observe correlation between *Clostridiales* abundance and M1 production in the stool samples. This may be due to the small number of samples used for this exploratory study and/or the quality of samples non-optimal for enzymatic assays. The presence of multiple factors affecting gut bacterial gene expression *in vivo* such as nutritional status of the gut may further explain why we do not observe a correlation between our *in vitro* culture-based results and *in vivo* abundance of gut bacteria. For example, the amino acid arginine was shown to repress the expression of the gene encoding digoxin-metabolizing enzyme in *E. lenta*, thus reducing digoxin elimination by gut bacteria (Haiser et al., 2013b). Obviously, *in vitro* culture-based systems do not fully reflect the bacterial functions activated in the physiological gut ecosystem.

We attempted to estimate the overall magnitude of tacrolimus metabolism in the human small intestine using *F. prausnitzii* as a model gut bacterium. *F. prausnitzii* was chosen because it is one of the most abundant bacterium (at the bacterial species level) in the human gut including the small intestine (Sokol et al., 2008; Qin et al., 2010; Lopez-Siles et al., 2015). Our estimation indicates that about 1.9 mg of M1 may be produced in the small intestine during drug transit through the organ. Considering that the typical oral dose of tacrolimus ranges from 2 to 5 mg, a significant fraction of the orally administered tacrolimus may be lost by gut bacterial metabolism before absorption. Our results suggest that tacrolimus conversion to M1 in the gut may represent a previously unrecognized pathway of tacrolimus elimination in the gut, potentially contributing to tacrolimus loss in

the gut. This suggests that changes in the gut microbiota via antibiotics or diet could impact tacrolimus trough variability. In a retrospective cohort study of 260 kidney transplant recipients, our group recently identified that antibiotic administration is associated with tacrolimus trough variability, thus indirectly supporting a potential role of the gut microbiota on tacrolimus trough variability (Zheng et al., 2019). On the other hand, it should be noted that our calculation may grossly overestimate or underestimate the true extent of tacrolimus metabolism in the gut because (1) bacterial gene expression (and thereby function) in the gut is likely different from that in the laboratory medium used in our study; (2) the capacity of other gut bacteria to metabolize tacrolimus may be widely different as compared to that of *F. prausnitzii*; and (3) a low solubility drug such as tacrolimus may reach the lower gastrointestinal tract (Sousa et al., 2008a) and be presented to a large amount of gut bacteria in the colon. Slow absorption of tacrolimus over a prolonged period has been reported clinically (Venkataramanan et al., 1995).

We also attempted to use rodent model to study the contribution of gut bacterial metabolism in oral drug exposure. However, we did not see significant difference in AUC between mice w/wo antibiotics' treatment. Incubation of tacrolimus with mice small intestinal content showed negligible conversion. Suggesting mouse small intestinal bacteria does not significantly metabolize tacrolimus. Comparing the bacterial composition between mouse and human reveals a significant difference in major bacterial taxa in major tacrolimus absorption site: human duodenum and jejunum harbors major tacrolimus metabolizing bacteria *Clostridia*, represent 31% and 10% of the total bacteria respectively (Wang et al., 2005; Nadal et al., 2007). While it only account for 5% in our mouse model (data not shown). Thus, lacking tacrolimus metabolizing bacteria in small intestine may explain the unexpected result. Species difference need to be taken into

consideration when performing translation study for drug metabolism (Nguyen et al., 2015).

Our mechanistic study revealed oxidoreductases that utilizing NADPH/NADH as proton donors are enzymes responsible for mediating tacrolimus to M1 conversions in *F. prausnitzii*. The nature of these enzymes being oxygen-sensitive for may be explained by the involvement of iron-sulfur clusters in the redox reaction, which is known to be decomposed by oxygen (Imlay, 2006). Through the heterogeneous expression of candidate oxidoreductases in *E. coli*, we found multiple oxidoreductases are capable of catalyzing ketone reduction of tacrolimus in *F. prausnitzii*. Their combined activity may explain the high conversion of tacrolimus to M1 by *F. prausnitzii*. This result may also explain the prevalence of tacrolimus metabolism by gut bacteria in previous *in vitro* experiments.

In summary, we present the evidence of tacrolimus metabolism by gut bacteria, providing potential explanations for its low oral bioavailability. Tacrolimus metabolism into M1 may represent a novel elimination pathway that occurs before intestinal absorption of tacrolimus. While the extent of gut metabolism of tacrolimus on variable tacrolimus exposure remains to be determined, our data provide a novel understanding of tacrolimus metabolism and may explain variability in tacrolimus exposures in kidney transplant recipients and patients with glomerular diseases on tacrolimus therapy.

CONCLUSION AND FUTURE DIRECTIONS

In my thesis project, we identified a bacteria-mediated tacrolimus elimination pathway. Both *in vitro* and *in vivo* results indicated that human gut bacteria could convert tacrolimus into less active metabolite M1 through ketone reduction. Beyond known contributing factors including CYP3A4/5 mediated oxidation and efflux by P-gp, bacterial metabolism of tacrolimus appears to be an additional important factor responsible for extensive intestinal extraction and low oral bioavailability observed in the clinic. From a mechanistic stand point, we discovered multiple oxidoreductases in *F. prausnitzii* that are capable of metabolizing tacrolimus to M1.

Tacrolimus exhibits a narrow therapeutic index, such that over- and under-exposure to tacrolimus increase the risks for drug-related toxicity and graft rejection, respectively. For a future direction, we aimed to investigate potential DDI resulted from inhibition of bacterial metabolism of tacrolimus. For example, co-administration of antiviral drugs, including telaprevir and boceprevir, were reported to increase tacrolimus AUC by 70 and 17-fold, respectively (Garg et al., 2011; Coilly et al., 2014). Interestingly, both compounds are structurally similar as tacrolimus that contain α-keto amide, where the bacterial metabolism occurs. Thus, in addition to inhibiting CYP3A4/5 activity, competition for metabolizing enzymes with tacrolimus may also be a major reason for significantly enhanced tacrolimus oral exposure observed in the clinic. Fully understanding their roles in inhibiting bacterial metabolism of tacrolimus may help to optimize tacrolimus dosage regimen and improving graft outcomes in transplant recipients in the long run.

CITED LITERATURE

Achilli C, Ciana A, and Minetti G (2015) The discovery of methionine sulfoxide reductase enzymes: An historical account and future perspectives. *Biofactors* **41:**135-152.

Ali Y, Hamid SA, and Rashid U (2018) Biomedical applications of aromatic azo compounds. *Mini Rev Med Chem* **18:**1548-1558.

Arumugam M, Raes J, Pelletier E, Le Paslier D, Yamada T, Mende DR, Fernandes GR, Tap J, Bruls T, Batto JM, Bertalan M, Borruel N, Casellas F, Fernandez L, Gautier L, Hansen T, Hattori M, Hayashi T, Kleerebezem M, Kurokawa K, Leclerc M, Levenez F, Manichanh C, Nielsen HB, Nielsen T, Pons N, Poulain J, Qin J, Sicheritz-Ponten T, Tims S, Torrents D, Ugarte E, Zoetendal EG, Wang J, Guarner F, Pedersen O, de Vos WM, Brunak S, Dore J, Meta HITC, Antolin M, Artiguenave F, Blottiere HM, Almeida M, Brechot C, Cara C, Chervaux C, Cultrone A, Delorme C, Denariaz G, Dervyn R, Foerstner KU, Friss C, van de Guchte M, Guedon E, Haimet F, Huber W, van Hylckama-Vlieg J, Jamet A, Juste C, Kaci G, Knol J, Lakhdari O, Layec S, Le Roux K, Maguin E, Merieux A, Melo Minardi R, M'Rini C, Muller J, Oozeer R, Parkhill J, Renault P, Rescigno M, Sanchez N, Sunagawa S, Torrejon A, Turner K, Vandemeulebrouck G, Varela E, Winogradsky Y, Zeller G, Weissenbach J, Ehrlich SD, and Bork P (2011) Enterotypes of the human gut microbiome. *Nature* **473:**174-180.

Azadkhan AK, Truelove SC, and Aronson JK (1982) The disposition and metabolism of sulphasalazine (salicylazosulphapyridine) in man. *Br J Clin Pharmacol* **13:**523-528.

Bäckman L, Nicar M, Levy M, Distant D, Eisenstein C, Renard T, Goldstein R, Husberg B, Gonwa TA, and Klintmalm G (1994) FK506 trough levels in whole blood and plasma in liver transplant recipients. Correlation with clinical events and side effects. *Transplantation* **57:**519-525.

Ballet F, Vrignaud P, Robert J, Rey C, and Poupon R (1987) Hepatic extraction, metabolism and biliary excretion of doxorubicin in the isolated perfused rat liver. *Cancer Chemother Pharmacol* **19:**240-245.

Barry A and Levine M (2010) A systematic review of the effect of CYP3A5 genotype on the apparent oral clearance of tacrolimus in renal transplant recipients. *Ther Drug Monit* **32:**708-714.

Barski OA, Tipparaju SM, and Bhatnagar A (2008) The aldo-keto reductase superfamily and its role in drug metabolism and detoxification. *Drug Metab Rev* **40:**553-624.

Basit AW and Lacey LF (2001) Colonic metabolism of ranitidine: implications for its delivery and absorption. *Int J Pharm* **227:**157-165.

Basit AW, Newton JM, and Lacey LF (2002) Susceptibility of the H2-receptor antagonists cimetidine, famotidine and nizatidine, to metabolism by the gastrointestinal microflora. *International journal of pharmaceutics* **237:**23-33.

Beckett AH, Gorrod JW, and Jenner P (1970) Absorption of (-)-nicotine-l-N-oxide in man and its reduction in the gastrointestinal tract. *J Pharm Pharmacol* **22:**722-723.

Birdwell K, Decker B, Barbarino J, Peterson J, Stein C, Sadee W, Wang D, Vinks A, He Y, Swen J, Leeder J, van Schaik R, Thummel K, Klein T, Caudle K, and MacPhee I (2015) Clinical Pharmacogenetics Implementation Consortium (CPIC) Guidelines for CYP3A5 Genotype and Tacrolimus Dosing. *Clinical Pharmacology & Therapeutics* **98:**19-24.

Birolli WG, Ferrreira IM, Jimenez DEQ, Silva BNM, Silva BV, Pinto AC, and Porto ALM (2017) First Asymmetric Reduction of Isatin by Marine-Derived Fungi. *Journal of the Brazilian Chemical Society* **28:**1023-1029.

Blair LM and Sperry J (2013) Natural products containing a nitrogen-nitrogen bond. *J Nat Prod* **76:**794-812.

Bodemar G, Norlander B, Fransson L, and Walan A (1979) The absorption of cimetidine before and during maintenance treatment with cimetidine and the influence of a meal on the absorption of cimetidine--studies in patients with peptic ulcer disease. *Br J Clin Pharmacol* **7:**23-31.

Brown JP (1981) Reduction of polymeric azo and nitro dyes by intestinal bacteria. *Appl Environ Microbiol* **41:**1283-1286.

Brunell D, Sagher D, Kesaraju S, Brot N, and Weissbach H (2011) Studies on the metabolism and biological activity of the epimers of sulindac. *Drug Metab Dispos* **39:**1014-1021.

Caillard S, Moulin B, Buron F, Mariat C, Audard V, Grimbert P, and Marquet P (2016) Advagraf®, a once-daily prolonged release tacrolimus formulation, in kidney transplantation: literature review and guidelines from a panel of experts. *Transplant International* **29:**860-869.

Cashman JR, Park SB, Yang ZC, Wrighton SA, Jacob P, 3rd, and Benowitz NL (1992) Metabolism of nicotine by human liver microsomes: stereoselective formation of trans-nicotine N'-oxide. *Chem Res Toxicol* **5:**639-646.

Celesk RA, Asano T, and Wagner M (1976) The size pH, and redox potential of the cecum in mice associated with various microbial floras. *Proc Soc Exp Biol Med* **151:**260-263.

Chen LZ, Sabo JP, Philip E, Rowland L, Mao Y, Latli B, Ramsden D, Mandarino DA, and Sane RS (2015) Mass balance, metabolite profile, and in vitro-in vivo comparison of clearance pathways of deleobuvir, a hepatitis C virus polymerase inhibitor. *Antimicrob Agents Chemother* **59:**25-37.

Cheng R, Tu T, Shackel N, and McCaughan GW (2014) Advances in and the future of treatments for hepatitis C. *Expert Rev Gastroenterol Hepatol* **8:**633-647.

Chitnis SD, Ogasawara K, Schniedewind B, Gohh RY, Christians U, and Akhlaghi F (2013) Concentration of tacrolimus and major metabolites in kidney transplant recipients as a function of diabetes mellitus and cytochrome P450 3A gene polymorphism. *Xenobiotica; the fate of foreign compounds in biological systems* **43:**641-649.

Choi JH, Lee YJ, Jang SB, Lee J-E, Kim KH, and Park K (2007) Influence of the CYP3A5 and MDR1 genetic polymorphisms on the pharmacokinetics of tacrolimus in healthy Korean subjects. *British Journal of Clinical Pharmacology* **64:**185-191.

Chow FS, Piekoszewski W, and Jusko WJ (1997) Effect of hematocrit and albumin concentration on hepatic clearance of tacrolimus (FK506) during rabbit liver perfusion. *Drug Metab Dispos* **25:**610-616.

Christians U, Braun F, Kosian N, Schmidt M, Schiebel H, Ernst L, Kruse C, Winkler M, Holze I, and Linck A (1991) High performance liquid chromatography/mass spectrometry of FK 506 and its metabolites in blood, bile, and urine of liver grafted patients, in: *Transplantation proceedings,* pp 2741.

Christians U, Braun F, Schmidt M, Kosian N, Schiebel H, Ernst L, Winkler M, Kruse C, Linck A, and Sewing K-F (1992) Specific and sensitive measurement of FK506 and its metabolites in blood and urine of liver-graft recipients. *Clinical chemistry* **38:**2025-2032.

Christians U, Schmitz V, and Haschke M (2005) Functional interactions between P-glycoprotein and CYP3A in drug metabolism. *Expert opinion on drug metabolism & toxicology* **1:**641-654.

Chung KT (2016) Azo dyes and human health: A review. *J Environ Sci Health C Environ Carcinog Ecotoxicol Rev* **34:**233-261.

Chung KT, Fulk GE, and Egan M (1978) Reduction of azo dyes by intestinal anaerobes. *Appl Environ Microbiol* **35:**558-562.

Circu ML and Aw TY (2011) Redox biology of the intestine. *Free Radic Res* **45:**1245-1266.

Clackson T, Yang W, Rozamus LW, Hatada M, Amara JF, Rollins CT, Stevenson LF, Magari SR, Wood SA, Courage NL, Lu X, Cerasoli F, Gilman M, and Holt DA (1998) Redesigning an FKBP–ligand interface to generate chemical dimerizers with novel specificity. *Proceedings of the National Academy of Sciences* **95:**10437-10442.

Clark DR and Kalman SM (1974) Dihydrodigoxin: a common metabolite of digoxin in man. *Drug Metab Dispos* **2:**148-150.

Clarke G, Sandhu KV, Griffin BT, Dinan TG, Cryan JF, and Hyland NP (2019) Gut reactions: Breaking down xenobiotic-microbiome interactions. *Pharmacol Rev* **71:**198-224.

Coilly A, Roche B, Dumortier J, Leroy V, Botta-Fridlund D, Radenne S, Pageaux G-P, Si-Ahmed S-N, Guillaud O, Antonini TM, Haïm-Boukobza S, Roque-Afonso A-M, Samuel D, and Duclos-Vallée J-C (2014) Safety and efficacy of protease inhibitors to treat hepatitis C after liver transplantation: A multicenter experience. *J Hepatol* **60:**78-86.

Colburn WA, Bekersky I, Min BH, Hodshon BJ, and Garland WA (1980) Contribution of gut contents, intestinal wall and liver to the first-pass metabolism of clonazepam in the rat. *Res Commun Chem Pathol Pharmacol* **27:**73-90.

Colebrook L, Buttle GAH, and O'Meara RAQ (1936) The mode of action of *p*-aminobenzenesulphonamide and prontosil in hemolytic Streptococcal infections. *Lancet* **228:**1323-1326.

Crespo M, Mir M, Marin M, Hurtado S, Estadella C, Guri X, Rap O, Moral R, Puig J, and Lloveras J (2009) De novo kidney transplant recipients need higher doses of Advagraf compared with Prograf to get therapeutic levels, in: *Transplantation proceedings*, pp 2115-2117, Elsevier.

Crofts TS, Sontha P, King AO, Wang B, Biddy BA, Zanolli N, Gaumnitz J, and Dantas G (2019) Discovery and characterization of a nitroreductase capable of conferring bacterial resistance to chloramphenicol. *Cell Chem Biol* **26:**559-570.e556.

Dai Y, Hebert MF, Isoherranen N, Davis CL, Marsh C, Shen DD, and Thummel KE (2006) EFFECT OF *CYP3A5* POLYMORPHISM ON TACROLIMUS METABOLIC CLEARANCE IN VITRO. *Drug Metabolism and Disposition* **34:**836-847.

Dajani R, Gorrod J, and Beckett A (1975a) Reduction in vivo of (−)-nicotine-1′-N-oxide by germ-free and conventional rats. *Biochemical pharmacology* **24:**648-650.

Dajani RM, Gorrod JW, and Beckett AH (1975b) In vitro hepatic and extra-hepatic reduction of (minus)-nicotine-1'-N-oxide in rats. *Biochem Pharmacol* **24:**109-117.

Dajani RM, Gorrod JW, and Beckett AH (1975c) Reduction in vivo of (minus)-nicotine-1'-N-oxide by germ-free and conventional rats. *Biochem Pharmacol* **24:**648-650.

Damani LA (1991) *N-Oxidation of drugs: Biochemistry, Pharmacology and Toxicology*. Springer Science.

Das KM, Eastwood MA, McManus JP, and Sircus W (1973) The metabolism of salicylazosulphapyridine in ulcerative colitis. I. The relationship between metabolites and the response to treatment in inpatients. *Gut* **14:**631-641.

Davies NM (1997) Clinical pharmacokinetics of nabumetone. The dawn of selective cyclo-oxygenase-2 inhibition? *Clin Pharmacokinet* **33:**404-416.

de Jonge H, Kuypers DR, Verbeke K, and Vanrenterghem Y (2010) Reduced C0 Concentrations and Increased Dose Requirements in Renal Allograft Recipients Converted to the Novel Once-Daily Tacrolimus Formulation. *Transplantation* **90:**523-529.

Dick AT, Dann AT, Bull LB, and Culvenok CCJ (1963) Vitamin B12 and the detoxification of hepatotoxic pyrrolizidine alkaloids in rumen liquor. *Nature* **197:**207-208.

Dietemann J, Berthoux P, Gay-Montchamp JP, Batie M, and Berthoux F (2001) Comparison of ELISA method versus MEIA method for daily practice in the therapeutic monitoring of tacrolimus. *Nephrol Dial Transplant* **16:**2246-2249.

Dieterle W, Faigle JW, and Moppert J (1980) New metabolites of sulfinpyrazone in man. *Arzneimittelforschung* **30:**989-993.

Dinos GP, Athanassopoulos CM, Missiri DA, Giannopoulou PC, Vlachogiannis IA, Papadopoulos GE, Papaioannou D, and Kalpaxis DL (2016) Chloramphenicol derivatives as antibacterial and anticancer agents: Historic problems and current solutions. *Antibiotics (Basel)* **5**.

Dobrinska MR, Furst DE, Spiegel T, Vincek WC, Tompkins R, Duggan DE, Davies RO, and Paulus HE (1983) Biliary secretion of sulindac and metabolites in man. *Biopharm Drug Dispos* **4:**347-358.

Dodd D, Spitzer MH, Van Treuren W, Merrill BD, Hryckowian AJ, Higginbottom SK, Le A, Cowan TM, Nolan GP, Fischbach MA, and Sonnenburg JL (2017) A gut bacterial pathway metabolizes aromatic amino acids into nine circulating metabolites. *Nature* **551:**648-652.

Domagk G (1957) Twenty-five years of sulfonamide therapy. *Ann N Y Acad Sci* **69:**380-384.

Duggan DE (1981) Sulindac: therapeutic implications of the prodrug/pharmacophore equilibrium. *Drug Metab Rev* **12:**325-337.

Duggan DE, Hare LE, Ditzler CA, Lei BW, and Kwan KC (1977a) The disposition of sulindac. *Clin Pharmacol Ther* **21:**326-335.

Duggan DE, Hooke KF, Risley EA, Shen TY, and Arman CG (1977b) Identification of the biologically active form of sulindac. *J Pharmacol Exp Ther* **201:**8-13.

Ehle M, Patel C, and Giugliano RP (2011) Digoxin: clinical highlights: a review of digoxin and its use in contemporary medicine. *Crit Pathw Cardiol* **10:**93-98.

Ehrlich J, Bartz QR, Smith RM, Joslyn DA, and Burkholder PR (1947) Chloromycetin, a new antibiotic from a soil *Actinomycete*. *Science* **106:**417.

Elmer GW and Remmel RP (1984) Role of the intestinal microflora in clonazepam metabolism in the rat. *Xenobiotica* **14:**829-840.

Emmons G and Rowland M (2010) Pharmacokinetic considerations as to when to use dried blood spot sampling. *Bioanalysis* **2:**1791-1796.

Espey MG (2013) Role of oxygen gradients in shaping redox relationships between the human intestine and its microbiota. *Free Radic Biol Med* **55:**130-140.

Etienne F, Resnick L, Sagher D, Brot N, and Weissbach H (2003) Reduction of Sulindac to its active metabolite, sulindac sulfide: assay and role of the methionine sulfoxide reductase system. *Biochem Biophys Res Commun* **312:**1005-1010.

Feng J, Cerniglia CE, and Chen H (2012) Toxicological significance of azo dye metabolism by human intestinal microbiota. *Front Biosci (Elite Ed)* **4:**568-586.

Floren LC, Bekersky I, Benet LZ, Mekki Q, Dressler D, Lee JW, Roberts JP, and Hebert MF (1997) Tacrolimus oral bioavailability doubles with coadministration of ketoconazole. *Clin Pharmacol Ther* **62:**41-49.

Friedman ES, Bittinger K, Esipova TV, Hou L, Chau L, Jiang J, Mesaros C, Lund PJ, Liang X, FitzGerald GA, Goulian M, Lee D, Garcia BA, Blair IA, Vinogradov SA, and Wu GD (2018) Microbes vs. chemistry in the origin of the anaerobic gut lumen. *Proc Natl Acad Sci U S A* **115:**4170-4175.

Fritz A, Busch D, Lapczuk J, Ostrowski M, Drozdzik M, and Oswald S (2019) Expression of clinically relevant drug-metabolizing enzymes along the human intestine and their correlation to drug transporters and nuclear receptors: An intra-subject analysis. *Basic & Clinical Pharmacology & Toxicology* **124:**245-255.

Fuller AT (1937) Is *p*-aminobenzenesulphonamide the active agent in prontosil therapy? *Lancet* **229:**194-198.

Gardiner KM, Tett SE, and Staatz CE (2016) Multinational evaluation of mycophenolic acid, tacrolimus, cyclosporin, sirolimus, and everolimus utilization. *Ann Transplant* **21:**1-11.

Garg V, van Heeswijk R, Eun Lee J, Alves K, Nadkarni P, and Luo X (2011) Effect of telaprevir on the pharmacokinetics of cyclosporine and tacrolimus. *Hepatology* **54:**20-27.

Geertz-Hansen HM, Blom N, Feist AM, Brunak S, and Petersen TN (2014) Cofactory: Sequence-based prediction of cofactor specificity of Rossmann folds. *Proteins: Structure, Function, and Bioinformatics* **82:**1819-1828.

Gewirtz DA (1999) A critical evaluation of the mechanisms of action proposed for the antitumor effects of the anthracycline antibiotics adriamycin and daunorubicin. *Biochem Pharmacol* **57:**727-741.

Gidai J, Acs N, Banhidy F, and Czeizel AE (2010) Congenital abnormalities in children of 43 pregnant women who attempted suicide with large doses of nitrazepam. *Pharmacoepidemiol Drug Saf* **19:**175-182.

Gill SR, Pop M, DeBoy RT, Eckburg PB, Turnbaugh PJ, Samuel BS, Gordon JI, Relman DA, Fraser-Liggett CM, and Nelson KE (2006) Metagenomic analysis of the human distal gut microbiome. *Science* **312:**1355-1359.

Gingell R, Bridges J, and Williams R (1969a) Gut flora and the metabolism of prontosils in the rat. *Biochemical Journal* **114:**5P.

Gingell R and Bridges JW (1971) Intestinal azo reduction and glucuronide conjugation of prontosil. *Biochem J* **125:**24p.

Gingell R, Bridges JW, and Williams RT (1969b) Gut flora and the metabolism of prontosils in the rat. *Biochem J* **114:**5p-6p.

Golovenko NY, Bogatskii AV, Orlyuk EI, Kurushin AA, and Karaseva TL (1977) Metabolism of nitrazepam in the intestine of albino rats. *Bull Exp Biol Med* **84:**981-984.

Gonschior AK, Christians U, Winkler M, Linck A, Baumann J, and Sewing KF (1996) Tacrolimus (FK506) metabolite patterns in blood from liver and kidney transplant patients. *Clin Chem* **42:**1426-1432.

Goto M, Masuda S, Kiuchi T, Ogura Y, Oike F, Okuda M, Tanaka K, and Inui K-i (2004) CYP3A5*1-carrying graft liver reduces the concentration/oral dose ratio of tacrolimus in recipients of living-donor liver transplantation. *Pharmacogenetics and Genomics* **14**.

Goulet M, Rupprecht K, Sinclar P, Wyvratt M, and Parsons W (1994) The medicinal chemistry of FK-506. *Perspectives in Drug Discovery and Design* **2:**145.

Gruber SA, Hewitt JM, Sorenson AL, Barber DL, Bowers L, Rynders G, Arrazola L, Matas AJ, Rosenberg ME, and Canafax DM (1994) Pharmacokinetics of FK506 after

intravenous and oral administration in patients awaiting renal transplantation. *Journal of clinical pharmacology* **34:**859-864.

Haiser HJ, Gootenberg DB, Chatman K, Sirasani G, Balskus EP, and Turnbaugh PJ (2013a) Predicting and manipulating cardiac drug inactivation by the human gut bacterium *Eggerthella lenta*. *Science* **341:**295-298.

Haiser HJ, Gootenberg DB, Chatman K, Sirasani G, Balskus EP, and Turnbaugh PJ (2013b) Predicting and manipulating cardiac drug inactivation by the human gut bacterium Eggerthella lenta. *Science* **341:**295-298.

Hamman MA, Haehner-Daniels BD, Wrighton SA, Rettie AE, and Hall SD (2000) Stereoselective sulfoxidation of sulindac sulfide by flavin-containing monooxygenases. Comparison of human liver and kidney microsomes and mammalian enzymes. *Biochem Pharmacol* **60:**7-17.

Hauso O, Martinsen TC, and Waldum H (2015) 5-Aminosalicylic acid, a specific drug for ulcerative colitis. *Scand J Gastroenterol* **50:**933-941.

Hedner T, Samulesson O, Wahrborg P, Wadenvik H, Ung KA, and Ekbom A (2004) Nabumetone: therapeutic use and safety profile in the management of osteoarthritis and rheumatoid arthritis. *Drugs* **64:**2315-2343; discussion 2344-2315.

Hewick DS and Shaw V (1978) The importance of the intestinal microflora in nitrazepam metabolism in the rat [proceedings]. *Br J Pharmacol* **62:**427p.

Hirata S, Izumi S, Furukubo T, Ota M, Fujita M, Yamakawa T, Hasegawa I, Ohtani H, and Sawada Y (2005) Interactions between clarithromycin and digoxin in patients with end-stage renal disease. *Int J Clin Pharmacol Ther* **43:**30-36.

Hoffmann F and Maser E (2007) Carbonyl reductases and pluripotent hydroxysteroid dehydrogenases of the short-chain dehydrogenase/reductase superfamily. *Drug Metab Rev* **39:**87-144.

Holt R (1967a) The bacterial degradation of chloramphenicol. *Lancet (London, England)* **1:**1259.

Holt R (1967b) The bacterial degradation of chloramphenicol. *Lancet* **1:**1259-1260.

Houston JB, Day J, and Walker J (1982) Azo reduction of sulphasalazine in healthy volunteers. *Br J Clin Pharmacol* **14:**395-398.

Ianiri G, Applen Clancey S, Lee SC, and Heitman J (2017) FKBP12-Dependent Inhibition of Calcineurin Mediates Immunosuppressive Antifungal Drug Action in Malassezia. *MBio* **8**.

Imlay JA (2006) Iron-sulphur clusters and the problem with oxygen. *Molecular Microbiology* **59:**1073-1082.

Ishihara K, Yamamoto H, Mitsuhashi K, Nishikawa K, Tsuboi S, Tsuji H, and Nakajima N (2004) Purification and characterization of alpha-keto amide reductase from Saccharomyces cerevisiae. *Biosci Biotechnol Biochem* **68:**2306-2312.

Iwasaki K (2007) Metabolism of tacrolimus (FK506) and recent topics in clinical pharmacokinetics. *Drug Metab Pharmacokinet* **22:**328-335.

IWASAKI K, SHIRAGA T, MATSUDA H, KAWAMURA A, HATA T, and Chasseaud L (1998a) Absorption, distribution and excretion of tacrolimus (FK506) in the baboon. *Drug Metabolism and Pharmacokinetics* **13:**478-483.

Iwasaki K, Shiraga T, Matsuda H, Nagase K, Tokuma Y, Hata T, Fujii Y, Sakuma S, Fujitsu T, and Fujikawa A (1995) Further metabolism of FK506 (tacrolimus). Identification and

biological activities of the metabolites oxidized at multiple sites of FK506. *Drug Metabolism and Disposition* **23:**28-34.

IWASAKI K, SHIRAGA T, MATSUDA H, TERAMURA Y, KAWAMURA A, HATA T, NINOMIYA S, and EsuMI Y (1998b) Absorption, distribution, metabolism and excretion of tacrolimus (FK506) in the rat. *Drug Metabolism and Pharmacokinetics* **13:**259-265.

Iwasaki K, Shiraga T, Nagase K, Tozuka Z, Noda K, Sakuma S, Fujitsu T, Shimatani K, Sato A, and Fujioka M (1993) Isolation, identification, and biological activities of oxidative metabolites of FK506, a potent immunosuppressive macrolide lactone. *Drug metabolism and disposition* **21:**971-977.

Jacquet JM, Bressolle F, Galtier M, Bourrier M, Donadio D, Jourdan J, and Rossi JF (1990) Doxorubicin and doxorubicinol: intra- and inter-individual variations of pharmacokinetic parameters. *Cancer Chemother Pharmacol* **27:**219-225.

Jourova L, Anzenbacher P, Matuskova Z, Vecera R, Strojil J, Kolar M, Nobilis M, Hermanova P, Hudcovic T, Kozakova H, Kverka M, and Anzenbacherova E (2019) Gut microbiota metabolizes nabumetone in vitro: Consequences for its bioavailability in vivo in the rodents with altered gut microbiome. *Xenobiotica* **49:**1296-1302.

Ju KS and Parales RE (2010) Nitroaromatic compounds, from synthesis to biodegradation. *Microbiol Mol Biol Rev* **74:**250-272.

Jusko WJ, Piekoszewski W, Klintmalm GB, Shaefer MS, Hebert MF, Piergies AA, Lee CC, Schechter P, and Mekki QA (1995) Pharmacokinetics of tacrolimus in liver transplant patients. *Clin Pharmacol Ther* **57:**281-290.

Kinouchi T and Ohnishi Y (1983) Purification and characterization of 1-nitropyrene nitroreductases from *Bacteroides fragilis*. *Appl Environ Microbiol* **46:**596-604.

Kitamura S, Sugihara K, and Tatsumi K (1999) A unique tertiary amine N-oxide reduction system composed of quinone reductase and heme in rat liver preparations. *Drug Metab Dispos* **27:**92-97.

Kitamura S, Tatsumi K, and Yoshimura H (1980) Metabolism in vitro of sulindac. Sulfoxide-reducing enzyme systems in guinea pig liver. *J Pharmacobiodyn* **3:**290-298.

Klotz U and Walker S (1990) Biliary excretion of H2-receptor antagonists. *Eur J Clin Pharmacol* **39:**91-92.

Kolars JC, Lown KS, Schmiedlin-Ren P, Ghosh M, Fang C, Wrighton SA, Merion RM, and Watkins PB (1994) CYP 3A gene expression in human gut epithelium. *Pharmacogenetics* **4:**247-259.

Koppel N, Bisanz JE, Pandelia ME, Turnbaugh PJ, and Balskus EP (2018) Discovery and characterization of a prevalent human gut bacterial enzyme sufficient for the inactivation of a family of plant toxins. *Elife* **7**.

Larriba J, Imperiali N, Groppa R, Giordani C, Algranatti S, and Redal MA (2010) Pharmacogenetics of immunosuppressant polymorphism of CYP3A5 in renal transplant recipients. *Transplant Proc* **42:**257-259.

Lavrijsen K, Van Dyck D, Van Houdt J, Hendrickx J, Monbaliu J, Woestenborghs R, Meuldermans W, and Heykants J (1995a) Reduction of the prodrug loperamide oxide to its active drug loperamide in the gut of rats, dogs, and humans. *Drug metabolism and disposition* **23:**354-362.

Lavrijsen K, van Dyck D, van Houdt J, Hendrickx J, Monbaliu J, Woestenborghs R, Meuldermans W, and Heykants J (1995b) Reduction of the prodrug loperamide oxide to its active drug loperamide in the gut of rats, dogs, and humans. *Drug Metab Dispos* **23:**354-362.

Lee JR, Muthukumar T, Dadhania D, Taur Y, Jenq RR, Toussaint NC, Ling L, Pamer E, and Suthanthiran M (2015) Gut microbiota and tacrolimus dosing in kidney transplantation. *PLoS One* **10:**e0122399.

Levin AA and Dent JG (1982) Comparison of the metabolism of nitrobenzene by hepatic microsomes and cecal microflora from Fischer-344 rats in vitro and the relative importance of each in vivo. *Drug Metab Dispos* **10:**450-454.

Levine WG (1991) Metabolism of azo dyes: implication for detoxication and activation. *Drug Metab Rev* **23:**253-309.

Lindenbaum J, Rund DG, Butler VP, Tse-Eng D, and Saha JR (1981) Inactivation of Digoxin by the Gut Flora: Reversal by Antibiotic Therapy. *New England Journal of Medicine* **305:**789-794.

Lindenbaum J, Rund DG, Butler VPJ, Tse-Eng D, and Saha JR (1981) Inactivation of digoxin by the gut flora: Reversal by antibiotic therapy. *N Eng J Med* **305:**789-794.

LinWu S-W, Syu C-J, Chen Y-L, Wang AH-J, and Peng F-C (2009a) Characterization of Escherichia coli nitroreductase NfsB in the metabolism of nitrobenzodiazepines. *Biochemical pharmacology* **78:**96-103.

Linwu SW, Syu CJ, Chen YL, Wang AH, and Peng FC (2009b) Characterization of Escherichia coli nitroreductase NfsB in the metabolism of nitrobenzodiazepines. *Biochem Pharmacol* **78:**96-103.

Liu G, Zhou J, Fu QS, and Wang J (2009) The *Escherichia coli* azoreductase AzoR is involved in resistance to thiol-specific stress caused by electrophilic quinones. *J Bacteriol* **191:**6394-6400.

Lopez-Siles M, Martinez-Medina M, Abella C, Busquets D, Sabat-Mir M, Duncan SH, Aldeguer X, Flint HJ, and Garcia-Gil LJ (2015) Mucosa-associated Faecalibacterium

prausnitzii phylotype richness is reduced in patients with inflammatory bowel disease. *Appl Environ Microbiol* **81:**7582-7592.

Luchi RJ and Gruber JW (1968) Unusually large digitalis requirements. A study of altered digoxin metabolism. *Am J Med* **45:**322-328.

MacLean C, Moenning U, Reichel A, and Fricker G (2008) Closing the gaps: a full scan of the intestinal expression of p-glycoprotein, breast cancer resistance protein, and multidrug resistance-associated protein 2 in male and female rats. *Drug Metab Dispos* **36:**1249-1254.

Madsen EL and Bollag J-M (1988) Pathway of indole metabolism by a denitrifying microbial community. *Archives of Microbiology* **151:**71-76.

Mahmood S, Khalid A, Arshad M, Mahmood T, and Crowley DE (2016) Detoxification of azo dyes by bacterial oxidoreductase enzymes. *Crit Rev Biotechnol* **36:**639-651.

Margulies EH, White AM, and Sherry S (1980) Sulfinpyrazone: a review of its pharmacological properties and therapeutic use. *Drugs* **20:**179-197.

Mattila MA and Larni HM (1980) Flunitrazepam: a review of its pharmacological properties and therapeutic use. *Drugs* **20:**353-374.

McCabe M, Sane RS, Keith-Luzzi M, Xu J, King I, Whitcher-Johnstone A, Johnstone N, Tweedie DJ, and Li Y (2015) Defining the Role of Gut Bacteria in the Metabolism of Deleobuvir: In Vitro and In Vivo Studies. *Drug Metab Dispos* **43:**1612-1618.

Mercier C, Chalansonnet V, Orenga S, and Gilbert C (2013) Characteristics of major *Escherichia coli* reductases involved in aerobic nitro and azo reduction. *J Appl Microbiol* **115:**1012-1022.

Merkel JR and Steers E (1953a) Relationship between "chloramphenicol reductase activity" and chloramphenicol resistance in Escherichia coli. *Journal of bacteriology* **66:**389.

Merkel JR and Steers E (1953b) Relationship between "chloramphenicol reductase activity" and chloramphenicol resistance in *Escherichia coli*. *J Bacteriol* **66:**389.

Messele T, Roos MT, Hamann D, Koot M, Fontanet AL, Miedema F, Schellekens PT, and Rinke de Wit TF (2000) Nonradioactive techniques for measurement of in vitro T-cell proliferation: alternatives to the [(3)H]thymidine incorporation assay. *Clin Diagn Lab Immunol* **7:**687-692.

Minematsu T, Sugiyama E, Kusama M, Hori S, Yamada Y, Ohtani H, Sawada Y, Sato H, Takayama T, Sugawara Y, Makuuchi M, and Iga T (2004) Effect of hematocrit on pharmacokinetics of tacrolimus in adult living donor liver transplant recipients. *Transplantation Proceedings* **36:**1506-1511.

Mix TCH, Kazmi W, Khan S, Ruthazer R, Rohrer R, Pereira BJG, and Kausz AT (2003) Anemia: A Continuing Problem Following Kidney Transplantation. *American Journal of Transplantation* **3:**1426-1433.

Möller A, Iwasaki K, Kawamura A, Teramura Y, Shiraga T, Hata T, Schäfer A, and Undre N (1999) The disposition of 14C-labeled tacrolimus after intravenous and oral administration in healthy human subjects. *Drug Metabolism and Disposition* **27:**633-636.

Moller A, Iwasaki K, Kawamura A, Teramura Y, Shiraga T, Hata T, Schafer A, and Undre NA (1999) The disposition of 14C-labeled tacrolimus after intravenous and oral administration in healthy human subjects. *Drug Metab Dispos* **27:**633-636.

Morgan KA and Ahlawat R (2019) Ranitidine, in: *StatPearls*, StatPearls Publishing LLC., Treasure Island (FL).

Morrison JM and John GH (2015) Non-classical azoreductase secretion in *Clostridium perfringens* in response to sulfonated azo dye exposure. *Anaerobe* **34:**34-43.

Morrison JM and John GH (2016) Growth and physiology of *Clostridium perfringens* wild-type and D*azoC* knockout: an azo dye exposure study. *Microbiology* **162:**330-338.

Morrison JM, Wright CM, and John GH (2012) Identification, Isolation and characterization of a novel azoreductase from *Clostridium perfringens*. *Anaerobe* **18:**229-234.

Moskovitz J, Flescher E, Berlett BS, Azare J, Poston JM, and Stadtman ER (1998) Overexpression of peptide-methionine sulfoxide reductase in Saccharomyces cerevisiae and human T cells provides them with high resistance to oxidative stress. *Proc Natl Acad Sci U S A* **95:**14071-14075.

Mouly S and Paine MF (2003) P-glycoprotein increases from proximal to distal regions of human small intestine. *Pharm Res* **20:**1595-1599.

Muthukumar A, Sangeetha S, and Sekar G (2018) Recent developments in functionalization of acyclic α-keto amides. *Organic & Biomolecular Chemistry* **16:**7068-7083.

Nadal I, Donant E, Ribes-Koninckx C, Calabuig M, and Sanz Y (2007) Imbalance in the composition of the duodenal microbiota of children with coeliac disease. *Journal of Medical Microbiology* **56:**1669-1674.

Nagase K, Iwasaki K, Nozaki K, and Noda K (1994) Distribution and Protein Binding of FK506, a Potent Immunosuppressive Macrolide Lactone, in Human Blood and Its Uptake by Erythrocytes. *Journal of Pharmacy and Pharmacology* **46:**113-117.

Nakanishi M, Yatome C, Ishida N, and Kitade Y (2001) Putative ACP phosphodiesterase gene (*acpD*) encodes an azoreductase. *J Biol Chem* **276:**46394-46399.

Namiki Y, Kihara N, Koda S, Hane K, and Yasuda T (1993) Tautomeric phenomenon of a novel potent immunosuppressant (FK506) in solution. I. Isolation and structure determination of tautomeric compounds. *J Antibiot (Tokyo)* **46:**1149-1155.

Nayfach S, Fischbach MA, and Pollard KS (2015) MetaQuery: a web server for rapid annotation and quantitative analysis of specific genes in the human gut microbiome. *Bioinformatics* **31:**3368-3370.

Nguyen TLA, Vieira-Silva S, Liston A, and Raes J (2015) How informative is the mouse for human gut microbiota research? *Dis Model Mech* **8:**1-16.

Olson RD, Mushlin PS, Brenner DE, Fleischer S, Cusack BJ, Chang BK, and Boucek RJ, Jr. (1988) Doxorubicin cardiotoxicity may be caused by its metabolite, doxorubicinol. *Proc Natl Acad Sci U S A* **85:**3585-3589.

Onderdonk AB, Kasper DL, Mansheim BJ, Louie TJ, Gorbach SL, and Bartlett JG (1979) Experimental animal models for anaerobic infections. *Reviews of infectious diseases* **1:**291-301.

Patel P, Patel H, Panchal S, and Mehta T (2012) Formulation strategies for drug delivery of tacrolimus: An overview. *Int J Pharm Investig* **2:**169-175.

Peng FC, Chaing HH, Tang SH, Chen PC, and Lu SC (2004) NADPH-cytochrome P-450 reductase is involved in flunitrazepam reductive metabolism in Hep G2 and Hep 3B cells. *J Toxicol Environ Health A* **67:**109-124.

Peppercorn MA and Goldman P (1972a) The role of intestinal bacteria in the metabolism of salicylazosulfapyridine. *J Pharmacol Exp Ther* **181:**555-562.

Peppercorn MA and Goldman P (1972b) The role of intestinal bacteria in the metabolism of salicylazosulfapyridine. *Journal of Pharmacology and Experimental Therapeutics* **181:**555-562.

Peres CM and Agathos SN (2000) Biodegradation of nitroaromatic pollutants: from pathways to remediation. *Biotechnol Annu Rev* **6:**197-220.

Perez-Silva G, Rodriguez D, and Perez-Silva J (1966) Dehydroxylation of caffeic acid by a bacterium isolated from rat faeces. *Nature* **212:**303-304.

Peternel L, Kristan K, Petruševska M, Rižner TL, and Legen I (2012) Suitability of Isolated Rat Jejunum Model for Demonstration of Complete Absorption in Humans for BCS-Based Biowaiver Request. *Journal of pharmaceutical sciences* **101:**1436-1449.

Peters U, Falk LC, and Kalman SM (1978) Digoxin metabolism in patients. *Arch Intern Med* **138:**1074-1076.

Picard N, Rouguieg-Malki K, Kamar N, Rostaing L, and Marquet P (2011) CYP3A5 genotype does not influence everolimus in vitro metabolism and clinical pharmacokinetics in renal transplant recipients. *Transplantation* **91:**652-656.

Pinder RM, Brogden RN, Speight TM, and Avery GS (1976) Clonazepam: a review of its pharmacological properties and therapeutic efficacy in epilepsy. *Drugs* **12:**321-361.

Piska K, Koczurkiewicz P, Bucki A, Wojcik-Pszczola K, Kolaczkowski M, and Pekala E (2017) Metabolic carbonyl reduction of anthracyclines - role in cardiotoxicity and cancer resistance. Reducing enzymes as putative targets for novel cardioprotective and chemosensitizing agents. *Invest New Drugs* **35:**375-385.

Prosser GA, Copp JN, Syddall SP, Williams EM, Smaill JB, Wilson WR, Patterson AV, and Ackerley DF (2010) Discovery and evaluation of *Escherichia coli* nitroreductases that activate the anti-cancer prodrug CB1954. *Biochem Pharmacol* **79:**678-687.

Qin J, Li R, Raes J, Arumugam M, Burgdorf KS, Manichanh C, Nielsen T, Pons N, Levenez F, Yamada T, Mende DR, Li J, Xu J, Li S, Li D, Cao J, Wang B, Liang H, Zheng H, Xie Y, Tap J, Lepage P, Bertalan M, Batto JM, Hansen T, Le Paslier D, Linneberg A, Nielsen HB, Pelletier E, Renault P, Sicheritz-Ponten T, Turner K, Zhu H, Yu C, Li S, Jian M, Zhou Y, Li Y, Zhang X, Li S, Qin N, Yang H, Wang J, Brunak S, Dore J, Guarner

F, Kristiansen K, Pedersen O, Parkhill J, Weissenbach J, Meta HITC, Bork P, Ehrlich SD, and Wang J (2010) A human gut microbial gene catalogue established by metagenomic sequencing. *Nature* **464:**59-65.

Radomski JL and Mellinger TJ (1962) The absorption, fate and excretion in rats of the water-soluble azo dyes, FD&C Red No. 2, FD&C Red No. 4, and FD&C Yellow No. 6. *J Pharmacol Exp Ther* **136:**259-266.

Rafii F and Cerniglia CE (1993) Comparison of the azoreductase and nitroreductase from *Clostridium perfringens*. *Appl Environ Microbiol* **59:**1731-1734.

Rafii F, Franklin W, and Cerniglia CE (1990) Azoreductase activity of anaerobic bacteria isolated from human intestinal microflora. *Appl Environ Microbiol* **56:**2146-2151.

Rafii F, Sutherland JB, Hansen EB, Jr., and Cerniglia CE (1997) Reduction of nitrazepam by Clostridium leptum, a nitroreductase-producing bacterium isolated from the human intestinal tract. *Clinical infectious diseases : an official publication of the Infectious Diseases Society of America* **25 Suppl 2:**S121-122.

Rafil F, Franklin W, Heflich RH, and Cerniglia CE (1991) Reduction of nitroaromatic compounds by anaerobic bacteria isolated from the human gastrointestinal tract. *Appl Environ Microbiol* **57:**962-968.

Renwick AG, Evans SP, Sweatman TW, Cumberland J, and George CF (1982a) The role of the gut flora in the reduction of sulphinpyrazone in the rat. *Biochemical pharmacology* **31:**2649-2656.

Renwick AG, Evans SP, Sweatman TW, Cumberland J, and George CF (1982b) The role of the gut flora in the reduction of sulphinpyrazone in the rat. *Biochem Pharmacol* **31:**2649-2656.

Rieger PG, Meier HM, Gerle M, Vogt U, Groth T, and Knackmuss HJ (2002) Xenobiotics in the environment: present and future strategies to obviate the problem of biological persistence. *J Biotechnol* **94:**101-123.

Robertson MD and Drummer OH (1995) Postmortem drug metabolism by bacteria. *J Forensic Sci* **40:**382-386.

Robinson P (2015) Enzymes: principles and biotechnological applications. *Essays In Biochemistry* **59:**1-41.

Roldan MD, Perez-Reinado E, Castillo F, and Moreno-Vivian C (2008) Reduction of polynitroaromatic compounds: the bacterial nitroreductases. *FEMS Microbiol Rev* **32:**474-500.

Rosenkranz HS and Mermelstein R (1983) Mutagenicity and genotoxicity of nitroarenes. All nitro-containing chemicals were not created equal. *Mutat Res* **114:**217-267.

Ryan AJ, Roxon JJ, and Sivayavirojana A (1968) Bacterial azo reduction: a metabolic reaction in mammals. *Nature* **219:**854-855.

Saha, Butler V, Neu H, and Lindenbaum J (1983a) Digoxin-inactivating bacteria: identification in human gut flora. *Science* **220:**325-327.

Saha JR, Butler VP, Neu HC, and Lindenbaum J (1983b) Digoxin-inactivating bacteria: Identification in human gut flora. *Science* **220:**325-327.

Scheline RR (1968) Metabolism of phenolic acids by the rat intestinal microflora. *Acta Pharmacol Toxicol (Copenh)* **26:**189-205.

Scheline RR (1973) Metabolism of foreign compounds by gastrointestinal microorganisms. *Pharmacol Rev* **25:**451-532.

Scheline RR and Midtvedt T (1970) Absence of dehydroxylation of caffeic acid in germ-free rats. *Experientia* **26:**1068-1069.

Schroder H and Gustafsson BE (1973) Azo reduction of salicyl-azo-sulphapyridine in germ-free and conventional rats. *Xenobiotica* **3:**225-231.

Sellés Vidal L, Kelly CL, Mordaka PM, and Heap JT (2018) Review of NAD(P)H-dependent oxidoreductases: Properties, engineering and application. *Biochimica et biophysica acta Proteins and proteomics* **1866:**327-347.

Sender R, Fuchs S, and Milo R (2016) Revised Estimates for the Number of Human and Bacteria Cells in the Body. *PLOS Biology* **14:**e1002533.

Skarydova L, Nobilis M, and Wsol V (2013) Role of carbonyl reducing enzymes in the phase I biotransformation of the non-steroidal anti-inflammatory drug nabumetone in vitro. *Xenobiotica* **43:**346-354.

Smith AL, Erwin AL, Kline T, Unrath WC, Nelson K, Weber A, and Howald WN (2007) Chloramphenicol is a substrate for a novel nitroreductase pathway in Haemophilus influenzae. *Antimicrob Agents Chemother* **51:**2820-2829.

Smith GN and Worrel CS (1950) The decomposition of chloromycetin (chloramphenicol) by microorganisms. *Arch Biochem* **28:**232-241.

Smith GN and Worrel CS (1953) Reduction of chloromycetin and related compounds by *Escherichia coli*. *J Bacteriol* **65:**313-317.

Smith TW and Haber E (1970) Digoxin intoxication: the relationship of clinical presentation to serum digoxin concentration. *The Journal of clinical investigation* **49:**2377-2386.

Sokol H, Pigneur B, Watterlot L, Lakhdari O, Bermudez-Humaran LG, Gratadoux JJ, Blugeon S, Bridonneau C, Furet JP, Corthier G, Grangette C, Vasquez N, Pochart P, Trugnan G, Thomas G, Blottiere HM, Dore J, Marteau P, Seksik P, and Langella P (2008) Faecalibacterium prausnitzii is an anti-inflammatory commensal bacterium

identified by gut microbiota analysis of Crohn disease patients. *Proc Natl Acad Sci U S A* **105:**16731-16736.

Soleim HA and Scheline RR (1972) Metabolism of xenobiotics by strains of intestinal bacteria. *Acta Pharmacol Toxicol (Copenh)* **31:**471-480.

Sousa T, Paterson R, Moore V, Carlsson A, Abrahamsson B, and Basit AW (2008a) The gastrointestinal microbiota as a site for the biotransformation of drugs. *Int J Pharm* **363:**1-25.

Sousa T, Paterson R, Moore V, Carlsson A, Abrahamsson B, and Basit AW (2008b) The gastrointestinal microbiota as a site for the biotransformation of drugs. *Int J Pharm* **363:**1-25.

Spanogiannopoulos P, Bess EN, Carmody RN, and Turnbaugh PJ (2016) The microbial pharmacists within us: a metagenomic view of xenobiotic metabolism. *Nat Rev Micro* **14:**273-287.

Speth PA, van Hoesel QG, and Haanen C (1988) Clinical pharmacokinetics of doxorubicin. *Clin Pharmacokinet* **15:**15-31.

Staatz CE and Tett SE (2004) Clinical pharmacokinetics and pharmacodynamics of tacrolimus in solid organ transplantation. *Clin Pharmacokinet* **43:**623-653.

Stanciu CN and Gnanasegaram SA (2017) Loperamide, the "Poor Man's Methadone": Brief review. *J Psychoactive Drugs* **49:**18-21.

Starzl TE (1987) First International Workshop on FK-506. A potential breakthrough in immunosuppression. Proceedings. *Transplantation proceedings* **19:**1-104.

Steinbach WJ, Reedy JL, Cramer RA, Jr., Perfect JR, and Heitman J (2007) Harnessing calcineurin as a novel anti-infective agent against invasive fungal infections. *Nat Rev Microbiol* **5:**418-430.

Størset E, Holford N, Midtvedt K, Bremer S, Bergan S, and Åsberg A (2014) Importance of hematocrit for a tacrolimus target concentration strategy. *Eur J Clin Pharmacol* **70:**65-77.

Strilchuk L, Fogacci F, and Cicero AF (2019) Safety and tolerability of available urate-lowering drugs: a critical review. *Expert Opin Drug Saf* **18:**261-271.

Strong HA, Renwick AG, and George CF (1984) The site of reduction of sulphinpyrazone in the rabbit. *Xenobiotica* **14:**815-826.

Strong HA, Renwick AG, George CF, Liu YF, and Hill MJ (1987) The reduction of sulphinpyrazone and sulindac by intestinal bacteria. *Xenobiotica* **17:**685-696.

Strong HA, Warner NJ, Renwick AG, and George CF (1985) Sulindac metabolism: the importance of an intact colon. *Clin Pharmacol Ther* **38:**387-393.

Suzuki H (2019) Remarkable diversification of bacterial azoreductases: primary sequences, structures, substrates, physiological roles, and biotechnological applications. *Appl Microbiol Biotechnol* **103:**3965-3978.

Svartz N (1942) Salazopyrin, a new sulfanilamide preparation. *Acta Medica Scandinavica* **110:**577-598.

Symons ZC and Bruce NC (2006) Bacterial pathways for degradation of nitroaromatics. *Nat Prod Rep* **23:**845-850.

Takeno S and Sakai T (1991) Involvement of the intestinal microflora in nitrazepam-induced teratogenicity in rats and its relationship to nitroreduction. *Teratology* **44:**209-214.

Tamura K, Kobayashi M, Hashimoto K, Kojima K, Nagase K, Iwasaki K, Kaizu T, Tanaka H, and Niwa M (1987) A highly sensitive method to assay FK-506 levels in plasma. *Transplant Proc* **19:**23-29.

Tamura S, Ohike A, Ibuki R, Amidon GL, and Yamashita S (2002) Tacrolimus is a class II low-solubility high-permeability drug: the effect of P-glycoprotein efflux on regional permeability of tacrolimus in rats. *Journal of pharmaceutical sciences* **91:**719-729.

Tamura S, Tokunaga Y, Ibuki R, Amidon GL, Sezaki H, and Yamashita S (2003) The site-specific transport and metabolism of tacrolimus in rat small intestine. *J Pharmacol Exp Ther* **306:**310-316.

Tatsumi K, Kitamura S, and Yamada H (1983) Sulfoxide reductase activity of liver aldehyde oxidase. *Biochim Biophys Acta* **747:**86-92.

Turpeinen M, Hofmann U, Klein K, Murdter T, Schwab M, and Zanger UM (2009) A predominate role of CYP1A2 for the metabolism of nabumetone to the active metabolite, 6-methoxy-2-naphthylacetic acid, in human liver microsomes. *Drug Metab Dispos* **37:**1017-1024.

Tuteja S, Alloway RR, Johnson JA, and Gaber AO (2001) The effect of gut metabolism on tacrolimus bioavailability in renal transplant recipients. *Transplantation* **71:**1303-1307.

Usami N, Kitahara K, Ishikura S, Nagano M, Sakai S, and Hara A (2001) Characterization of a major form of human isatin reductase and the reduced metabolite. *Eur J Biochem* **268:**5755-5763.

Vamos M, Erath JW, and Hohnloser SH (2015) Digoxin-associated mortality: a systematic review and meta-analysis of the literature. *Eur Heart J* **36:**1831-1838.

van Kessel SP, Frye AK, El-Gendy AO, Castejon M, Keshavarzian A, van Dijk G, and El Aidy S (2019) Gut bacterial tyrosine decarboxylases restrict levels of levodopa in the treatment of Parkinson's disease. *Nature communications* **10:**310.

Venkataramanan R, Jain A, Warty VW, Abu-Elmagd K, Furakawa H, Imventarza O, Fung J, Todo S, and Starzl TE (1991) Pharmacokinetics of FK 506 following oral administration: a comparison of FK 506 and cyclosporine. *Transplant Proc* **23:**931-933.

Venkataramanan R, Swaminathan A, Prasad T, Jain A, Zuckerman S, Warty V, McMichael J, Lever J, Burckart G, and Starzl T (1995) Clinical pharmacokinetics of tacrolimus. *Clin Pharmacokinet* **29:**404-430.

Vincent SH, Karanam BV, Painter SK, and Chiu S-HL (1992) In vitro metabolism of FK-506 in rat, rabbit, and human liver microsomes: Identification of a major metabolite and of cytochrome P450 3A as the major enzymes responsible for its metabolism. *Archives of Biochemistry and Biophysics* **294:**454-460.

Wallemacq PE and Verbeeck RK (2001) Comparative clinical pharmacokinetics of tacrolimus in paediatric and adult patients. *Clin Pharmacokinet* **40:**283-295.

Wallis RB (1983) Mechanisms of action of sulphinpyrazone. *Thromb Res Suppl* **4:**31-38.

Wang M, Ahrné S, Jeppsson B, and Molin G (2005) Comparison of bacterial diversity along the human intestinal tract by direct cloning and sequencing of 16S rRNA genes. *FEMS Microbiology Ecology* **54:**219-231.

Watanabe K, Yamashita S, Furuno K, Kawasaki H, and Gomita Y (1995) Metabolism of omeprazole by gut flora in rats. *J Pharm Sci* **84:**516-517.

Williams MF, Dukes GE, Heizer W, Han YH, Hermann DJ, Lampkin T, and Hak LJ (1992) Influence of gastrointestinal site of drug delivery on the absorption characteristics of ranitidine. *Pharm Res* **9:**1190-1194.

Winter ME (2004) *Basic clinical pharmacokinetics*. Lippincott Williams & Wilkins.

Woodings EP, Dixon GT, Harrison C, Carey P, and Richards DA (1980) Ranitidine--a new H2-receptor antagonist. *Gut* **21:**187-191.

Xu H, Heinze TM, Paine DD, Cerniglia CE, and Chen H (2010) Sudan azo dyes and Para Red degradation by prevalent bacteria of the human gastrointestinal tract. *Anaerobe* **16:**114-119.

Yamashita K, Nakate T, Okimoto K, Ohike A, Tokunaga Y, Ibuki R, Higaki K, and Kimura T (2003) Establishment of new preparation method for solid dispersion formulation of tacrolimus. *International Journal of Pharmaceutics* **267:**79-91.

Yan A, Culp E, Perry J, Lau JT, MacNeil LT, Surette MG, and Wright GD (2018) Transformation of the Anticancer Drug Doxorubicin in the Human Gut Microbiome. *ACS Infect Dis* **4:**68-76.

Yu LX, Crison JR, and Amidon GL (1996) Compartmental transit and dispersion model analysis of small intestinal transit flow in humans. *International Journal of Pharmaceutics* **140:**111-118.

Yu S, Li S, Yang H, Lee F, Wu J-T, and Qian MG (2005) A novel liquid chromatography/tandem mass spectrometry based depletion method for measuring red blood cell partitioning of pharmaceutical compounds in drug discovery. *Rapid Communications in Mass Spectrometry* **19:**250-254.

Zahir H, McCaughan G, Gleeson M, Nand RA, and McLachlan AJ (2004) Factors affecting variability in distribution of tacrolimus in liver transplant recipients. *British journal of clinical pharmacology* **57:**298-309.

Zahir H, McLachlan AJ, Nelson A, McCaughan G, Gleeson M, and Akhlaghi F (2005) Population Pharmacokinetic Estimation of Tacrolimus Apparent Clearance in Adult Liver Transplant Recipients. *Ther Drug Monit* **27**.

Zahir H, Nand RA, Brown KF, Tattam BN, and McLachlan AJ (2001) Validation of methods to study the distribution and protein binding of tacrolimus in human blood. *Journal of Pharmacological and Toxicological Methods* **46:**27-35.

Zheng Y, Masand A, Wagner M, Kapur S, Dadhania D, Lubetzky M, and Lee JR (2019) Identification of Antibiotic Administration as a Potentially Novel Factor Associated With Tacrolimus Trough Variability in Kidney Transplant Recipients: A Preliminary Study. *Transplantation Direct* **5**.

Ziegler DM (1988) Flavin-containing monooxygenases: catalytic mechanism and substrate specificities. *Drug Metab Rev* **19:**1-32.

Zou Y, Xue W, Luo G, Deng Z, Qin P, Guo R, Sun H, Xia Y, Liang S, Dai Y, Wan D, Jiang R, Su L, Feng Q, Jie Z, Guo T, Xia Z, Liu C, Yu J, Lin Y, Tang S, Huo G, Xu X, Hou Y, Liu X, Wang J, Yang H, Kristiansen K, Li J, Jia H, and Xiao L (2019) 1,520 reference genomes from cultivated human gut bacteria enable functional microbiome analyses. *Nat Biotechnol* **37:**179-185.

APPENDICES

Appendix A Permission letter for manuscript used in Chapter 1

Can I include/use my article in my thesis/dissertation? –

Yes. Authors can include their articles in full or in part in a thesis or dissertation for non-commercial purposes.

Which uses of a work does Elsevier view as a form of 'prior publication'? +

How do I obtain permission to use Elsevier Journal material such as figures, tables, or text excerpts, if the request falls within the STM permissions guidelines? +

How do I obtain permission to use Elsevier Journal material such as figures, tables, or text excerpts, if the amount of material I wish to use does not fall within the free limits set out in the STM permissions guidelines? +

How do I obtain permission to use Elsevier Book material such as figures, tables, or text excerpts? +

How do I obtain permission to use Elsevier material that is NOT on ScienceDirect or Clinical Key? +

Can I use material from my Elsevier journal article within my thesis/dissertation? –

As an Elsevier journal author, you have the right to Include the article in a thesis or dissertation (provided that this is not to be published commercially) whether in full or in part, subject to proper acknowledgment; see the Copyright page for more information. No written permission from Elsevier is necessary.

Appendix B Permission letter for manuscript used in Chapter 2

December 2, 2020

Yukuang Guo
Pharmaceutical Sciences
University of Illinois at Chicago
833 S Wood St
Chicago, IL 60612

Email: yukuangguo@gmail.com

Dear Yukuang Guo:

This is to grant you permission to include the following article in your dissertation entitled "The role of gut bacteria in tacrolimus dispostion" for the University of Illinois at Chicago:

Y Guo, CM Crnkovic, K-J Won, X Yang, JR Lee, J Orjala, H Lee, and H Jeong (2019) Commensal Gut Bacteria Convert the Immunosuppressant Tacrolimus to Less Potent Metabolites, *Drug Metab Dispos*, 47(3): 194-202; DOI: https://doi.org/10.1124/dmd.118.084772

The following must be included with your citation to the article:

Reprinted with permission of the American Society for Pharmacology and Experimental Therapeutics. All rights reserved.

If you present the article as it was published in the journal, the original copyright line published with the paper must be shown on the copies included with your dissertation.

Sincerely yours,

Richard Dodenhoff
Journals Director

Appendix C Permission letter for manuscript used in Chapter 2

JOURNAL POLICIES

Originality

Materials submitted to *Transplantation Direct* must not be under consideration elsewhere or previously published. Doing so is a violation of the policies of the Committee on Publication Ethics to which the journal belongs. This does not apply to meeting abstracts, which may be submitted in article form. Material that formed part of a student dissertation will be permitted, provided it does not appear in a citable journal.

Transplantation Direct endorses the policies of the International Committee of Medical Journal Editors regarding overlapping publications.

VITA

NAME: Yukuang Guo

EDUCATION:

2015 - present   Ph.D. in Pharmacognosy

University of Illinois at Chicago, US

2013 – 2014   M.Sc. in Pharmaceutics

King's College London, UK

2009 – 2013   B.Sc. in Pharmacognosy

Chengdu University of Traditional Chinese Medicine, China

HONORS

• Oscar Robert Oldberg Award, 2020, UIC College of Pharmacy, Chicago, IL, USA

• Paul Sang Award, 2019, UIC College of Pharmacy, Chicago, IL, USA

• Travel Award for PhD Students, 2019, UIC College of Pharmacy, Chicago, IL, USA

• American Heart Association (AHA) Pre-doctoral fellowship, 2019 (2 years $53,688)

• 2nd place in Images of Research, 2018, UIC College of Pharmacy, Chicago, IL, USA

• Best podium presentation in Translational Science category, Third annual GEMS Research Symposium, 2018, Chicago, IL, USA

• Best poster presentation in Clinical and Translational Science (CCTS) category, COP research day, 2018, UIC College of Pharmacy, Chicago, IL, USA

• 2nd place in Images of Research, 2015, UIC College of Pharmacy, Chicago, IL, USA

• Distinct graduate student. 2014, College of pharmacy, King's College London,

PUBLICATIONS

• Guo, Y., Lee, H., Edusei, E., Albakry, S., Jeong, H., & Lee, J. R. (2020). Blood Profiles of Gut Bacterial Tacrolimus Metabolite in Kidney Transplant Recipients. Transplantation direct, 6(10), e601.

• Guo, Y., Lee, H., & Jeong, H. (2020). Gut microbiota in reductive drug metabolism. Progress in Molecular Biology and Translational Science, 171, 61-93.

• Guo, Y., Crnkovic, C. M., Won, K. J., Yang, X., Lee, J. R., Orjala, J., ... & Jeong, H. (2019). Commensal gut bacteria convert the immunosuppressant tacrolimus to less potent metabolites. Drug Metabolism and Disposition, 47(3), 194-202.

• Mei, K. C., Guo, Y., Bai, J., Costa, P. M., Kafa, H., Protti, A., ... & Al-Jamal, K. T. (2015). Organic Solvent-Free, One-Step Engineering of Graphene-Based Magnetic-Responsive Hybrids Using Design of Experiment-Driven Mechanochemistry. ACS applied materials & interfaces, 7(26), 14176-14181.

ABSTRACTS

• Yukuang Guo, Camila Crnkovic, John Lee, Jimmy Orjala, Hyunwoo Lee, Hyunyoung Jeong (Podium) Commensal Gut Bacteria Convert Tacrolimus to Less Potent Metabolites. Keystone meeting (Microbiome: Chemical Mechanisms and Biological Consequences)-2019, Montreal, Canada

• Yukuang Guo, Camila Crnkovic, John Lee, Jimmy Orjala, Hyunwoo Lee, Hyunyoung Jeong (Poster) Commensal gut bacteria metabolize tacrolimus. PGSRM-2018, University of Minnesota, Minneapolis, MN, USA

• Yukuang Guo, Camila Crnkovic, John Lee, Jimmy Orjala, Hyunwoo Lee, Hyunyoung Jeong. (Podium Award) Commensal gut bacteria metabolize tacrolimus. Third annual

GEMS Research Symposium-2018, University of Illinois at Chicago, Chicago, IL, USA

• Yukuang Guo, Camila Crnkovic, John Lee, Jimmy Orjala, Hyunwoo Lee, Hyunyoung Jeong. (Poster) Commensal gut bacteria metabolize tacrolimus. PGSRM-2018, University of Minnesota, Minneapolis, MN, USA

• Yukuang Guo, Camila Crnkovic, John Lee, Jimmy Orjala, Hyunwoo Lee, Hyunyoung Jeong. (Poster) Commensal gut bacteria metabolize tacrolimus. Great Lakes Drug Metabolism and Disposition Group Meeting-2018, Indianapolis, IN, USA

• Yukuang Guo, Camila Crnkovic, John Lee, Jimmy Orjala, Hyunwoo Lee, Hyunyoung Jeong. (Poster Award) Commensal gut bacteria metabolize tacrolimus. COP research day-2018, University of Illinois at Chicago, Chicago, IL, USA

• Yukuang Guo, Sungjoon Cho, Kyoung-Jae Won, Eunah Chung, Joo-Seop Park, Hyunyoung Jeong. (Poster) Differential gut microbiota leads to altered hepatic expression of Drug Disposition Genes (DDG) in mice. PGSRM-2017, University of Michigan, Ann Arbor, MI, USA

• Yukuang Guo, Sungjoon Cho, Kyoung-Jae Won, Eunah Chung, Joo-Seop Park, Hyunyoung Jeong. (Poster) Differential gut microbiota leads to altered hepatic expression of Drug Disposition Genes (DDG) in mice. COP research day-2017, UIC College of Pharmacy, Chicago, IL, USA

• Yukuang Guo, Sungjoon Cho, Kyoung-Jae Won, Eunah Chung, Joo-Seop Park, Hyunyoung Jeong. (Poster) Structural differences in gut microbiota lead to altered hepatic expression of Drug Disposition Genes (DDG) in mice. Experimental Biology-2017, Chicago, IL, USA